UNIVERSITY OF THE
WITWATERSRAND,
JOHANNESBURG

High Temperature Sulphidation and Naphthenic Acid Corrosion Modelling in Crude Oil Refining

by

Nonkululeko P. Nancy Xaba

(768692)

A dissertation submitted to the Faculty of Engineering and the Built Environment, University of the Witwatersrand, in fulfilment of the requirements for the degree of Master of Science in Engineering

16 November 2018

DECLARATION

I declare that this dissertation is my own unaided work. It is being submitted for the degree of Master of Science in Engineering to the University of the Witwatersrand, Johannesburg. It has not been submitted before for any degree or examination in any other university. The data produced and used in the research was obtained whilst in the employ of SAPREF, who approved the use of the data for research purposes in collaboration with Mintek, DST and the university.

Signature N.P.N. Xaba:

16 November 2018

ACKNOWLEDGEMENTS

The Lord

Thank you to God for the opportunity and ability to embark on this study.

My supervisor

Thank you to my supervisor, Professor Lesley Cornish, for her patience and support even as we encountered data access issues as well as time issues when I was sent on expatriation assignment.

Technical assistance

Thank you to Dr. John Pugh and Marion van den Hoogen for their participation and work on this study.

Institutions and Organisations

Thank you to the DST, NRF, Mintek, AMI and DST-NRF CoE in Strong Materials for sponsoring the research project. A thank you to SAPREF for participating in the study and allowing review of internal records for the research purposes.

My family

I would like to thank my family, parents and my husband, Björn Pietruschka, for supporting and encouraging me throughout the research study.

ABSTRACT

High temperature sulphidic (HTS) and naphthenic acid corrosion (NAC) pose not only reliability, but also health, safety and environmental threats to crude oil distillation unit operations. Based on an oil refinery's crude oil diet properties, materials of construction and operational conditions in the distillation units, these high temperature corrosion phenomena occur in varying severity. In a bid to improve profit margins, oil refineries may choose to process opportunity crude oils at the risk of aggravating these corrosion mechanisms. In order to predict corrosion rates due to HTS and NAC, an industry corrosion model, Predict Crude^{TM}, was used on a refinery's atmospheric and vacuum distillation units. The model was based largely on empirical data from a 4-year joint industry program that collected NAC and HTS corrosion rate data. The model provided qualitative corrosion rates for different distillation product streams for three model cases, based on total acid number (TAN) namely crude blend TAN 0.35, TAN 0.5 and TAN 0.8. The corrosion rates produced by the model for the 0.35 and 0.5 TAN cases were assessed against the measured corrosion rates, using conventional (industrial ultrasonic thickness and profile radiography) plant inspection techniques. Good agreement between the model predicted corrosion rates for the 0.35 and 0.5 TAN cases and the practically observed corrosion rates was found. The 0.8 TAN case was used to assess upset (unusual) conditions only, as the plant did not process 0.8 TAN crude blends. The 0.8 TAN case model data also explained some of the higher than modelled corrosion rates that were measured. Thus, the model provided a closely accurate prediction of corrosion rates to be expected in the atmospheric and vacuum distillation units.

CONTRIBUTIONS OF THIS STUDY

N. Xaba, L.A. Cornish and F.M.L. Mulaudzi, Challenges in the Development of a High Temperature Corrosion Model for a Crude Oil Refinery Unit, Nuclear Materials Development Network Conference, AMI, SAIMM Symposium Series S87, pp. 113-121, NMMU, Port Elizabeth, 28^{th} – 30^{th} October 2015. ISBN 978-1-920410-78-0

N. Xaba, L.A. Cornish and F.M.L. Mulaudzi, Measurement and Monitoring of Naphthenic Acid Corrosion in a Crude Oil Refinery's Crude Distillation Fired Heater, AfriCORR 2016, p. 67, Midrand, 25^{th} – 29^{th} July 2016. (Poster)

A presentation was given at AfriCORR 2018:

N. Xaba, L.A. Cornish and F.M.L. Mulaudzi, Modelling and Measurement of Naphthenic Acid Corrosion in a Crude Oil Refinery's Distillation Units, AfriCORR 2018, Book of Abstracts, p. 19, Johannesburg, 18th – 20^{th} July 2018.

TABLE OF CONTENTS

DECLARATION....2
ACKNOWLEDGEMENTS....3
ABSTRACT....4
CONTRIBUTIONS OF THIS STUDY....5
TABLE OF CONTENTS....6
LIST OF FIGURES....8
LIST OF TABLES....9
1. INTRODUCTION....10
1.1 Crude Oil Sources....10
1.2 Crude Oil Price....11
1.3 Crude Oil Refining....12
1.4 High Temperature Corrosion in Oil Refining....14
1.5 Historical corrosion Issues at SAPREF....14
1.6 Problems with Corrosion Modelling in Oil Refining....15
1.7 Purpose of this Work....16
1.8 Objectives....16
2. LITERATURE REVIEW....17
2.1 High Temperature Sulphidic Corrosion....17
2.2 Naphthenic Acid Corrosion....19
2.3 The interaction between NAC and HTS....19
2.4 Previous attempts at prediction and current practices....23
2.5 Corrosion Measurements systems....26
2.5.1 Ultrasonic Wall Thickness Testing....26
2.5.2 Profile Radiography....28
3. PROJECT DESCRIPTION AND METHODOLOGY....30
3.1 Corrosion Process Loop Definition....30
3.2 Pro/II Modelling....31
3.3 Corrosion Modelling....32
3.3.1 Exclusions....33
3.4 Corrosion Rate Measurement and Inspection History Review....34

3.4.1 Historical Corrosion Rate Determination 34
4. RESULTS 40
4.1 Corrosion Process Loop Definition...43
4.2 Sulphur and TAN Distributions 44
4.2.1 Atmospheric Distillation Sulphur and TAN Distributions...44
4.2.2 Vacuum Distillation Sulphur and TAN Distributions 46
4.3 Corrosion Rates Results 48
4.3.1 Atmospheric Distillation Modelled Corrosion Rates Profile..48
4.3.2 Atmospheric Distillation Actual Corrosion Rates History 52
4.3.3 Vacuum Distillation Modelled Corrosion Rates Profile 54
4.3.4 Vacuum Distillation Actual Corrosion Rates History..58
5. DISCUSSION 60
5.1 Crude Oil Feed Sulphur and TAN 60
5.2 Sulphur Distribution..60
5.2.1 Sulphur Distribution – Atmospheric Pressure Distillation...60
5.2.2 Sulphur Distribution – Vacuum Pressure Distillation...61
5.3 TAN Distribution 61
5.3.1 TAN Distribution – Atmospheric Pressure Distillation...62
5.3.2 TAN Distribution – Vacuum Pressure Distillation 62
5.4 Comparison of Modelled Corrosion Rates and Inspection History......................................62
5.4.1 Behavior of Different Materials in HTS & NAC Conditions..68
5.5 Limitations & Potential Error Sources 70
6. CONCLUSIONS 72
7. RECOMMENDATIONS FOR FUTURE WORK 74
REFERENCES 75
APPENDICES...82
Appendix 1...83
Appendix 2...94
Appendix 3 98

LIST OF FIGURES

Figure 1.1: Changes in crude oil price (Global Petrol Prices, 2015). 12
Figure 1.2: Basic process flow of atmospheric and vacuum distillation units (Parker Kittiwake, 2015). 13
Figure 2.1: Modified McConomy curves (Hucinska, 2006). 18
Figure 2.2: Internal pitting observed on vacuum distillation furnace tube bends (Xaba et al., 2015). 22
Figure 2.3: Comparison of laboratory corrosion rate data for VGO (TAN 3, 0.6wt%) and prediction methods from API 581, McConomy and Predict Crude^{TM} (Kane & Chambers, 2011). 25
Figure 2.4: Principle of ultrasonic wall thickness testing with a contact transducer, with an A-scan representation of the readings displayed on the right (Spectro, 2010). 27
Figure 2.5: Double wall technique radiography (Zscherpel et al., 2006). 28
Figure 3.1: Corrosion rate estimation flowchart. 38
Figure 4.1: Transition of crude oil diet from mainly PG to WAF. 40
Figure 4.2: Crude feed measured TAN and sulphur (March 2005 to January 2011). 41
Figure 4.3: Crude feed measured TAN and sulphur (June 2013 to July 2014). 42
Figure 4.4: Crude feed measured TAN and sulphur (June 2013 to July 2014). 45
Figure 4.5: TAN distribution in atmospheric distillation cuts for the three modelled cases. 46
Figure 4.6: Sulphur distribution in vacuum distillation cuts for the three modelled cases. 47
Figure 4.7: TAN distribution in vacuum distillation cuts for the three modelled cases. 47
Figure 4.8: Atmospheric distillation unit corrosion map for 0.35 TAN model case. 49
Figure 4.9: Atmospheric distillation unit corrosion map for 0.5 TAN model case. 50
Figure 4.10: Atmospheric distillation unit corrosion map for 0.8 TAN model case. 51
Figure 4.11: Vacuum distillation unit corrosion map for 0.35 TAN model case. 55
Figure 4.12: Vacuum distillation unit corrosion map for 0.5 TAN model case. 56
Figure 4.13: Vacuum distillation unit corrosion map for 0.8 TAN model case. 57

LIST OF TABLES

Table 3.1: Corrosion rate range definition. 36
Table 4.1: Model cases crude mixes. 43
Table 4.2: Corrosion process loops. 44
Table 4.3: Comparison of model and Actual Corrosion Rate (CR) Results for Atmospheric Distillation Circuits. 52
Table 4.4: Atmospheric distillation major corrosion events. 53
Table 4.5: Comparison of model and Actual Corrosion Rate (CR) Results for Vacuum Distillation Circuits. 58
Table 4.6: Vacuum distillation major corrosion events. 59

1. INTRODUCTION

This chapter serves to give background to the oil refining industry and the associated corrosion issues. The background information is intended to set the scene for the relevance of this research to everyday life and the oil industry. The modern world depends largely, and runs, on oil derived products. From the automotive, plastics and cosmetics industry to clothing, construction and many other industries rely on a constant supply of fuel oils, lubricants, base chemicals and many more. Whereas access to crude oil sources has been increasingly unlocked in terms of deep sea or unconventional sources, refineries remain the crucial choke point between oil extraction and the insatiable thirst for oil derived products for the global economy, with each interruption causing global delays and problems.

1.1 Crude Oil Sources

Oil can be found and produced from a variety of sources globally. It exists in reservoirs in the earth's crust. World oil production comes largely from what are termed as conventional sources. Today, conventional oil sources are considered to be oil fields and offshore oil deposits. The definition of conventional and unconventional depends largely on the cost of extraction, as well as the availability of the related technology. For this reason, the classification of conventional and unconventional oil sources can shift over time depending on technological advances in the industry. As an example, 50 years ago offshore oil deposits were also considered to be unconventional crude oil sources.

Crude oil varies in properties depending on its source, and crude oil traders also supply assays which provide detailed analyses of the crude oil with density, characterization of product yields and the boiling point ranges, as well as the concentrations of key elements, salts and contaminants. The data contained within the crude assay are used for refinery engineering and product planning, commonly referred to as scheduling; they can be used to determine whether a crude oil could potentially cause yield, quality, production, environmental or any other issues.

1.2 Crude Oil Price

Crude oil pricing has a history of being volatile and has varied immensely based on supply and demand dynamics and political influences, as shown in Figure 1.1 (Global Petrol Prices, 2015). Downstream crude oil refining began in the 20th century and subsequently expanded in the 21st century, with developments in the transportation and energy industry. As the industry grew, economic constraints threatened the profitability of the business, particularly when crude oil prices peaked in 2008 and 2014. Most refineries were built at a time when crude oil prices were relatively low, up to the 1970s, and refinery equipment were designed for a crude oil diet composition that has increased significantly in cost. However, crude diet however has significant impact on Gross Refinery Margins (GRM), with higher prices putting a squeeze on profitable operation of the plants. The cost of crude oil can account for up to 90% of refineries' expenditure therefore there is an incentive for purchasing crude oils of lower prices (Qing, 2010). No two crude oils are the same, differing not only in product yields and availability, but also in corrosivity and cost (U.S. Energy Information Administration, 2012) It is no wonder that oil refineries seek out opportunity crudes to boost profitability margins, although these crudes often come at the cost of integrity and reliability of the units (Yeung, 2006). Opportunity crude oils are termed as such due to the possibility they afford refineries to bolster margins. However, many opportunity crudes contain more organic acids which can be more corrosive to the refining equipment.

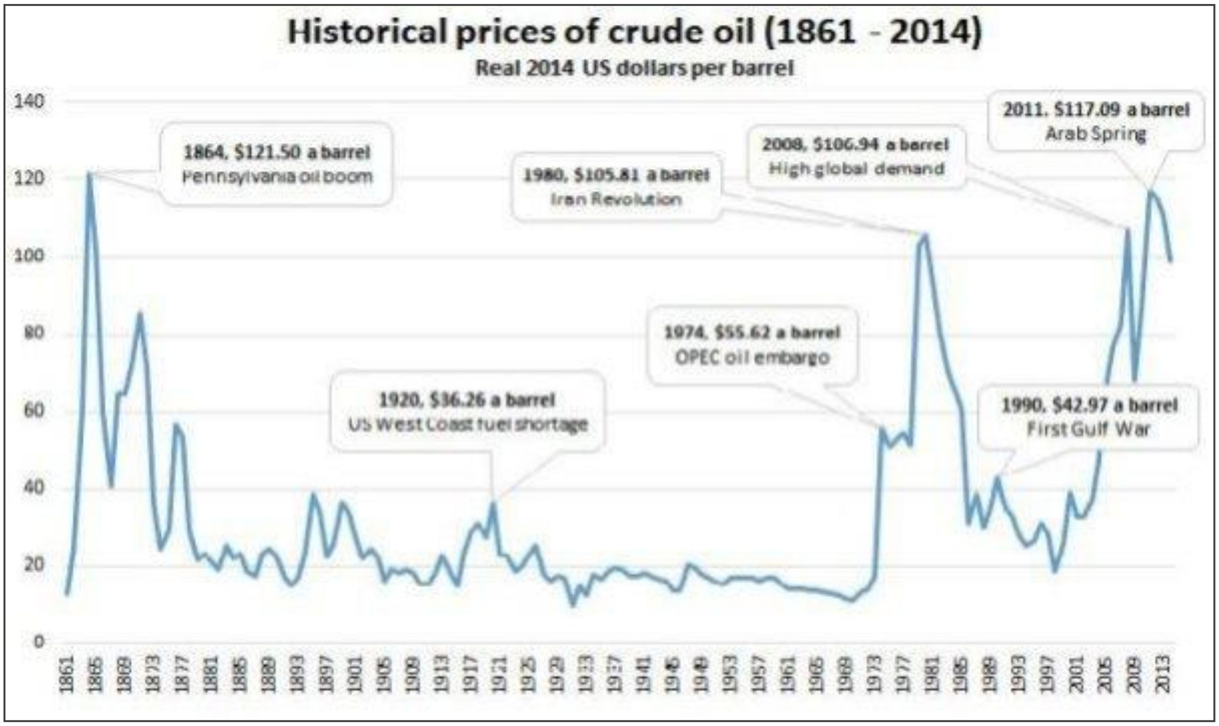

Figure 1.1: Changes in crude oil price (Global Petrol Prices, 2015).

1.3 Crude Oil Refining

A “unit” is a term used for a basic chemical reaction step in a process. In the oil refining process, atmospheric and vacuum distillation are both considered separate units. The basic design of the atmospheric and vacuum distillation units is presented in Figure 1.2 (Parker Kittiwake, 2015). The crude oil is firstly desalted to remove salts and sludge. The salts and sludge can cause damage to the refinery equipment by promoting scale formation and causing blockages, as well as causing corrosion in lower temperature systems with an aqueous water phase. The crude oil is then preheated in a series of heat exchangers, before being sent to the furnace where the crude oil is heated to a maximum temperature of 360˚C for distillation in the atmospheric column. Various relatively light products are distilled from the atmospheric distillation step. The heavier long residue from the bottom of the atmospheric column is routed to the vacuum distillation section where it is further heated in the vacuum furnace. More gasoil fractions, namely the waxy distillates and washoil, as well as heavy residue, are then distilled in the vacuum column.

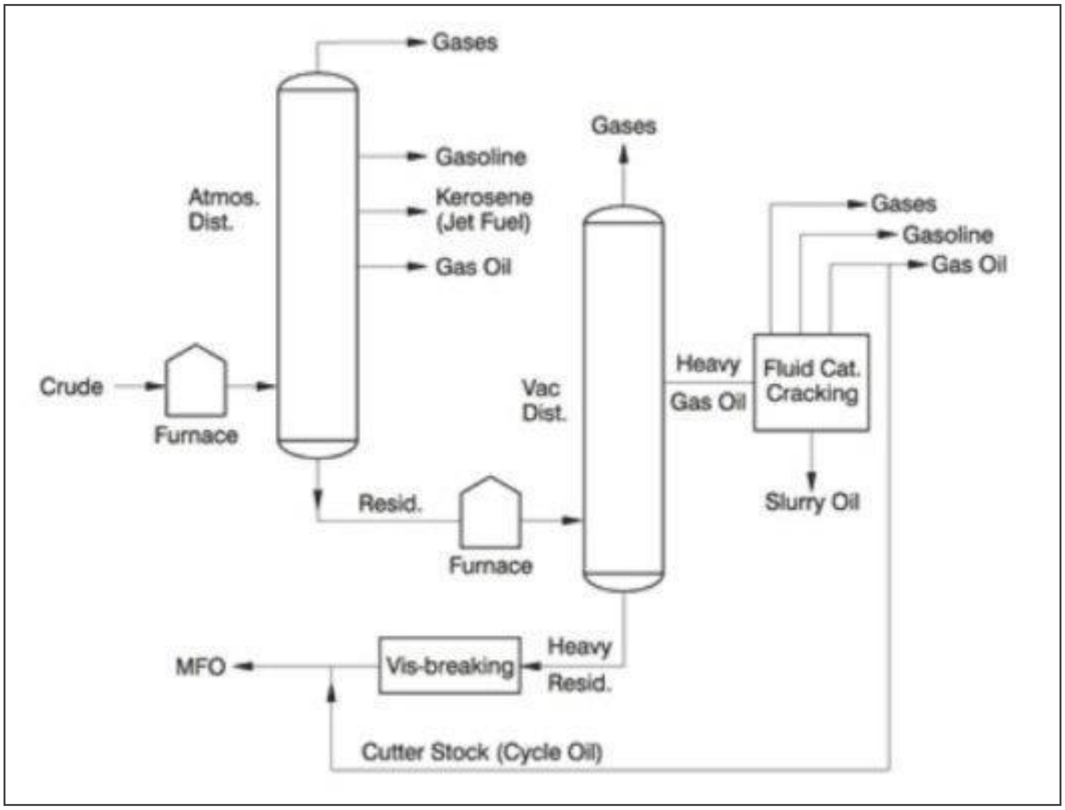

Figure 1.2: Basic process flow of atmospheric and vacuum distillation units (Parker Kittiwake, 2015).

There is a wide range of products that can be derived from crude oil, which differ in distillation temperatures and number of carbon atoms in their molecules. The principle of distillation, also called fractionation, employed in both the atmospheric and vacuum distillation columns, is based on this difference in boiling temperatures of the various compounds in the crude oil feedstock. However, the atmospheric distillation step cannot separate the heavy product called long residue at the bottom of the column without additional heat input, which would result in thermal cracking. Thermal cracking of the residue alters the chemical structure of the products and causes resultant issues with coke formation. Vacuum distillation is therefore carried out at pressures as low as 1.33×10^3 and 2×10^3 Pa to keep temperatures lower. The true boiling point (TBP) curve, together with the density curves of a given crude oil can be used to characterize the products emanating from fractionation of that crude.

1.4 High Temperature Corrosion in Oil Refining

Depending on the process conditions in the distillation process and the materials of construction of the equipment and interconnecting piping, varying corrosion mechanisms can occur. High temperature corrosion poses one of the largest risks to unit operations as corrosion leaks cannot be repaired without interruption of operations which has a direct impact on GRM. There is also the environmental aspect; as some refinery processes are above auto-ignition temperature and can result in fires of the process equipment. Common high temperature corrosion mechanisms in oil refining include high temperature oxidation, metal dusting, high temperature sulphidation (HTS) and naphthenic acid corrosion (NAC). While high temperature oxidation and metal dusting only affect furnace tubes, HTS and NAC impact all piping and equipment operating at elevated temperatures. HTS and NAC could therefore be considered the most problematic. Both mechanisms occur in the same temperature range and interact with one another, particularly when combined with flow effects. They have differing morphologies; while HTS is a general corrosion that cannot be visually identified by any particular pattern, NAC is identified by pitting in localised areas.

1.5 Historical corrosion Issues at SAPREF

SAPREF is South Africa's largest crude oil refinery, built in 1960 and commissioned in 1963. The refinery has a capacity of 8.5 million tons per year and between 180 000 and 190 000 barrels per day, depending on the type of crude oil processed. Apart from being the largest oil refinery in the country, the refinery has additional strategic importance given its location and role in coordinating approximately 80% of the crude oil import into the country at the Single Buoy Mooring (SBM), where tankers offload crude oil. The refinery produces petrol, diesel, paraffin, aviation fuel, liquid petroleum gas, base oil, solvents and marine fuel oil, making a large contribution in addressing the country's and the greater southern African region's fuel demands.

The oil refinery in South Africa, SAPREF, had a history of poor reliability in its atmospheric and vacuum distillation units, due to leak incidents from corrosion on high temperature circuits, resulting in small fires and shutdown of unit operations for repairs. The leaks were determined to be from HTS and NAC from detailed failure investigations, there was only one incident recorded from metal dusting (Dube, 2012) and none from oxidation. These incidents followed after gradual increases in processing of opportunity crude oils by the refinery. Leaks occurred on both the atmospheric and vacuum furnaces, as well as on transfer piping from the furnace to the distillation columns. For this reason, it was highly advantageous to employ the use of industrially available corrosion modelling tools to determine areas of risk for HTS and NAC.

1.6 Problems with Corrosion Modelling in Oil Refining

Corrosion models can be either mathematical, semi-empirical or empirical. Given the limited understanding of the corrosion mechanisms quantifying the influencing factors effects on corrosion rates and the interaction of the mechanisms with one another, mathematical models have proven unsuccessful at predicting corrosion behaviour. There needs to be a firm understanding of how each corrosion influencing parameter affects corrosion rates and how the combined effect of changes in these parameters impacts corrosion. No such mathematical model has successfully been developed and implemented. The success of semi-empirical and empirical models in the prediction of high temperature corrosion rates is unknown, and experience on industrially available models is not shared within refining industry, for the sake of confidentiality and competition (and one such confidentiality agreement has been entered into with the parties involved in this investigation, and a sample thereof is attached in Appendix 2.

The questions arising include:-

- Is it possible to model the combination of HTS and NAC?
- Can flow effects be included in corrosion rate modelling?
- Do modelled data agree with the corrosion rates observed in practice on an operational plant?
- What are the pitfalls of attempting to model HTS and NAC?

1.7 Purpose of this Work

This investigation sought to verify the corrosion rates predicted by an empirical industry corrosion model that was run on three different crude oil blend compositions, with crude oils from different locations and varying also in characteristics. The actual corrosion rates observed and measured on the refining equipment were compared to the modelled results relating to the blends closest to those actually processed on the units, to determine the effectiveness of the model in estimating the corrosion rates. The issues encountered in the use of the model and with the suitability of the input data for such a model were also discussed.

1.8 Objectives

a. Literature had to be reviewed and the historically observed corrosion mechanisms in crude oil atmospheric and vacuum distillation units studied. This was done to determine where high temperature sulphidation (HTS) and naphthenic acid corrosion (NAC) mechanisms could be expected in the high temperature circuits of a crude oil atmospheric and high vacuum distillation unit. The HTS and NAC corrosion rates were modelled for three different crude feed total acid number (TAN) cases, using a commercially available model based on empirical data. As an outcome of the modelling, a high temperature corrosion map of the refinery distillation unit was provided.
b. This research project sought to determine whether the use of an industry corrosion model, on an oil refinery using more opportunity crudes as part of its diet could provide accurate corrosion rate predictions for major high temperature equipment and components in the oil refining process.
c. Determine the effect of changes in crude feed TAN had on the following:
    i. Sulphur distribution in the crude distillation cuts,
    ii. TAN distribution in the crude distillation cuts,
    iii. Corrosion rates.

2. LITERATURE REVIEW

2.1 High Temperature Sulphidic Corrosion

High temperature sulphidic corrosion, also called high temperature sulphidation (HTS), is a term given to the oxidation of metallic surfaces by the action of sulphur and its compounds at elevated temperatures. These corrosive sulphur compounds include hydrogen sulphide, polysulphides, mercaptans, disulphides and aliphatic sulphides. Carbon steels form an iron sulphide (FeS) scale that generally adhere to the metal substrate and retard corrosion rates whereas low alloy steels that contain chromium form a two-layer scale – the inner layer is a sulpho-spinel ($FeCr_2S_4$) and the outer layer is the FeS (NACE 34103, 2014). HTS can occur by the direct reaction of active sulphur species, like mercaptans, with metallic surfaces to form iron sulphide or iron and chrome sulphide products. The second method of HTS is the thermal decomposition of active sulphur compounds to form H_2S which then reacts with metal surfaces to form iron sulphide or sulpho-spinels. In crude oil refining, the most common form of HTS is that by hydrogen sulphide, sulphur and mercaptans. The corrosion is difficult to detect visually as it takes the form of general wall loss of the substrate (Rebak, 2011), although the black solid iron suphide layer can be seen on the surface of the corroded metal. The presence or absence of hydrogen also affects corrosion rates and the Couper-Gourman curves are used to predict corrosion rates in hydrogen rich process conditions (Lai, 2007, page 212). McConomy curves, which are used for HTS corrosion rate prediction, have been found to be overly conservative and predict exceedingly high corrosion rates. Modified McConomy curves, Figure 2.1 (Hucinska, 2006), were introduced in 1986 to correct the corrosion rate prediction by introducing a multiplier. However, modified McConomy have still been found to provide overly conservative corrosion rate predictions (Kane & Chambers, 2011).

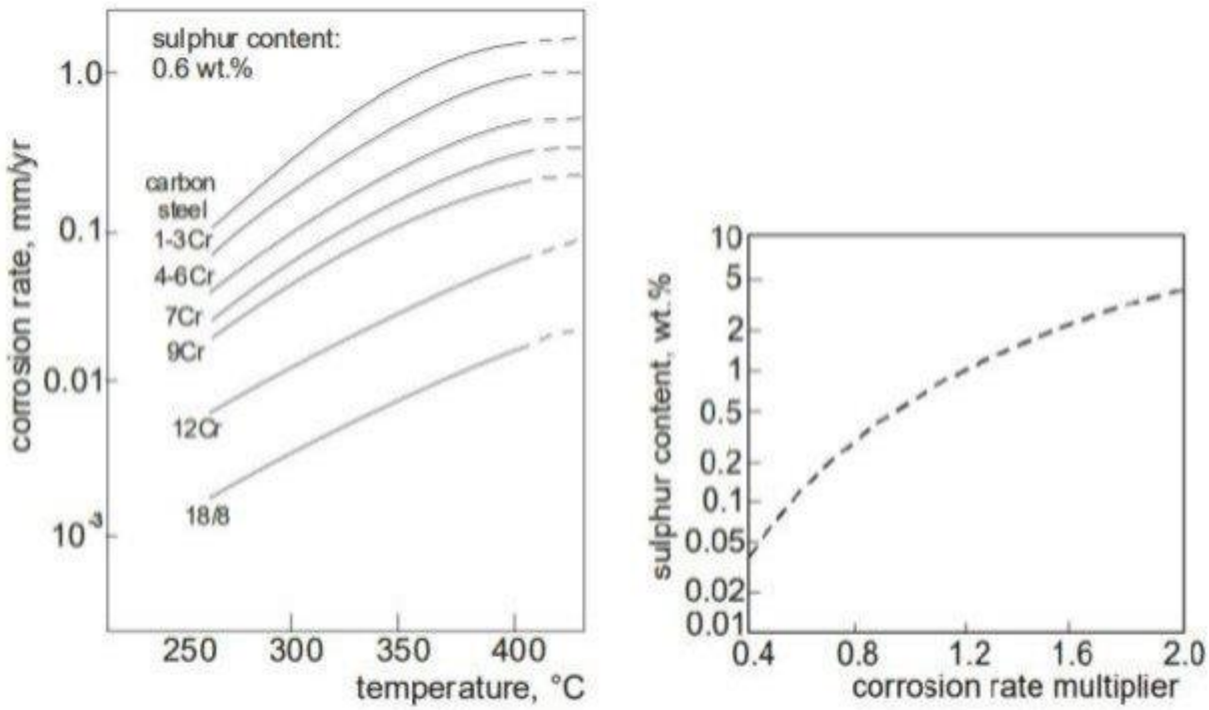

Figure 2.1: Modified McConomy curves (Hucinska, 2006).

Much work has been done on predicting the corrosion behavior of different materials in high temperature sulphidation environments. The McConomy curves, which differentiate between corrosion rates for carbon steels, low alloy and stainless steels, were presented in 1963, but they only demonstrate the effect of increases in the chromium content of the steel. Since then, research on the influence of alloying elements on corrosion rates has demonstrated that for carbon steels, reduced amounts of silicon (Si <0.1 wt%) leads to higher corrosion rates (API RP 939-C, 2008). Alloying of common metals by the refractory metals, niobium and molybdenum, considerably improves corrosion resistance with respect to highly sulphidising atmospheres (Przybylski & Mrowec, 2003). Each of the before-mentioned alloying elements (Si, Cr, Nb, Mo) all serve to produce more stable sulphide scales on the surface of the steel, which passivate and protect the material from further corrosion. It was also suggested by Farrell & Roberts (2010) that chromium may poison the decomposition of sulphur compounds, thus obstructing the corrosion process.

2.2 Naphthenic Acid Corrosion

"Naphthenic acids" is a term given to organic acids naturally occurrent in crude oils. The acids are chemically represented by $R[CH_2]_n$-COOH, where R is a single or more saturated ring structures (usually cyclopentane or cyclohexane). Corrosion by naphthenic acids is most severe at their boiling point or upon condensation (Slavcheva, 1999). Although other means do exist, the most popular measurement used to quantify the amount of naphthenic acids in a crude oil is the Total Acid Number (TAN) (Piehl, 1988). TAN is measured by titration of 1g of an oil sample using KOH, where the amount of KOH, in mg, used to neutralise the sample is the TAN. TAN is considered an ineffective way of measurement as this includes the reaction of not just naphthenic acids but sulphides and other acid gases as well (Kane, 2006). The technique is deficient in differentiating between the various acidic species that also react with the KOH. Although crude oils with higher TAN were generally considered as being more corrosive Hau et al. (2003) showed that using iron powder tests, there were anomalous cases where oil samples having larger values of TAN exhibited less corrosivity than others having much lower values of TAN, and also cases where oils show completely different corrosivity despite having similar or the same TAN.

Similar to HTS, the increase of chromium in steels increases NAC resistance because of the improved stability of the sulphide scale on the surface of the steel. Interestingly, the benefit of 5Cr over carbon steel was shown to be minimal (El Kamel et al., 2010). Stainless steels, particularly those containing higher amounts of molybdenum are considered the most effective against NAC (Farraro & Stellina, 1996).

2.3 The interaction between NAC and HTS

The factors which influence NAC corrosion rates are similar to those for HTS (Bota et al., 2010), namely:

- Materials of construction.

Materials with higher chromium, niobium and/or molybdenum content exhibit better resistance to corrosion by both HTS and NAC.

- Process temperatures: HTS corrosion rates increase with temperature. Similarly, NAC rates tend to increase with increased temperature but are also most severe at the boiling point of the naphthenic acids concerned.
- Flow regime: In annular flow both HTS and NAC corrosion rates are lower than in high velocity, turbulent two phase or mist flow conditions. The resultant wall shear stresses in high velocity, turbulent and two-phase flow conditions tend to remove the corrosion products that protect the metal substrate promoting further corrosion.
- Active sulphur content, as well as the concentration and type of naphthenic acid of the process streams. In general, higher concentrations lead to higher corrosion rates.

The relationship of the mechanisms' corrosion rates with each of these influencing parameters is not linear in nature, and becomes all the more complex when the parameters are assessed in combination with each other. Nugent and Dobis (1998) discovered that although naphthenic acid corrosion was previously thought to be most severe at high TAN levels (typically classified as crude TAN above 0.5 and crude fractions with TAN greater than 1.5), NAC corrosion rates can also be high for sweeter crudes, crude oil with sulphur content below 0.5 wt%, with low TANs. In the early 1990s failures of major process equipment occurred following the processing low TAN primarily West African Crudes (WAF) on crude distillation and high vacuum units designed for sour Persian Gulf (PG) Crudes. These findings were later supported by the joint industry project (Chambers et al., 2012) which proposed an apparent window of sulphidic corrosion inhibition in which sulphur acted as an agent of protection against naphthenic acid corrosion, for sulphur levels between 0.1 wt% and 2.2 wt%. In this range, the measured corrosion rates were lower than for both the low and high sulphur concentrations.

Naphthenic acids have been broadly grouped into two categories: α and β naphthenic acids by Kane (2006), which differ in characteristics and more interestingly corrosivity. This difference in corrosivity is attributed to their difference in molecular weights; α naphthenic acids have lower molecular weights than β naphthenic acids. Steric hindrance reduces the reactivity of the larger more complex β naphthenic acids (Turnbull et al., 1998); the α acids are more easily absorbed into the material's surface than the β acids. This idea was supported by the findings Hau et al. (2003) that oils with the same or similar TAN can have varying corrosivities.

In addition to this, the different type of acids may be corrosive at varying temperatures. Naphthenic acid corrosion occurs in the liquid phase and has its most severe effects at temperatures close to the naphthenic acid boiling points and upon condensation (Derungs, 1956). Naphthenic acids have differing boiling points, for α naphthenic acids it is temperatures up to 385°C, whereas β naphthenic acids boil at between 357°C and 816°C. Above 400°C, some naphthenic acids begin thermally decomposing and much less corrosion is expected above this temperature.

Equations 2.1-2.3 represent the classical naphthenic acid corrosion theory for α acids (Babaian-Kibala, 1999). Equation 2.1 is the formation of iron naphthenate from corrosion of the metal by α naphthenic acid with the general chemical formula RCOOH. In Equation 2.2 the metal is also corroded by the action of sulphides in the process stream. The aggressive nature of naphthenic acid corrosion is shown by Equation 2.3, where the sulphides in the crude oil stream in solution with the unstable iron naphthenate corrosion product of Equation 2.1 (which is highly soluble in oil) react to form more naphthenic acids. The local resultant TAN at the metal substrate is therefore much higher than the measured TAN of the crude oil. This results in the heavily pitted morphology which is characteristic of NAC, observed in the failure of one of the furnace outlet bends, Figure 2.2 (Xaba et al., 2015). Figure 2.2 also shows the combined effect of flow effects and NAC resulting in the scalloped surface profile of the steel.

$$Fe + 2RCOOH \Leftrightarrow Fe(RCOO)_2 + H_2 \qquad \text{(Equation 2.1)}$$

$$Fe + H_2S \Leftrightarrow FeS + H_2 \qquad \text{(Equation 2.2)}$$

$$Fe(RCOO)_2 + H_2S \Leftrightarrow FeS + 2RCOOH \qquad \text{(Equation 2.3)}$$

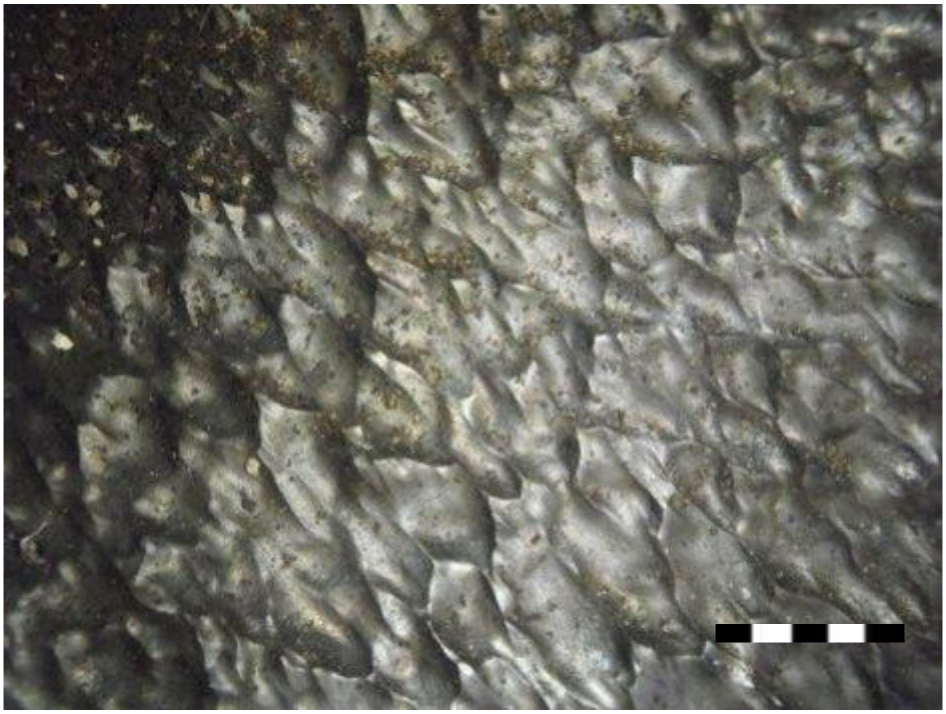

Figure 2.2: Internal pitting observed on vacuum distillation furnace tube bends (Xaba et al., 2015).

Dettman et al. (2009) found in laboratory experiments that there is a fourth equation that further complicates the corrosion theory presented above. Upon heating, the two carbon-sulphur bonds are broken creating two olefin hydrocarbon fragments and hydrogen sulphide. Once hydrogen sulphide is formed, it was observed to participate in the corrosion mechanisms outlined in Equations 2.2 and 2.3. The iron sulphide layer formed during high temperature sulphidation, which was once thought to be insoluble, may be dissolved by naphthenic acid (Groysman et al., 2005). The result is a self-perpetuating combined corrosion mechanism.

$$FeS + 2RCOOH \rightarrow Fe(RCOO)_2 + H_2S \qquad \text{(Equation 2.4)}$$

Due to the complex relationship between naphthenic acid and sulphidic corrosion, the Naphthenic acid corrosion index (NACI) has been proposed by Craig (1996) as a tool to potentially determine which of the two mechanisms is more dominant. It is expressed as the ratio of the corrosion rate to the weight of corrosion product. The underlying principle is that sulphidation produces an insoluble iron sulphide layer and the naphthenic acid corrosion product, iron naphthenate, is said to be oil soluble. NACI values above 10 are for naphthenic acid corrosion, and any values above 100 constitute a system with severe naphthenic acid corrosion. Kanukantla et al. (2009) also supported the notion that there was a threshold TAN value above which NAC becomes more dominant than HTS. Kane and Cayard [2002] demonstrated with hot oil flow loop (HOFL) tests that NAC attack is more prominent at higher TANs as well as higher fluid flow rates. Above 100fps, the effects of impingement attack were observed. This index is therefore not favoured, since the iron sulphide layer may be mechanically removed in systems with high flow velocities or turbulence.

2.4 Previous attempts at prediction and current practices

Although found to be overly conservative, the modified McConomy curves are still used in industry for HTS prediction. For NAC, some progress has been made in attempts at modelling corrosion rates; Craig (1996) developed a mathematical model for naphthenic acid corrosion that includes velocity effects and Qu et al. (2005) also investigated the flow effect of naphthenic acid corrosion using jet impingement. The latter discovered that depending on TAN concentration and the type of alloy used, the naphthenic acid corrosion rate can either increase linearly with velocity, or exhibit a velocity threshold, above which the corrosion rate sharply increases. Since in crude oil refining, HTS and NAC are active in the same systems within the same temperature ranges, it is of more value for operational distillation units to predict a combined HTS and NAC corrosion rate. The API 581 (2016) has tables designed for determining combined naphthenic and sulphidic corrosion rates which also attempt to account for flow effects by employing multiplying factor 5 when flow velocities exceed 30.48 m/s. The estimated corrosion rates on these tables is a function of material of construction, sulphur, TAN, and temperature. The flaw in the use of these tables is the absence of the sulphur species NAC inhibition phenomenon for medium sulphur levels.

Despite some of the developments made in mathematical modelling of NAC corrosion rates, the interaction between NAC and HTS is not well understood and is yet to be quantified by these means. A joint industry program (JIP) that was sponsored and lead by numerous major petroleum and engineering companies, generated considerable amounts of experimental research data on NAC and HTS (Kane & Chambers, 2011). These experimental data, along with historical corrosion rate data of operational units with known corrosion influencing parameters inputs, were used as the basis for the development of an empirical model. The model is commercially available for use by refiners, under the registered trademark "Predict Crude" ("Honeywell Process", 2018). Kane and Chambers (2011) used an experimental VGO set-up to assess the performance of the Predict Crude™ JIP model corrosion rates against API 581 and McConomy data as shown in Figure 2.3. Kane and Chambers found that Predict Crude™ had the best agreement with the experimental data for a wider range of materials. The graph shows the performance of materials with varying Cr alloying additions, as well as molybdenum content on the corrosion rates. Carbon steel has the highest corrosion rate and the corrosion rate decreases with increasing Cr alloying content, from 5% Cr to 9%, 13% and the 300 series stainless steels, with 18% Cr having the lowest corrosion rates. 317L SS, with the highest molybdenum content, has the lowest corrosion rate of all the stainless steels.

The carbon steel corrosion rates were over-predicted by both the McConomy curves and the API 581 prediction tables. API 581 prediction tables were mostly too conservative for all materials except 317L SS which had higher molybdenum content (3 wt%) than 316L SS (2 wt%). The 304L SS had the highest corrosion rate of the stainless steels as it has no molybdenum additions. The McConomy curves, however, under-predicted corrosion rates for all materials except the 300 series stainless steels (18 wt% Cr) as they did not account for the influence of naphthenic acid corrosion.

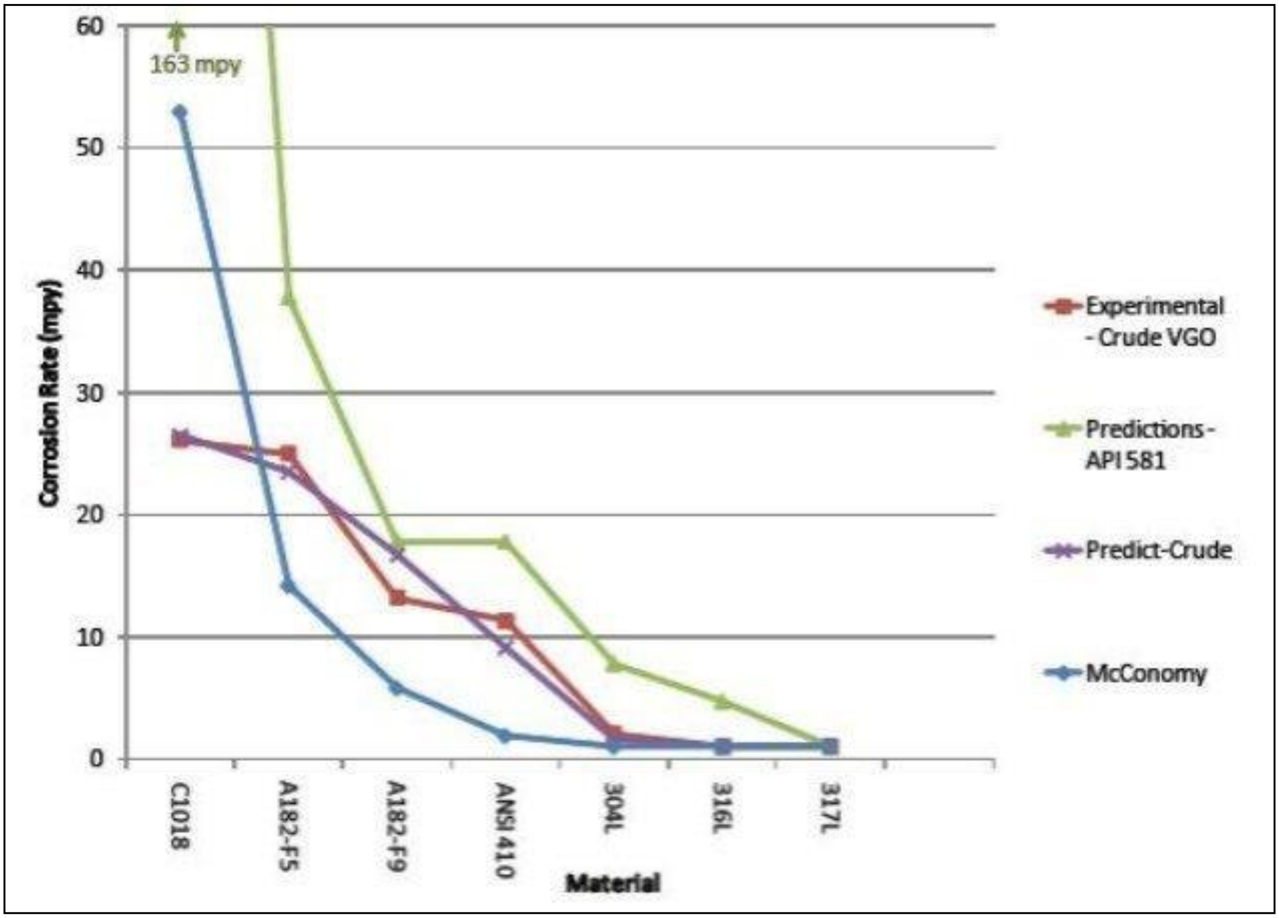

Figure 2.3: Comparison of laboratory corrosion rate data for VGO (TAN 3, 0.6wt%) and prediction methods from API 581, McConomy and Predict Crude^{TM} (Kane & Chambers, 2011).

As there are no mathematical means to calculate corrosion rates, the question remains: Can a model developed largely on experimental data accurately predict combined HTS and NAC corrosion rates on an industrial crude oil distillation unit in active operation?

For input to a corrosion model, TAN and sulphur data are among the parameters required and these may be acquired in one of two ways. The first option is by physical measurement of the crude oil blend and the distillation cuts' TAN and sulphur. The second method is by calculation/ modelling of these parameters. In the absence of measured data, modelling is possible if the crude oil blend constituents are known. There are numerous simulation packages commercially available for example, Aspen, Hysys, ProSim and Pro/II. These simulation software tools are typically used for process design, optimization, energy management and trouble shooting. Working steps like the correct selection of actual field efficiencies, choosing appropriate thermodynamic models, feed characterization and analysis of actual hydraulic behaviour, have a strong influence on the accuracy of the model's results. One of the most important factors in crude oil distillation simulation is the correct selection of thermodynamic model for the purpose of the model (Kolmetz, 2007). Doust et al. (2012) and Haydary & Pavlik (2009) recommended the use of the Braun K10 (BK10) thermodynamic model CDU modelling as it is suitable for mixtures of heavier hydrocarbons at pressures under 700 kPa and temperatures from 170°C to 430°C. Doust et al. (2012) continue to endorse BK10 primarily for modeling crude and vacuum columns operating near atmospheric or vacuum pressure.

2.5 Corrosion Measurements systems

In laboratory experiments, corrosion rates may be measured using several methodologies namely, polarization curves, electrochemical potential measurements, AC impedance and weight-loss measurement. In a practical crude oil refining environment, the interest in corrosion is based on the key goal of preventing loss of primary containment (LOPC) for environmental, as well as personal and process safety. It is also not feasible to use the before-mentioned techniques on systems that are still in use and are also intended for future use. Having wall thickness data on piping and equipment enables mechanical engineering design pressure containment calculations. For this reason, corrosion rates in industry are measured by wall thickness loss. To determine remaining wall thickness of piping and equipment following operational periods, two testing methods are mainly used, ultrasonic wall thickness (UT) and industrial profile radiography (RT).

2.5.1 Ultrasonic Wall Thickness Testing

Ultrasonic thickness testing deduces the wall thicknesses of pipes and vessels by measuring the total distance travelled by the ultrasonic pulses, which is represented by the distance from the initial pulse at the front surface to the reflection from the back surface (Bhowmick, 2011). Sound travels through metallic materials at known speeds which are used to calculate material thicknesses from the time taken to transmit and receive a backwall reflection from a transducer in contact with the surface of the metal being tested, as shown in Figure 2.4 (Spectro, 2010).

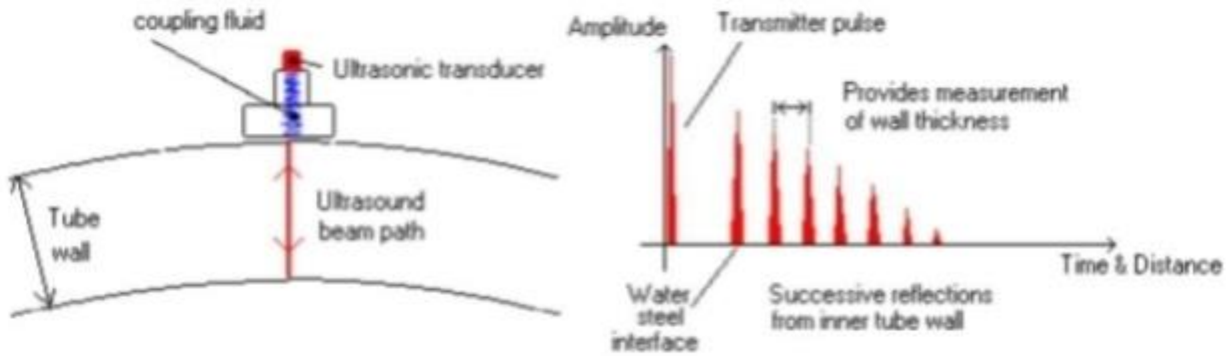

Figure 2.4: Principle of ultrasonic wall thickness testing with a contact transducer, with an A-scan representation of the readings displayed on the right (Spectro, 2010).

Schempp et al. (2016) analysed the results of continuous online ultrasonic wall thickness measurements taken on crude oil distillation units, and found that increasing surface roughness from a corroded surface reduced wall thickness measurements' accuracy. Although HTS in the absence of flow is considered a general wall loss corrosion mechanism and is normally monitored by spot UT wall thickness measurement techniques in industry, this approach is not suitable for the estimation of NAC. NAC leaves a rough surface and can also be localized and therefore easily missed by sampling inspection methods like spot UT.

In an ultrasonic C-scan presentation, the transducer scans the part and initially displays the A-scan in which radio frequency waveforms show the ultrasonic signals reflected from the component (Kumar et al. 2006). The A-scan images of the preset data points, which are then converted to a colour or grayscale image called a C-scan, which shows the variations in thickness of the component being tested. Separate C-scan images are produced which allow the component to be profiled through a top view, similar to a profile radiographic shot. The results of the scan are provided as an image, showing the sectional view of the component (Turcotte et al., 2016)

2.5.2 Profile Radiography

Profile radiography testing (RT) is also popularly used in industry to measure wall thickness of thinner walled piping and cylindrical components. The process of profile radiography in industry involves the use of a radioactive source (X-rays or gamma rays) penetrating through the workpiece being inspected and a detector film on the opposite side of the workpiece, as depicted in Figure 2.5 (Zscherpel et al., 2006). The detector film is usually a sheet of photographic film, held in a light-tight envelope or cassette having a very thin front surface that allows the X-rays to pass through easily. The process can be either wet or dry. For the "wet" process, chemicals are required to develop the radiographic image on the film. The dry process has been developed more recently and involves the use of computers; it is given the term digital or computer aided radiography.

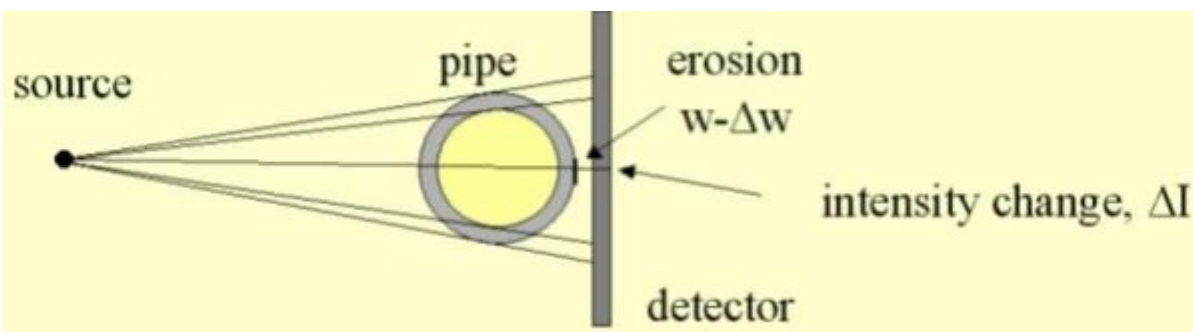

Figure 2.5: Double wall technique radiography (Zscherpel et al., 2006).

There are two methods for measuring wall thickness depending on the type of RT taken (Zscherpel et al., 2006). When the double wall technique (DWT) is used, the wall thickness measurement is based on the difference of radiation intensity. Due to the lower amount of material that radiation penetrates in the thinner wall sections, radiation intensity that reaches the film will be higher. When penetrating matter, radiation photons interact with matter which leads to absorption. Reduction of initial radiation intensity after penetrating through matter can be expressed by Beer's absorption law:

$$I_w = I_0 \, e^{-\mu w} \qquad \text{(Equation 2.5)}$$

where w = wall thickness, I_w = the radiation dose, I_0 = the radiation dose at w=0 and μ = the attenuation coefficient.

The second method used for wall thickness calculation is related to the tangential radiographic potential technique (TRT). With this technique, the magnification factor inherent to the test set-up is calculated (Cobanoglu and Altinsoy, 2014). This can be achieved in two ways; the first uses a comparator of known dimensions which is included in the radiographic shot to adjust the wall thickness measurement taken directly from the film/image. Alternatively, a correction on the evaluated wall thickness may be done if the dimensions of the geometrical testing set-up are known. The following correction can be applied; the true wall thickness (w) is:

$$w = \frac{f\, w' \cdot (f - R)}{R} \qquad \text{(Equation 2.6)}$$

where w' = the apparent wall thickness on the radiograph, R = the pipe radius (including insulation), f = source film distance (SFD).

3. PROJECT DESCRIPTION AND METHODOLOGY

Britannica reports that crude oil distillation and refining began in the 19th century and is somewhat well understood and applied (2018). Based on the theoretical understanding of the high temperature corrosion mechanisms, the areas of the atmospheric and distillation units that are susceptible to HTS and NAC were mapped out and divided into process loops. The modelling of the corrosion rates was based on the high temperature corrosion limit of 220°C, which is an accepted minimum temperature for active NAC to occur (Derungs, 1956). The project was divided into the steps detailed below, to ultimately perform a comparison of the modelled corrosion rates against the actual measured corrosion rates on the unit equipment and piping. In line with the objective of testing the suitability of an empirical industry model on an operational crude distillation process unit, the methodology was structured to suit the application of the research results.

3.1 Corrosion Process Loop Definition

Corrosion process loops were set mainly by the crude assay distillation curves, and they were further defined by either a change in processing step, medium and/or materials of construction. In the atmospheric distillation unit, the crude oil is heated first by convection in the feed preheat exchanger train, which is the first corrosion process loop starting where the minimum temperature of 220°C is exceeded. The next corrosion process loop is the furnace coil. The coils are divided into two main areas, namely the convection bank and radiant heater. The hot, partially vaporized crude oil is sent to the distillation column. The transfer piping to the column is defined as a separate corrosion process loop from the furnace coils, since the coils are also subject to oxidation on their external surface, as well as internal coking and creep degradation. In the distillation column, the crude oil is distilled into products that are also each defined as separate corrosion process loops.

3.2 Pro/II Modelling

Pro/II is a steady state process engineering simulation software licensed to and marketed by Invensys. It is designed to perform rigorous heat and material balance calculations for a wide range of chemical processes. The process simulation tool has capability extending from oil refining to chemicals production and pharmaceuticals applications. It has a variety of thermodynamic models and with access to thousands of crude assay data, the application is able to model crude column distillation of desired crude oil blends (Schneider Electric, 2018). The SAPREF oil refinery already uses and has extensive experience with Pro/II simulation software for process planning and optimization; for this reason, Pro/II was also used in this study to determine the crude blends' properties. The inputs to the Pro/II model were the crude blend constituents and ratios of mixing. The crude assay data may also be loaded into the model where it has been updated or does not already feature in the software databank. The results of the simulation in Pro/II were the product yields, an estimation of the TAN and sulphur for each distillation cut and the temperatures at which they would distill. The process loops under consideration were modelled with Pro/II Simulation software to determine the TAN and sulphur concentrations at each point in the distillation process where NAC and HTS may occur.

Crude oil properties such as TAN and sulphur are linearly additive and have additivity of mass. It is assumed that P_{mix} is the blended property, P_i is the property of i^{th} crude oil, and R_i is the mass fraction of the i^{th} selected crude oil (Huihua et al., 2014). With respect to the properties of mass additivity, Equation 3.1 can be used to calculate P_{mix}:

$$P_{mix} = \Sigma_{i=1}^{n} R_i P_i \qquad \text{(Equation 3.1)}$$

The simulation software package Pro/II is able to perform these calculations using preloaded crude assay data and thermodynamic theory to determine the crude oil blend product yields and the properties of the produced cuts. The software uses various thermodynamic models, for this simulation of the crude oil atmospheric and vacuum distillation, the BK10 equations of state were used in the atmospheric and vacuum distillation towers simulation.

The refinery alters its crude blend every week to two weeks, but the diet is determined by the desired product yields emanating from industry-related demands. In addition to this, the crude blend had changed considerably since the commissioning of the plant, and the resultant crude feed properties that affected corrosion, including the operational temperatures, were adjusted over time. For this reason, three sets of corrosion modelled data were created for this assessment. The first selected model case was 0.35 TAN, which was the original design basis for the unit. It should be noted that in reality, the TAN may have been much lower than the modelled crude blend and the blend used in the assessment would have contained much more PG and less WAF and other opportunity crudes. A 0.5 TAN case was also assessed, which is more representative of the current operational TAN limit, and the blend was selected such that the current required product yields could be met. Finally, a 0.8 TAN case was modelled to represent upset conditions, namely cases where unexpected crude diets were processed and the risk of crude layering and insufficient mixing of crudes with different densities resulted in running crudes of slightly higher TAN than expected.

3.3 Corrosion Modelling

The Predict Crude^{TM} corrosion modeling software that was used produces a corrosion rate from the Joint Industry Project (JIP) database for a material in any given process conditions (“Honeywell Process”, 2018). The JIP corrosion rate is inter- or extrapolated from the JIP experimental and shared corrosion rates database. Predict Crude^{TM} was selected as the most accurate known commercially available model that may be used by operating units.

The following input data were required for the calculation of corrosion rates by the Predict Crude^{TM} model:

- the materials of construction of the equipment or piping components
- the operational temperature of the process medium
- the flow regime, i.e. fully liquid or two-phase flow
- TAN and sulphur of the process medium.

The equipment general arrangement drawings, design data books and/or material certificates of equipment and piping assessed in the model were referenced for confirmation of the materials of construction. The process temperatures used for the modelling were extracted from the online process measurement system. These historical process temperatures were averaged over the operational history of the equipment to avoid using temperature excursions from operational upsets as input for the corrosion model. The TAN and sulphur results of the Pro/II model were used as inputs for the corrosion model in the absence of physical process measurement data. This resulted in three sets of predicted corrosion rates (for 0.35 TAN, 0.5 TAN and 0.8 TAN) for the distillation units based on each crude diet's properties.

3.3.1 Exclusions

The following elements were excluded from the corrosion models:

g. It is possible for certain areas to have had localised high TAN concentrations due to boiling and condensation effects, which could result in higher naphthenic acid corrosion rates in those areas. The model did not include these effects.

h. Further limitations included wall shear stresses which are not accounted for, which would also require geometric modelling of the plant, which as not practical for an operational unit.

i. The model was limited in its prediction of corrosion rates, as it did not differentiate between active and total sulphur content in the process stream. The model also did not use actual TAN and sulphur for corrosion rate estimation for the crude fractions, since these measurements could not be taken, because of the lack of sample points.

j. Temperature excursions from operational upsets were excluded from model (corrosion can be higher during these periods: start-up/shutdown etc.) To include these effects, an integrated corrosion model would have needed to have been set up for each operational temperature and the duration thereof, to arrive at a closer estimate of actual corrosion rates. This analysis was excluded from the assessment as this could not be done in the normal operation of a plant.

3.4 Corrosion Rate Measurement and Inspection History Review

Measurement of corrosion rates in an active running plant poses a challenge and cannot be measured using typical laboratory set-ups and equipment (Kane et al., 2002). The piping and equipment may be inaccessible and measurements whilst the plant is online are not regular practice for health, safety, security, environment (HSSE) concerns. The result is that measurements are taken at long intervals of up to years, and specific process conditions cannot be correlated with changes in corrosion rates. In this project, historical corrosion rates were assessed in a holistic way, including elements of location of corrosion, morphology and profile thereof and the measured pits and/or wall thicknesses. Furthermore, Piehl (1988) has shown that it is not possible to associate a set TAN value with a corrosion rate, thus corrosion rates in this project are therefore being presented qualitatively.

3.4.1 Historical Corrosion Rate Determination

The inspection history was reviewed to determine the actual corrosion rating for comparison against the modelled data. The modelled output data were classified in terms of corrosion rate (CR) ranges set at: Low (L), Medium (M) and High (H). Wall thickness measurements from radiographic and ultrasonic testing methods were collected, and the history of visual inspections, leaks and major findings or equipment and piping replacements were also taken into consideration. Since the material wastage expected from NAC and HTS was at localized areas, it was not practical to measure actual corrosion rates as calculated by the model for a system that was actively in use, where components could be readily removed and measured for mass loss.

The various types of corrosion data were weighted to provide a qualitative corrosion rate of Low, Medium or High that could be compared with the modelled results. The numerical measured corrosion rate data for the equipment and piping are confidential and cannot be published for commercial reasons. In Appendix 3, equipment history summaries for the major equipment, which were compiled from historical inspection reports, are presented.

In pressure equipment design practice, the effects of the expected corrosion losses are typically catered for by corrosion allowances, which are added to the thickness of the element calculated in static analyses (Krivy, 2012). In assessing corrosion rates, the desired design life of equipment and piping is considered. From the concept of a desired design life, a design corrosion rate is calculated for each equipment component and piping. A design corrosion rate (CR_d) is defined as the corrosion rate it would take to consume the corrosion allowance as per design within the desired design life, expressed in Equation 3.2 as follows:

$$CR_d = \frac{\text{Corrosion allowance (mm)}}{\text{Design life (years)}} \qquad \text{(Equation 3.2)}$$

In cases where failures had been historically recorded before the design life of the component was fulfilled, the corrosion rate was taken as high. The corrosion rate levels reported from the modelled corrosion data were in ranges and were compared to the measured corrosion rates and reported inspection history, as per Table 3.1.

Table 3.1: Corrosion rate range definition.

Corrosion Rate Range	**Model Corrosion Rate**	**Characteristics of Inspection History**
Low (L)	$CR_m < 0.5CR_d$	Minimal corrosion was observed from inspections
Medium (M)	$0.5CR_d \leq CR_m \leq CR_d$	Corrosion rates were within design expectations and predictable
High (H)	$CR_m > CR_d$	Failures/ leaks, replacements within design life. Measured corrosion rate above design conditions.

CR_m ≡ measured corrosion rate; CR_d ≡ design corrosion rate

Since measurements in the plant have a certain degree of uncertainty, due to the difficulty in obtaining repeatable results and calibration of measurements, surface conditions, and the range in competence of technicians taking the measurements, a procedure was developed to extend or reduce the measured corrosion rate range based on the measurement technique used and the confidence level in the measurement. Figure 3.1 presents the decision tree developed to define the corrosion rate range based on operational history review and the measured corrosion rates, including consideration for the measurement technique used. As NAC is very localized, credit was given for visual inspection or profile radiography for detection of corrosion prior to measurement of remaining wall thickness either by UT scan methods. Measurements of wall thickness without prescreening for locations of corrosion were considered invalid, and all measurements had to meet the criteria of:

- pre-screening with visual or profile radiography, and
- measurement of wall thickness using UT (grid) scan or C-scanning.

Inspection of areas with High and Medium predicted corrosion rates (CR) according to the 0.5 TAN case were prioritized over those of Low CR equipment and piping. The Low predicted CR areas (according to the 0.5 TAN case model) were not re-inspected unless these had never been measured before, due to limited budget and resources. For this reason, where there was already a measured CR on predicted Low CR equipment and piping, no new measurements were requested even if the measurement technique(s) did not meet the prescribed measurement criteria of the project.

There was a maintenance event in May 2015 during which the distillation units were shut down for inspection and maintenance activities. It was during this event that corrosion rate measurements were taken. Prior to that, measurements were taken in 2011. All modelled corrosion rates were compared to data extending up to and including April 2015.

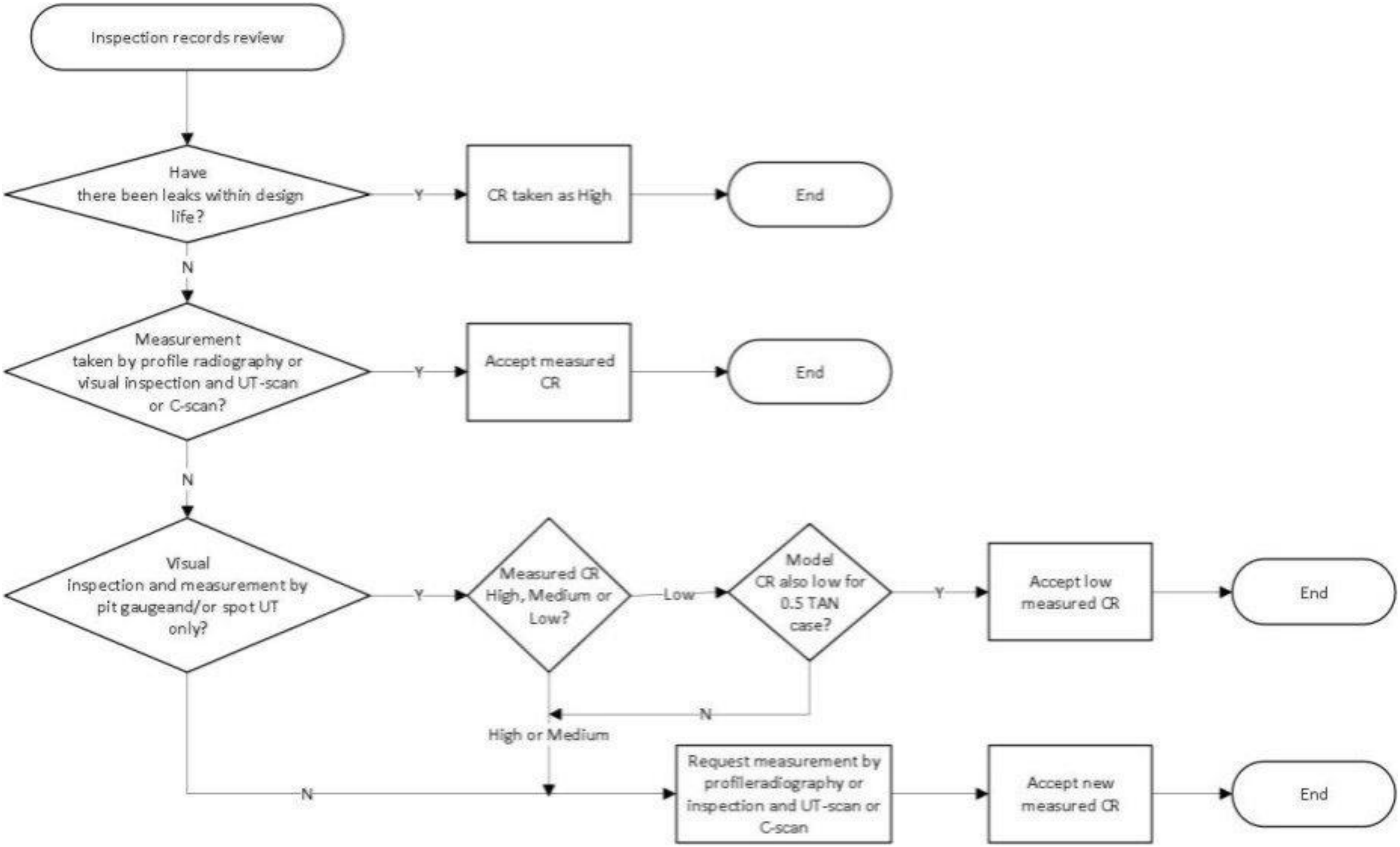

Figure 3.1: Corrosion rate estimation flowchart.

It should be noted that the 0.8 TAN case model data were not compared to the measured corrosion rates and inspection history as 0.8 TAN crude blends have not been processed on the distillation units. The 0.8 TAN model case data were analysed against the measured corrosion rates that exceeded the 0.5 TAN case data. Since the crude blends processed consist of crudes with varying individual TANs and densities, in the event of improper mixing or blending, it may be possible that the units' equipment and piping were exposed to higher or lower TANs than those of the blends.

4. RESULTS

With an increase in crude oil prices, SAPREF sought after more opportunity crude oils to try maintain the GRM. From the years 2005 to 2014, the refinery implemented a gradual change in crude diet; there was a transition from a predominantly Persian Gulf (PG) diet, from 80% at commissioning of the plant, up until 28% in 2014. More West African crudes (WAF) were incorporated into the crude oil diet of the plant, as shown in Figure 4.1.

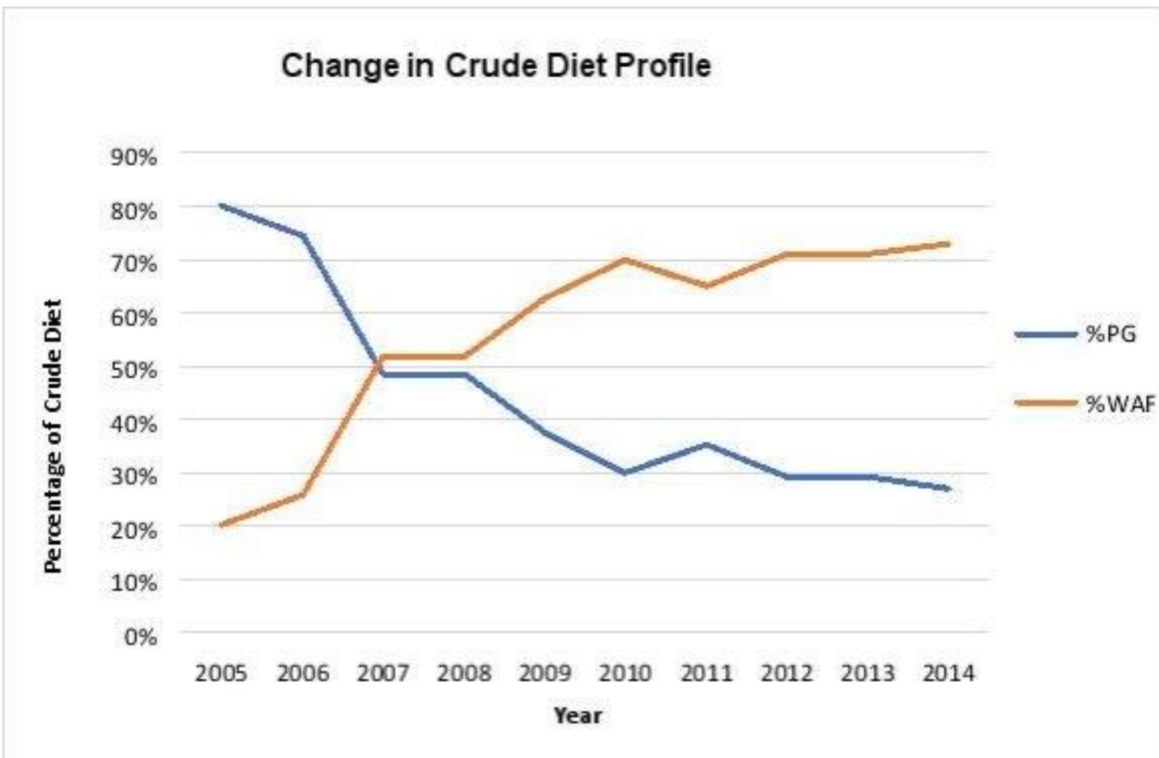

Figure 4.1: Transition of crude oil diet from mainly PG to WAF.

Figure 4.2 shows the measured processed crude TAN and sulphur values from 2005 to 2011. There was a steady decline in sulphur during this period in combination with a slight increase in TAN over the same period. No measurements were taken in the period from January 2011 to June 2013. In Figure 4.3, the TAN and sulphur measurements are presented for the period June 2013 to July 2014. By July 2014, the minimum measured sulphur was as low as 0.32wt% and the TAN measurements reached a maximum of 0.57, with sporadic high measurements up to 0.92, having started at 0.1 in March 2005 when measurements were first taken. The Pro/II model for each case was run on the crude oil composition shown in Table 4.1; the 0.35 TAN case consisted of 58% WAF, 0.5 TAN was 61% WAF and the 0.8 TAN case was 82% WAF. There were no recorded crude blend TAN and sulphur measurements between July 2014 and May 2015.

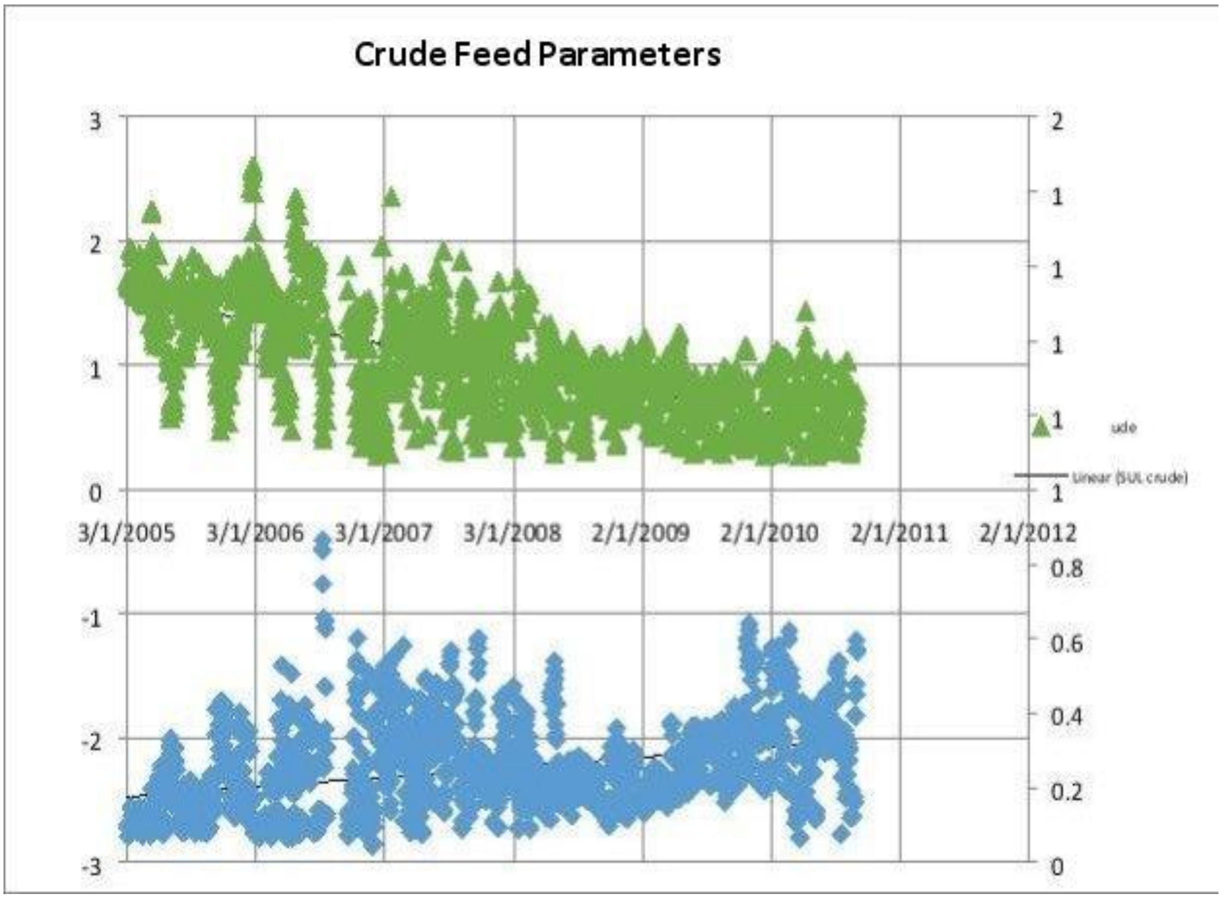

Figure 4.2: Crude feed measured TAN and sulphur (March 2005 to January 2011).

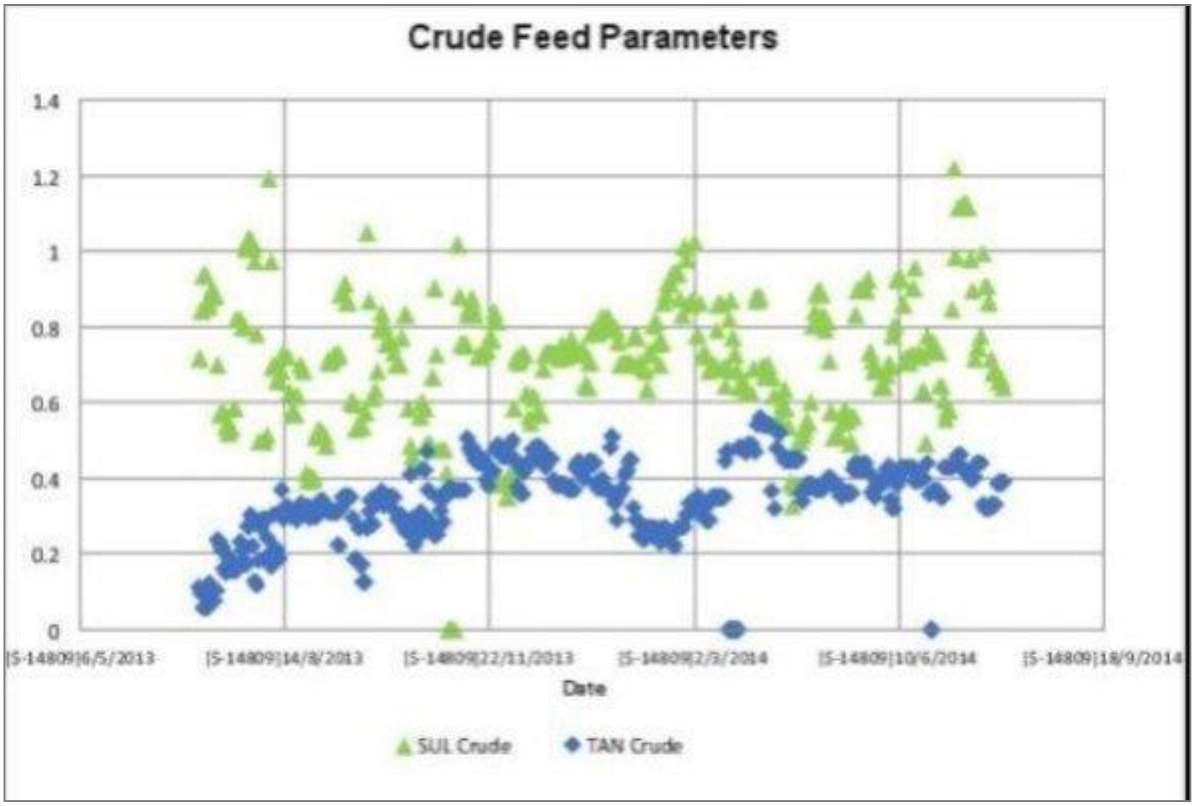

Figure 4.3: Crude feed measured TAN and sulphur (June 2013 to July 2014).

Table 4.1: Model cases crude mixes.

No.	Type/ Location	Crude	TAN 0.35 Mix Ratio	TAN 0.5 Mix Ratio	TAN 0.8 Mix Ratio
1	WAF	WAF1	0.09	0.05	-
2	PG	PG1	-	0.08	-
3	PG	PG2	-	-	0.01
4	WAF	WAF2	0.14	0.07	-
5	PG	PG3	0.08	0.04	-
6	WAF	WAF3	-	0.09	-
7	WAF	WAF4	-	0.03	-
8	WAF	WAF5	0.08	0.04	0.56
9	PG	PG4	0.14	0.07	-
10	PG	PG5	0.08	0.07	0.09
11	WAF	WAF6	0.13	0.2	-
12	PG	PG6	0.14	0.07	-
13	WAF	WAF7	-	0.05	0.26
14	WAF	WAF8	0.14	0.08	-
15	PG	PG7	-	0.06	0.07
16	PG	PG8	-	-	0.01
%WAF			58	61	82
%PG			42	39	18
			1.00	1.00	1.00

4.1 Corrosion Process Loop Definition

The process flow description of the distillation units was used to divide the units into corrosion process loops. Blended crude oil feed from the tank farm was preheated in a series of shell and tube exchangers and washed in a desalter to eliminate geological debris prior to entering the lower temperature convection bank of the crude oil heater at ~250°C. In the convection bank of the fired heater, the warm crude oil passing through the coils was heated by hot flue gas coming from the radiant section of the heater to ~300°C, before passing through the radiant section where the crude was heated to ~360°C.

The heated crude oil was transferred to the first distillation column which works under atmospheric pressure. Here the product's long residue, heavy gasoil, light gasoil and kerosene are distilled out at decreasing temperatures. Kerosene distilled below 220°C and was therefore not included in the high temperature corrosion assessment.

Long residue was lined to the vacuum distillation unit. It was preheated in the vacuum furnace up to 410°C before distillation in the vacuum column. The product's short residue, dirty washoil, heavy waxy and light waxy were separated out at decreasing temperatures in the column. Vacuum gasoil distilled below 220°C, and was therefore not included in the high temperature corrosion assessment.

Using the process flow description above, the corrosion process loops were divided as per Table 4.2.

Table 4.2: Corrosion process loops.

Corrosion Process Loop Name	Basis	Equipment
Hot Desalted Crude	HTS, NAC	E7108A-H CH, E7136 CH, E7701A/B CH, E7714 CH, E7715 CH
Atmospheric Furnace	HTS, NAC, Coking, Creep, Oxidation, Metal Dusting	F7101A, F7101B, F7101C
Atmospheric Transfer Lines	HTS, NAC	
Light gasoil (LGO)	HTS, NAC	C7101, C7103, E7104 SH
Heavy gasoil (HGO)	HTS, NAC	C7101, C7102, V7107, E7110A/B SH, E7109A/B SH, E7135 SH
Long residue (LR)	HTS, NAC	C7101
Vacuum Furnace	HTS, NAC, Coking, Creep, Oxidation	F7701B, F7701A
Vacuum Transfer Lines	HTS, NAC	
Light waxy distillate (LWD)	HTS, NAC	C7701, V7703, E7708A/B SH
Heavy waxy distillate (HWD)	HTS, NAC	C7701, V7702, E7206 CH, E7108A-H SH, E7102C/D SH, S7710A/B
Dirty washoil (DWO)	HTS, NAC	C7701, V7712, E7714 SH, E7702A/B SH
Short residue (SR)	HTS, NAC	C7701, E7715 SH, E7701A/B SH, E7711A/B, E7102A/B SH, S7711

SH ≡ shell, CH ≡ channel

4.2 Sulphur and TAN Distributions

4.2.1 Atmospheric Distillation Sulphur and TAN Distributions

In Figure 4.4 the distribution of sulphur for the atmospheric distillation of the three modelled cases is presented. Sulphur concentrated in the heaviest cuts in all cases, with concentrations reducing from long residue to heavy gasoil and light gasoil. The 0.8 TAN case had the lowest overall sulphur concentration, as well as the lowest concentration in all cuts. The behaviour of the organic acid distribution differed as shown in Figure 4.5; for the 0.35 TAN and 0.5 TAN cases the concentration of gases reduced with the heavier cuts. The 0.8 TAN case differed from the other two cases and showed a peak of organic acids in the heavy gasoil cut.

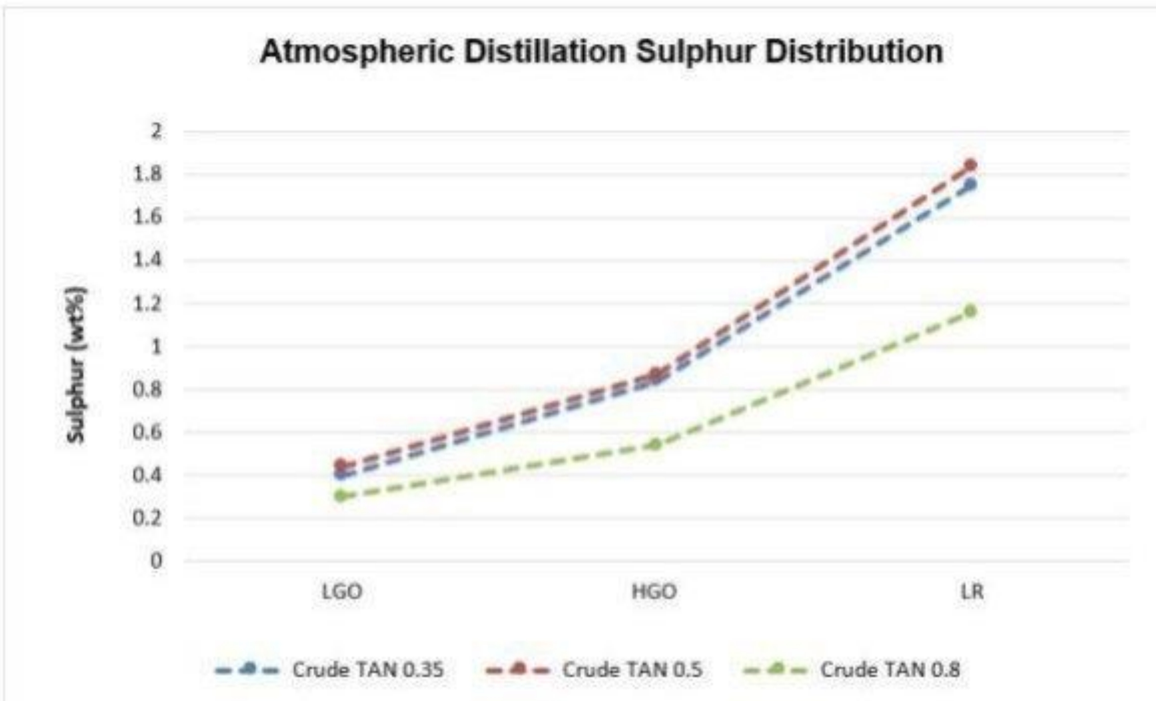

Figure 4.4: Crude feed measured TAN and sulphur (June 2013 to July 2014).

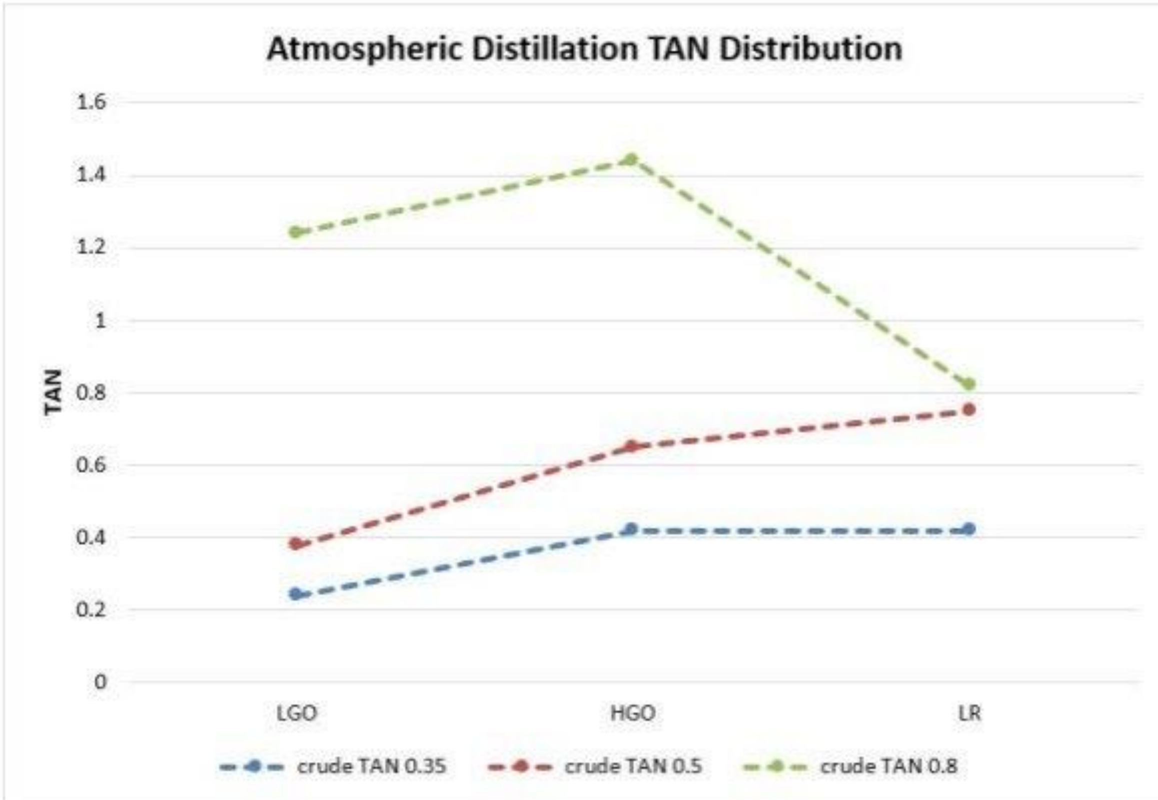

Figure 4.5: TAN distribution in atmospheric distillation cuts for the three modelled cases.

4.2.2 Vacuum Distillation Sulphur and TAN Distributions

Figure 4.6 presents the distribution of sulphur for the vacuum distillation of the three modelled cases. Sulphur concentration increased in the heavier cuts in the 0.35 and 0.5 TAN cases. The 0.8 TAN case had the lowest sulphur concentrations in all cuts. The behaviour of the organic acid distribution differed from the atmospheric distillation distribution as shown in Figure 4.7; the lightest distillate had the highest amount of organic acids and it reduced as the cuts were heavier. The distribution of organic acids for the 0.35 and 0.5 TAN cases behaved similarly to the atmospheric distillation curves in Figure 4.5.

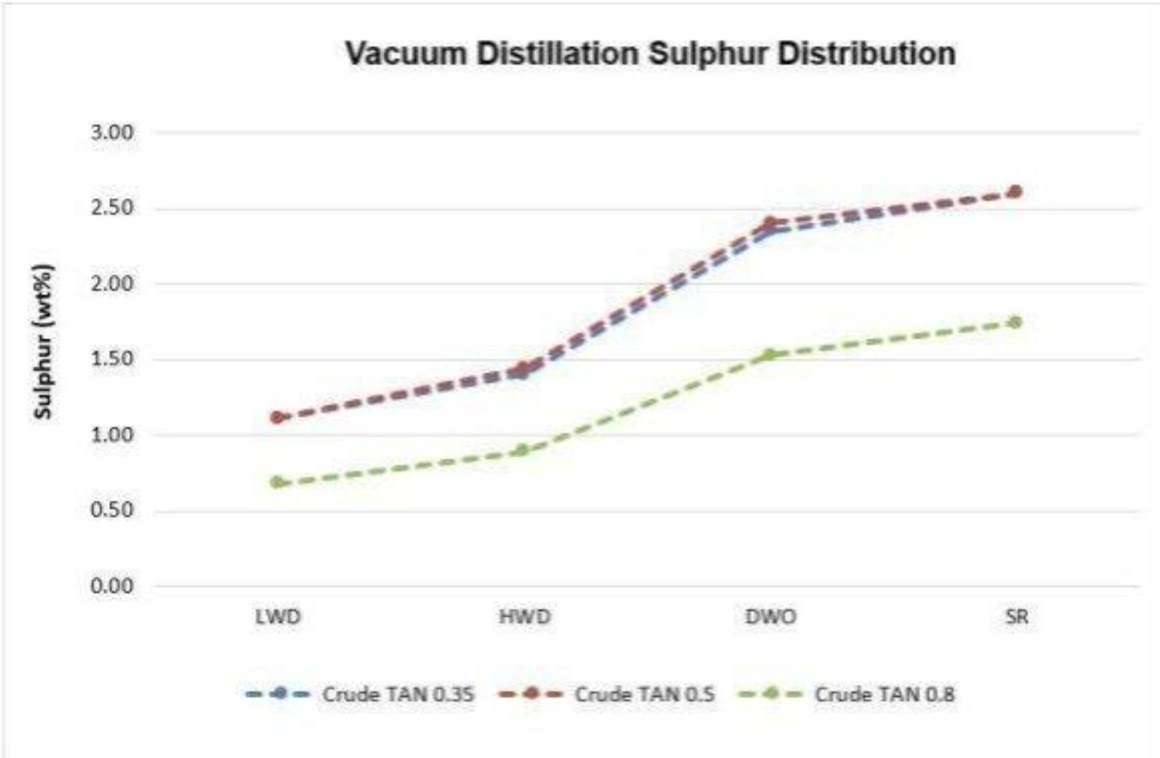

Figure 4.6: Sulphur distribution in vacuum distillation cuts for the three modelled cases.

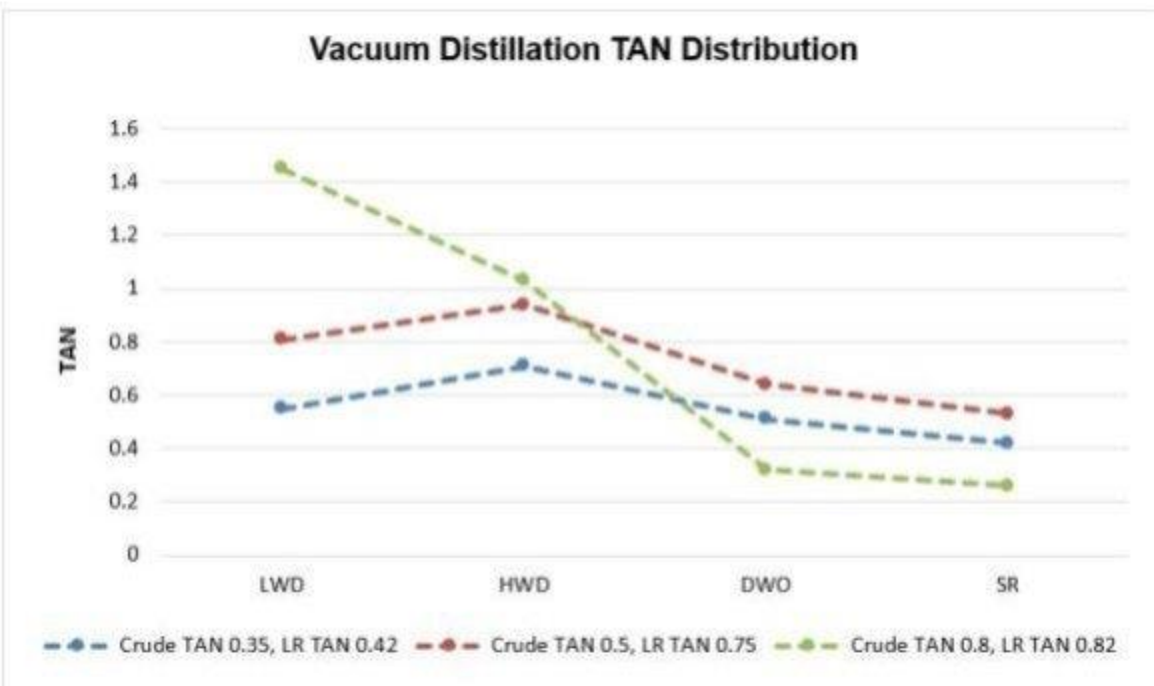

Figure 4.7: TAN distribution in vacuum distillation cuts for the three modelled cases.

4.3 Corrosion Rates Results

4.3.1 Atmospheric Distillation Modelled Corrosion Rates Profile

In Figure 4.8, a schematic representation of the plant is shown with colour coding for low, medium and high modelled corrosion result areas for the 0.35 TAN case. Figure 4.9 shows the representation of the 0.5 TAN case modelled results. The TAN and sulphur data points from the Pro II model of process constituents were used in the corrosion model. The outcome showed low corrosion rates in the hot desalted crude loop, i.e. all components upstream the crude heater. The corrosion rates increased from low to medium in the convection bank of the furnace coil where the crude oil was still in the liquid phase, remaining at medium then increasing to high in the radiant section of the heater, as the temperatures of the tubes, i.e. crude, increased. The corrosion rates for the two-phase crude oil, in the transfer lines from the radiant heater to the atmospheric distillation column, were medium in the 0.35 TAN case, but high for the 0.5 TAN case. The transfer line corrosion rates modelled as low in both TAN cases where the piping was clad with 316 SS. Similarly, inside the crude distillation column, the corrosion rates were rated low in the bottom section where there was 405 SS internal lining. The HGO section pipelines and equipment were mainly of carbon steel construction, and all rated medium, but components below 280°C rated low. The LGO equipment and piping were also carbon steel construction materials, and rated low. The long residue lines and equipment were all 5Cr0.5Mo material and rated medium for 0.35 TAN and high for 0.5 TAN according to the model. Table 4.3 shows the output of the 0.35 and 0.5 TAN corrosion models and the actual corrosion rates observed on the unit.

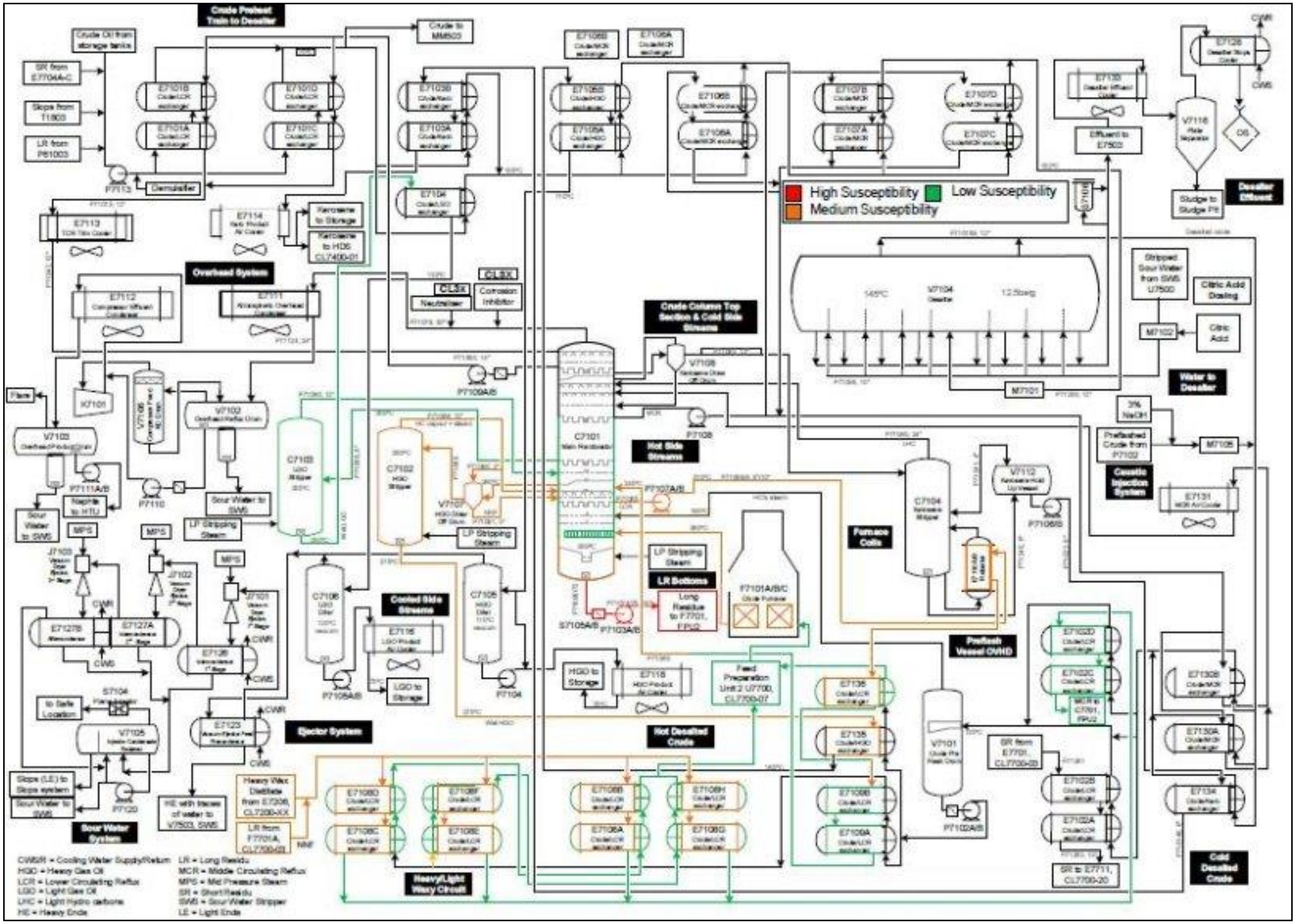

Figure 4.8: Atmospheric distillation unit corrosion map for 0.35 TAN model case.

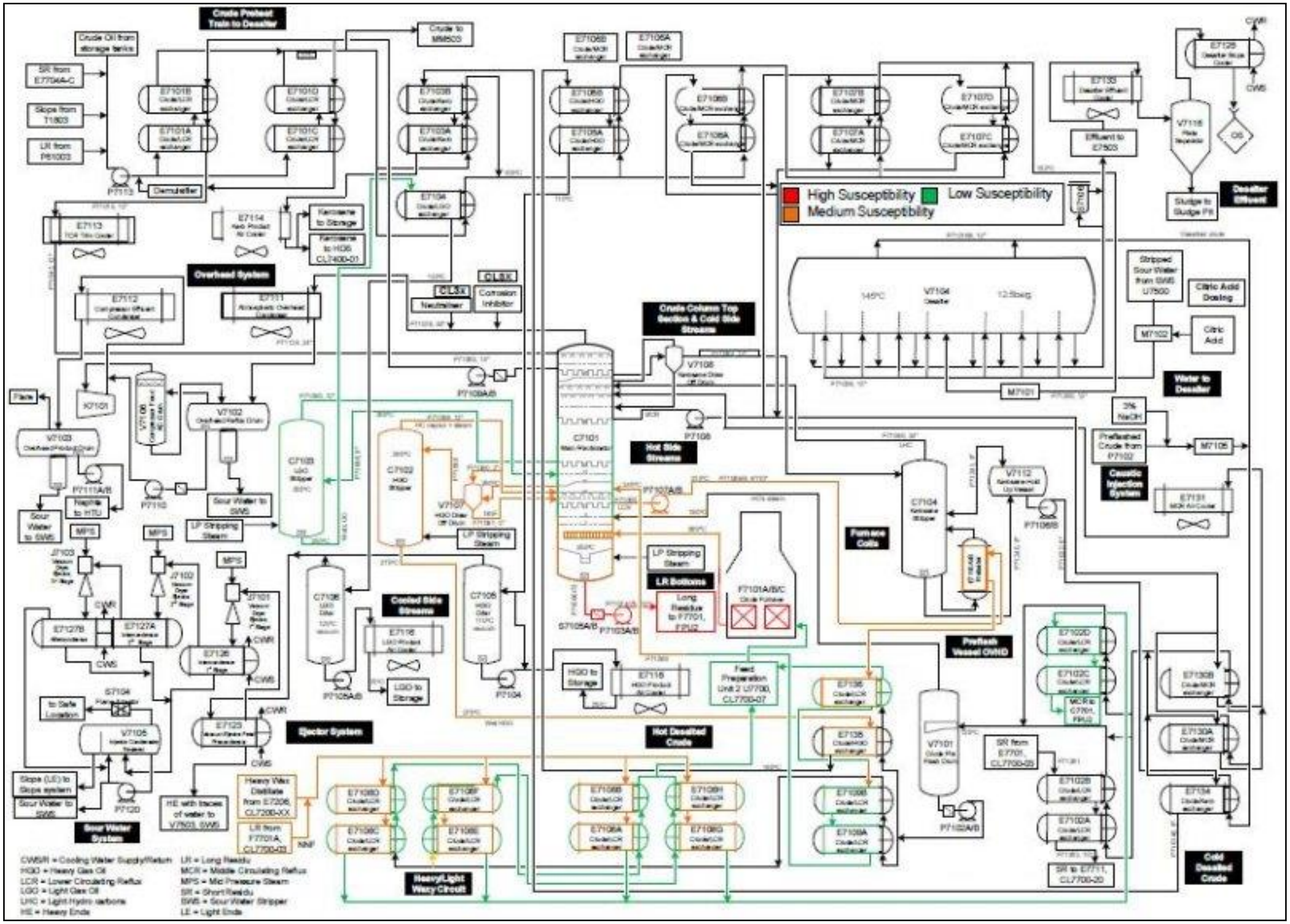

Figure 4.9: Atmospheric distillation unit corrosion map for 0.5 TAN model case.

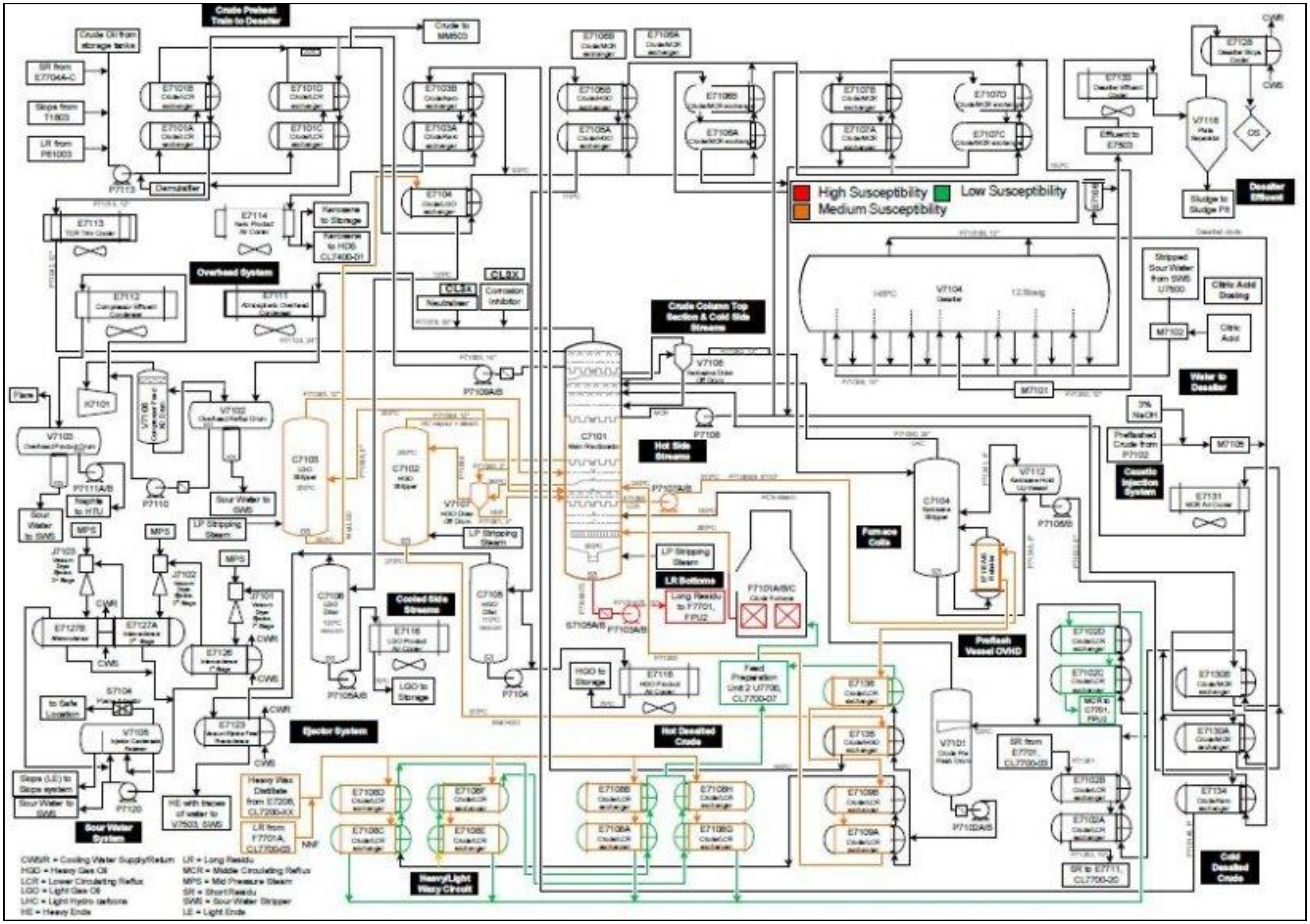

Figure 4.10: Atmospheric distillation unit corrosion map for 0.8 TAN model case.

Table 4.3: Comparison of model and Actual Corrosion Rate (CR) Results for Atmospheric Distillation Circuits.

Corrosion Process Loop	**Material**	**Max Temp (°C)**	**Flow**	**Model CR (TAN 0.35)**	**Model CR (TAN 0.5)**	**Actual CR**	**Model CR (TAN 0.8)**
Hot desalted crude	Carbon steel	260	liquid	L	L	L-M	L-M
Furnace Coil	5 Cr 0.5Mo	360	2 phase	M-H	M-H	M-H	M-H
Transfer Lines	5Cr0.5Mo	360	2 phase	L-M	L-H	H	H
Long Residue	5Cr0.5Mo	350	liquid	M	M-H	M	M-H
Heavy Gasoil	Carbon steel	315	liquid	L-M	M	H	M-H
Light Gasoil	Carbon steel	255	liquid	L	L	L	M

L=Low, M=Medium, H=High

4.3.2 Atmospheric Distillation Actual Corrosion Rates History

There have been numerous leak incidents and corrosion findings in the atmospheric furnace radiant coils as well as on the convection bank, although the convection bank incidents were attributed to localized overheating (due to coking) and/or creep ruptures not wall thinning phenomena. There was a leak on the HGO section of the distillation column in 1998, and as a result, the internal 405 SS cladding height was increased to above the HGO section. The light gasoil corrosion process loop reported low corrosion rates, the same as the modelled corrosion outputs. A brief summary of the major corrosion equipment and piping failure events and replacements is presented in Table 4.4.

Table 4.4: Atmospheric distillation major corrosion events.

Year	Major Failure/ Repair Event	Corrosion Process Loop
1976	Units commissioned.	
1992	F7101C Tube leak from localized overheating	Furnace Coils - convection
1992	Crude furnace radiant section carbon steel tubes replaced with 5Cr0.5Mo due to series of leaks in the preceding years 1986, 1988, 1989.	Furnace Coils - radiant
1992	F7101C Shock tube leak due to localized overheating.	Furnace Coils - convection
1996	F7101C Tube leak from localized overheating.	Furnace Coils - convection
1998	Distillation column C7101 HGO Section Perforation reported.	HGO
1998	F7101C Tube leak from localized overheating.	Furnace Coils - convection
1999	Crude preheat exchanger E7714A and B replaced with full stainless steel exchanger due to high HTS corrosion rates. No wall loss measured or corrosion issues reported since material upgrade. Last inspected in 2011.	Hot desalted crude
2010	F7101C Tube leaks from creep damage.	Furnace Coils - convection
2011	Pipeline renewed.	HGO
2009	Crude preheat exchanger E7701B Bundle retubed following high measured wall losses, commissioned 1976. Up to 40% wall loss measured in 2015.	Hot desalted crude
2012	F7101C Finned tube leak due to localized overheating	Furnace Coils - convection
2013	Leak and fire in November 2013 due to NAC on bend of transfer pipeline from F7101A furnace to column. Pipelines inspected in 2015 with numerous findings and renewals of pipelines.	Transfer lines
2013	F7101C Tubes replaced.	Furnace Coils - convection
2014	F7101A 5CR0.5Mo Tube leaked due to NAC damage	Furnace Coils - radiant
2015	Preheat exchanger E7701A Bundle retubed following recommendation from 2011 with high measured wall loss (commissioned 1976).	Hot desalted crude
2015	F7101A/B 5CR0.5Mo Tubes with severe NAC replaced.	Furnace Coils - radiant

4.3.3 Vacuum Distillation Modelled Corrosion Rates Profile

In Figure 4.10 a schematic representation of the plant is shown with colour coding for low, medium and high modelled corrosion result areas for the 0.35 TAN case. Figure 4.11 shows the representation of the 0.5 TAN case modelled results. The TAN and sulphur data points from the Pro/II model of process constituents were used in the corrosion model. In the long residue feed corrosion process loop, the corrosion rates modelled were medium in both the 0.35 and 0.5 TAN cases. The corrosion rates increased from medium to high in the convection bank of the furnace coil, as well as for the entire radiant section of the heater. The corrosion rates for the two-phase crude oil in the transfer lines, from the radiant heater to the atmospheric distillation column, were high in both modelled cases. Corrosion rates in the bottom section of the vacuum distillation column were medium. The hot short residue system, made of 5Cr0.5Mo materials was rated medium. The dirty washoil corrosion process loop in 316 SS was rated low. Corrosion rates increased to medium in the heavy and low waxy distillate corrosion process loops, which were both constructed of carbon steel materials. Table 4.5 shows the output of the corrosion model and the actual corrosion rates observed on the unit.

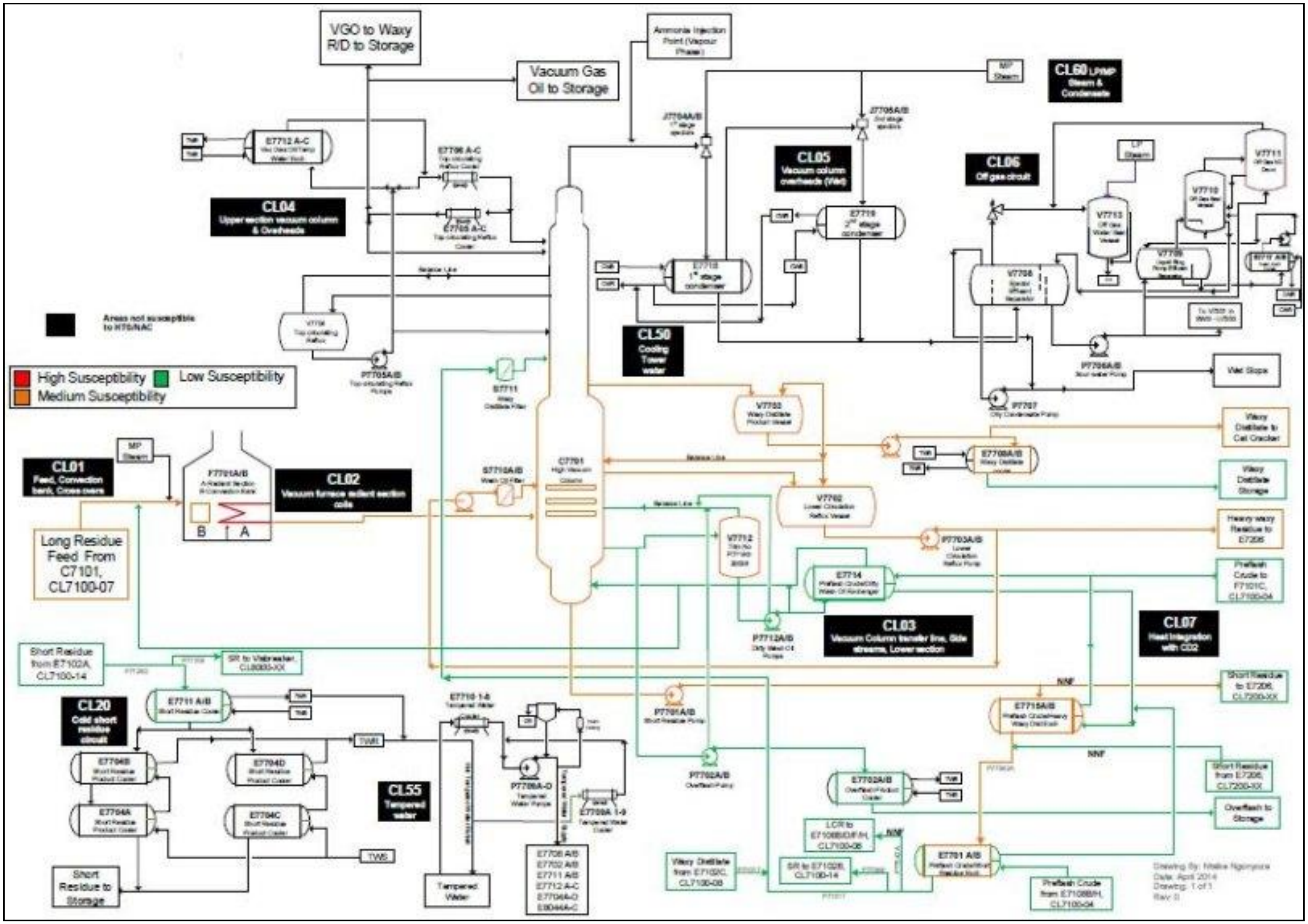

Figure 4.11: Vacuum distillation unit corrosion map for 0.35 TAN model case.

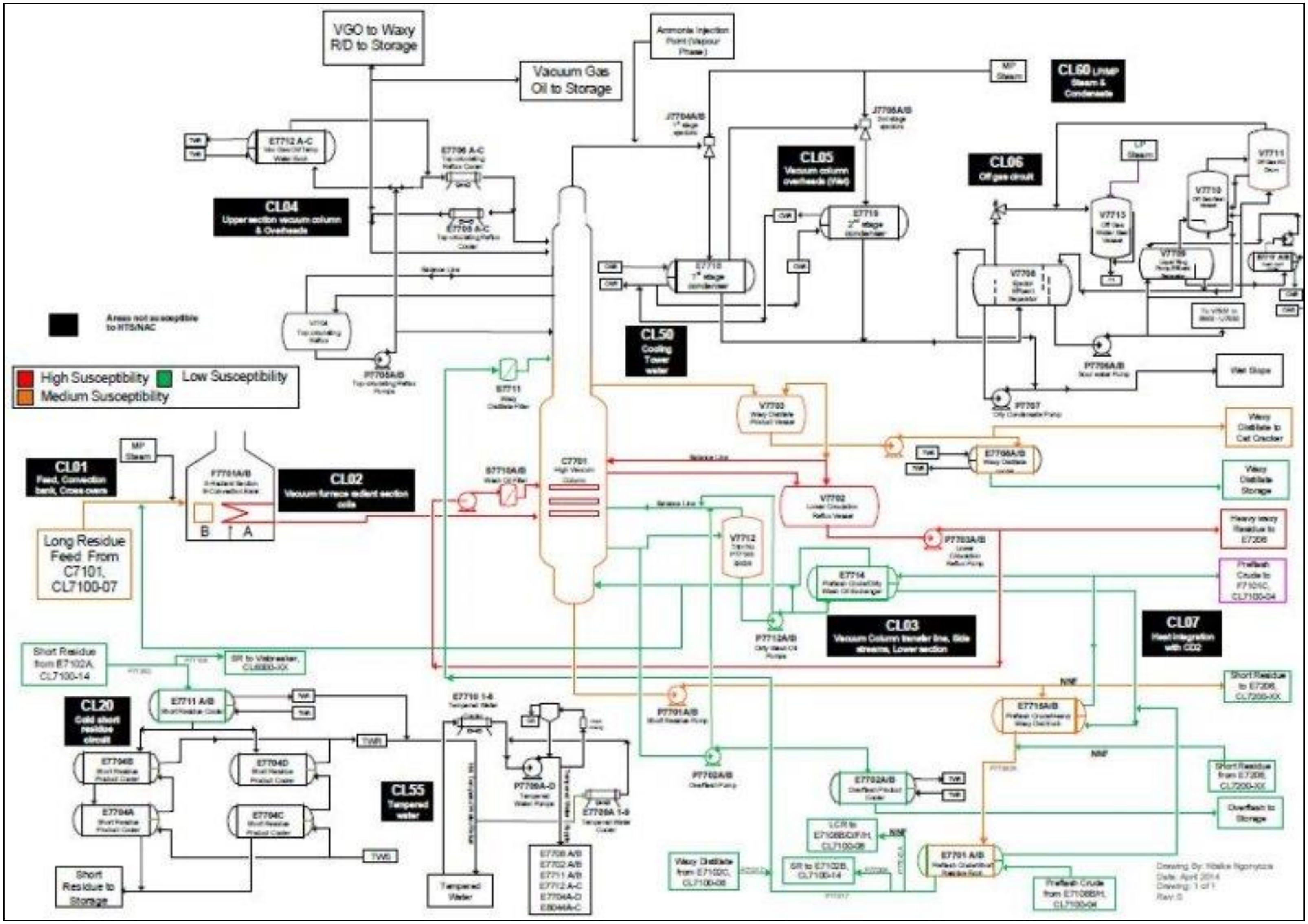

Figure 4.12: Vacuum distillation unit corrosion map for 0.5 TAN model case.

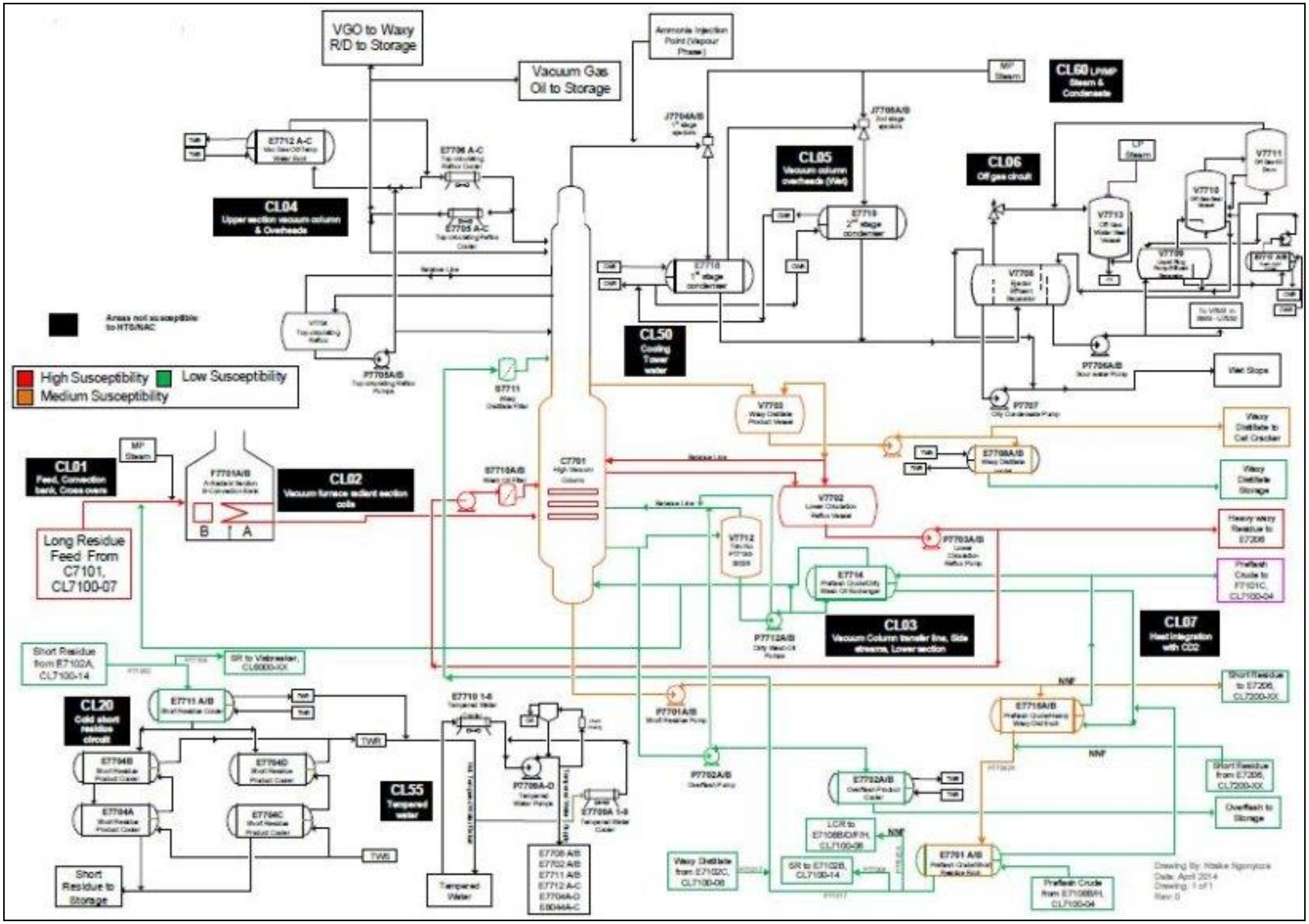

Figure 4.13: Vacuum distillation unit corrosion map for 0.8 TAN model case.

Table 4.5: Comparison of model and Actual Corrosion Rate (CR) Results for Vacuum Distillation Circuits.

Corrosion Process Loop	Material	Max Temp (°C)	Flow	Model CR (TAN 0.35)	Model CR (TAN 0.5)	Actual CR	Model CR (TAN 0.8)
Long Residue	5Cr0.5Mo	350	liquid	M	M	M	M-H
Furnace Coil	5Cr0.5Mo	410	2-phase	H	H	H	H
Transfer Lines	5Cr0.5Mo	410	2-phase	H	H	H	H
Short residue	5Cr0.5Mo	350	liquid	M	M	M	M
Dirty Washoil	316 SS	300	liquid	L	L	L	L-M
Heavy Waxy Distillate	Carbon steel	280	liquid	L-M	H	M	H
Light Waxy Distillate	Carbon steel	250	liquid	L-M	M	M	M

L=Low, M=Medium, H=High

4.3.4 Vacuum Distillation Actual Corrosion Rates History

There have been many leaks on the radiant section tubes from high temperature corrosion and erosion effects, as predicted by the 0.35 TAN case and in most cases the 0.5 TAN case model too. The convection section also had corrosion findings, resulting in a recommendation for replacement of both the radiant and convection sections. Although a leak was reported on a short residue pipe, it was already beyond the line's design life, so the corrosion rate was still considered medium. The dirty washoil corrosion process loop's reports reflected negligible corrosion rates, also in agreement with both the 0.35 and 0.5 TAN models. Severe wall thinning has been reported in the heavy and light waxy distillate piping corrosion process loops including the vessels, and in some cases corrosion allowances were completely consumed A brief summary of the major corrosion equipment and piping failure events and replacements is presented in Table 4.6.

Table 4.6: Vacuum distillation major corrosion events.

Year	Major Failure/ Repair Event	Corrosion Process Loop
1976	Unit commissioned.	
1999	Crude preheat exchangers E7714A&B-Shell replaced with full stainless steel exchangers due to high HTS corrosion rates in 1999. No wall loss measured or corrosion issues reported since material upgrade. Last inspected in 2011.	DWO
2006-2015	F7701A Transfer piping to column from furnace historic failures	Transfer lines
2009	Crude preheat exchanger E7701B Bundle retubed following high measured wall losses, commissioned 1976. Up to 40% wall loss measured in 2015.	Short Residue
2010 - 2015	F7701A Numerous NAC failure incidents from 2010 to date. Some bends replaced and hard-faced with stellite for erosion resistance.	Furnace coil - radiant
2011	Corrosion of 316L SS internal lining of F7701A transfer piping from furnace to column reported historically. Last inspected in 2011 and large sections weld repaired.	Transfer lines
2011	S7701A/B filters renewed.	Heavy waxy distillate
2013-2015	Numerous leaks on walking sticks and F7701A radiant tubes. Unit shutdown several times a year to repair NAC leaks.	Transfer lines
2015	Preheat exchanger E7701A Bundle retubed following recommendation from 2011 with high measured wall loss (commissioned 1976).	Short Residue
2015	C7701 vacuum column draw-off pipeline replaced due to high measured wall loss, leaking draw off trays.	Heavy waxy distillate
2015	Lower circulation reflux vessel V7702 high wall loss measured and vortex breaker replaced.	Heavy waxy distillate
2015	C7701 vacuum column light waxy trays leaking, wall loss measured on distillation column shell.	Light waxy distillate
2015	Vessel V7703 high wall loss measured and vortex breaker replaced.	Light waxy distillate
2015	Heavy waxy line replaced due to severe wall loss measured	Heavy waxy distillate

5. DISCUSSION

5.1 Crude Oil Feed Sulphur and TAN

A steady decline in crude sulphur content was observed in the actual measurements taken on the crude campaigns processed in the SAPREF distillation units from 2005 to 2014, from a maximum measured of 2.64 wt% down to a minimum measured value of 0.32 wt%. In that same period, the percentage WAF processed in the plant increased dramatically from 20% to 72%. The measured crude TAN levels increased also in that same period, Figures 4.2 and 4.3.

The Pro/II model was used to calculate the resultant crude blend feed sulphur for the three model cases. For the 0.35 TAN case, with the lowest WAF proportion, the corresponding crude sulphur level was 0.96 wt%. It increased slightly to 0.99 wt% for the 0.5 TAN case, then decreased to 0.67 wt% for the 0.8 TAN case; this also explains why the curves in Figures 4.4 and 4.6, the 0.5 TAN case, had the highest sulphur levels in all cuts, and the 0.8 TAN case had the lowest. Although in the measured results, there was an overall decrease in the sulphur level associated with the increase in crude feed TAN during this period, no direct correlation between the sulphur and TAN could be identified when plotted against each other for that same period. It is apparent from the Pro/II modelling that the concentration of sulphur in relation to changes in TAN of crude oil blends was mainly dependent on the crude oils mixed into that blend.

5.2 Sulphur Distribution

5.2.1 Sulphur Distribution – Atmospheric Pressure Distillation

No measurements of actual sulphur levels in the cuts were taken that could demonstrate the resultant change in sulphur concentrations of the cuts with reducing crude feed sulphur.

The Pro/II model did, however, indirectly show the effect of reduction in crude input sulphur on the various crude oil cuts for both the atmospheric and vacuum distillations. In general, sulphur was most concentrated in the heaviest cuts with the highest amount in the LR, HGO, then LGO with the lowest amount for all cases, Figure 4.4. The curves for the various TAN cases were also almost identical in shape, but the increase in concentration for the HGO and LR cuts was less pronounced in the 0.8 TAN case compared to the 0.35 and 0.5 TAN cases. The existing data set does not allow for analysis to investigate these effects further to explain why the concentration of sulphur in the heavier cuts was less pronounced in the 0.8 TAN case. However, the current results can lead to the potential assumption that there may be a link between the distribution of the sulphur among the fractions and the crudes that are mixed into a specific blend.

5.2.2 Sulphur Distribution – Vacuum Pressure Distillation

In the vacuum distillation, the sulphur distribution also showed a general tendency to concentrate in the heavier cuts, but the behaviour was not as linear as in the atmospheric distillation, Figure 4.6. The patterns for the 0.35 and 0.5 TAN cases were again quite similar, but the 0.8 TAN vacuum distillation case differed in that the sulphur concentrations were much lower for all cuts than the other two cases. Overall, there were still higher sulphur concentrations in the heavier cuts, with the highest concentration in the short residue for all cases. The distribution curve for the 0.8 TAN case was again flatter than that for the 0.35 and 0.5 TAN cases, indicating a reduction in the effect of higher sulphur concentrations in the heavier fractions. Similar to the atmospheric distillation section, the existing data set does not allow for analysis to investigate these effects further. However, the current results can lead to the potential assumption that there may be a link between the distribution of the sulphur among the fractions and the crudes that are mixed into a specific blend, or a reduction in differences between fraction sulphur concentrations with increases in TAN.

5.3 TAN Distribution

There was a slight increase in TAN in the period 2005 to 2014 during which the WAF processing was also increased, as per Figure 4.2 and 4.3. The crude TAN level was considered low (Nugent and Dobis, 1998), but there were varying effects on the different crude cuts as discussed in the following sections of the atmospheric and vacuum distillation sections.

5.3.1 TAN Distribution – Atmospheric Pressure Distillation

For the 0.8 crude TAN case, the TAN level generally decreased in the heavier cuts, but peaked in the HGO before reducing in the long residue, Figure 4.4. For the other two cases, 0.35 and 0.5 crude TAN, the TAN level tended to increase in heavier cuts, with the long residue having the highest TAN, but without a peak TAN in the HGO. The "curves" also have a lower gradient than the 0.8 TAN case. The marked difference in the 0.8 TAN case from the other two cases suggests there may be a difference in the TAN distribution behaviour of a more WAF based diet. More data in the form of measured TAN, in both WAF and PG crudes, per distillation cut could help in determining this. Since α naphthenic acids boil from 357°C (Kane & Chambers, 2011), most of the β naphthenic acids would concentrate in the long residue cut. However, this assumption does not however explain the distribution behaviour observed in the 0.8 TAN case curve.

5.3.2 TAN Distribution – Vacuum Pressure Distillation

In the vacuum distillation section, the TAN distribution for all model cases displayed similar behaviour to that observed in the atmospheric distillation for the 0.8 TAN case only, i.e. TAN decreased in the heavier cuts. The 0.35 and 0.5 crude TAN cases had a similar TAN distribution profile to one another, which peaked in the heavy waxy distillate, although The 0.8 crude TAN case displayed a sharp drop in TAN in the heavier DWO and SR, which was even lower than both the 0.35 and 0.5 TAN cases.

5.4 Comparison of Modelled Corrosion Rates and Inspection History

According to the McConomy curves (1963), the higher temperature and active sulphur concentrations should have increased the sulphidic corrosion rate. The outputs of all the models supported this idea. The HTS corrosion rates of the 0.5 and 0.35 TAN cases were approximately equal for all cuts, since the distillation temperatures remained constant and the sulphur levels in these two cases were almost equal, with slight variations depending on the crude blend. Since the unit was never continuously operated at crude feed TAN level of 0.8, it was not possible to assess the actual corrosion rate against the modelled corrosion rates.

In the hot desalted crude loop, which was constructed of carbon steel materials and had a maximum temperature of 260°C, the measured corrosion rates were low throughout and there were never any failures or leaks found. Some of the preheat train heat exchanger tube bundles had been pre-emptively replaced due to reducing wall thicknesses; they were nearing their end of life, but corrosion rates were steady and predictable over long periods, indicating a dominance of sulphidic corrosion over the more aggressive NAC mechanism. Most of the equipment had exceeded its design life of 30 years for pressure vessels and 20 years for tube bundles. Two of the preheat exchangers was upgraded to 316L SS following corrosion observed in 1999, Table 4.4; for this reason, the actual corrosion rate for this loop was medium. The difference in 0.35 and 0.5 TAN cases modelled corrosion rates and the findings on the preheat exchangers could be attributed to the error introduced by averaging historic operational temperatures.

The furnace coils of the atmospheric furnace had carbon steel tubes in the convection bank, as well as the first eight tubes of the radiant heater section. The remaining tubes were constructed of 5Cr0.5Mo material. The highest temperatures in the furnace were at the outlet tubes, at 360°C. Numerous leak incidents were reported in the operational history of this furnace. The convection bank suffered tube ruptures in the shock tubes, the top row of the convection bank exposed to the highest flue gas temperatures. These leak incidents were attributed to localized over-heating from internal coke build up, which was supported by metallographic analysis that indicated carburisation of the tube material microstructure and intergranular cavities (Dube et al., 2012). In the radiant section of the furnace, the operational history had been marred with various leak failures from internal corrosion of both the carbon steel and low alloy 5Cr0.5Mo tubes. In 2014, flow assisted NAC caused a leak of the last tube outlet bend, tube 30. In followup inspections, more NAC was found on the hottest outlet tubes of the radiant section. The 0.35 and 0.5 TAN case models estimated medium corrosion rates for the lower temperature carbon steel section and high corrosion for the hottest outlet 5CrMo tubes in which the crude oil begins to vaporize; this was the same as the observations on the furnace tube history.

The transfer lines from the radiant section of the heater to the atmospheric distillation column were all 5Cr0.5Mo material, and the hot crude oil was at temperatures up to 360°C, which is still in the two-phase flow regime following vaporization of the crude oil in the radiant section of the furnace. Extensive NAC damage and leaks in operation were found on these lines, particularly at bends and reducers. This section was ranked high for corrosion in the 0.5 TAN case, but medium in the 0.35 TAN case. It was observed that corrosion rates increased in the period between 2013 and 2015, which correlated with the increased corrosion prediction of the 0.35 to 0.5 TAN case models for increased corrosion rates with an increase in TAN over the years as shown by Figures 4.2 and 4.3.

Long residue corrosion rates were estimated at medium for the 0.35 TAN, and high for the 0.5 and 0.8 TAN cases. All the construction materials of the piping in this corrosion process loop were low alloy 5Cr0.5Mo and no leak incidents were reported here. No repairs were conducted in the operational and maintenance history and measured corrosion rates were within design. The measured corrosion rates were in agreement with the modelled corrosion rates for the 0.35 TAN case. The 0.5 TAN case model corrosion rates were higher than the actual observed corrosion on the long residue piping. This could be explained by the errors introduced in the set-up of the model, namely that the TAN is a measure of all acids, including dissolved acid gases in the crude oil sample and secondly, TAN values modelled from Pro/II were used for the corrosion models input. There may have been less actual naphthenic acids in the long residue than modelled by Pro/II. Furthermore, the corrosion model does not differentiate between types of naphthenic acids (Turnbull et al., 1998), and treats all TAN as being equally corrosive. It was shown by Hau et al. (2003) that it is possible for crude oils with the same amount of naphthenic acids to have differing corrosivities.

The heavy gasoil corrosion process loop was predicted by the 0.5 TAN case model to have medium corrosion rates. The lines and equipment were of carbon steel construction with maximum temperatures of 315°C. The actual corrosion rates were above that predicted by the corrosion model. This difference in corrosion rates could be partly due to a difference in the modelled acid content of the stream using Pro/II and the actual TAN of the stream. In addition to the error introduced by the uncertainty in actual TAN in the heavy gasoil, the construction material used for the corrosion model was 405 SS, however, the section which had a failure (22 years into the 30-year design life) was in the carbon steel section of the distillation column. As a result of the leak incident, the internal 405 SS, the weld overlay was increased to include the area that had leaked. Carbon steel is more susceptible to HTS and NAC (Bota et al., 2010).

The light gasoil reached a temperature of 255°C and all components in this circuit were carbon steel. The low predicted corrosion rates of the 0.35 and 0.5 TAN case models were in agreement with the measured corrosion rates. All pipelines and equipment had exceeded their design life. This is in accordance with the theory that HTS and NAC are reduced at lower temperatures (Bota et al., 2010).

In the vacuum distillation section, the long residue coming from the atmospheric distillation column was fully liquid at 350°C. The modelled corrosion rates for the 0.5 and 0.35 TAN cases were medium, and consistent with the predicted corrosion rates for the components in this circuit, which were all low alloy 5Cr0.5Mo.

In the vacuum furnace convection section and radiant section, all tubes were 5Cr0.5Mo material. The 0.5 and 0.5 TAN case models predicted high corrosion rates for the highest operational temperatures in the radiant section at 410°C. The convection section predicted corrosion rates were medium. In the convection section, general wall loss was measured on the tubes and they were replaced in 2015, due to low measured wall thicknesses. The radiant tubes of the furnace suffered multiple leaks throughout operation. The measured corrosion rates of both the convection and radiant sections were in agreement with the predictions of the modelled data for both cases. This was as expected for two-phase flow, which results in increased shear stresses that can mechanically remove the protective corrosion product scales on the substrate of the material as demonstrated by Kane et al. (2003). The furnace coil tubes were also of increasing diameter which promoted vaporization of the long residue at the operational temperatures of the furnace coil of up to 410°C (Xaba et al., 2012) and it is known that NAC is most aggressive during phase changes, i.e. the first drops of condensation or when boiling (Derungs, 1956).

The transfer lines from the vacuum furnace to the vacuum distillation column, which were also 5Cr0.5Mo with two-phase long residue at 410°C, were predicted to have high corrosion rates, similar to the radiant section coil. There were frequent leaks and repairs on these pipelines in the period from 2013 and 2015. These lines were also in agreement with the 0.35 and 0.5 TAN case corrosion models.

The short residue circuit lines from the bottom of the vacuum distillation column were all 5Cr0.5Mo material. The measured and the predicted corrosion rates from the 0.35 and 0.5 TAN case models were the same. Similarly, the dirty washoil system corrosion rates were accurately predicted low by the 0.35 and 0.5 TAN case model.

The heavy and light distillate section equipment and piping components were of carbon steel material. Predicted corrosion rates differed, depending on operational temperatures of each equipment and pipeline. For the 0.35 TAN case, the modelled corrosion rate was medium at the maximum temperature of 280°C, and for the 0.5 TAN case the maximum predicted corrosion rate was high. The actual measured corrosion rates on the piping and equipment were medium. Steady predictable general wall loss was observed on the piping and equipment, in agreement with the model predictions for the 0.35 TAN case. This could again be attributed to the uncertainty in actual TAN in the heavy waxy distillate which could be lower than the TAN modelled in Pro/II.

Although the historic actual fed TAN for the unit fluctuated drastically as shown in Figures 4.2 and 4.3, the predicted corrosion rates were in good agreement with the actual measured corrosion rates and observed corrosion throughout the units. The corrosion model results were at least more conservative than actual measurements, except for the hot desalted crude oil and heavy gasoil in the atmospheric distillation section. It should, however, be noted that the models predicted corrosion for defined crude oil blends and did not account for issues with mixing of the crude oil blends. Crudes do not always mix homogenously, and some crude tanks do not have efficient mixers or the crudes themselves do not blend well, which may result in layering of crudes with differing densities and sulphur and TAN concentrations (Warner, 2017). Therefore, it is possible to run a crude blend varying from the expected blend properties if crude mixing is not managed effectively. In addition to this, the model was based on only three crude blend variations, which in practice were varied approximately every two weeks, depending on the products the refinery needed to supply to the market. The crude campaigns were altered every week or two to meet market demands, and even discrete changes in the crudes that make up a blend can change the TAN and sulphur distribution, which then would affect corrosion rates. The TAN and sulphur data were produced from the Pro/II model which used crude ASSAY data to calculate the sulphur concentrations and TAN of each distillation cut; however, these crude ASSAY data are not always updated. There are also operational practices that can affect the processed crude feed properties, such as uncontrolled recycling of slops, waxy and long residues of possibly higher TAN, and unknown sulphur content into the crude feed, resulting in unpredictable effects on the various distillation cut properties (Xaba et al., 2015).

The actual TAN had a much smaller range of variance than the measured sulphur contents in the crude feed in the period between 2013 and 2014. This tends to support the notion that the sulphur concentration of the feed was much more influenced by the crudes blended and their proportions, rather than the crude feed TAN. This can also be controlled for through crude selection. In the period between 2013 and 2014, it was also observed that there was higher incidence of failures from NAC, while TAN increased and sulphur decreased. This observation supports the theory of Nugent and Dobis (1998) that corrosion rates may be aggravated by the reduction of sulphur content, which is understood to reduce the formation of the somewhat protective iron sulphide layer from the HTS reaction, leaving the substrate surface more vulnerable to NAC, even at relatively low TAN levels. The interaction of NAC and HTS is still not well understood and this notion requires further investigation. Another possible explanation for the increased corrosion rates could be organic acids measured in the TAN. Although the effective TAN increase was quite low in this period, a change to more corrosive organic acids can result in higher corrosion rates, since TAN is a measure of all organic acids, rather than the purely naphthenic acid content of a crude oil. According to NAC theory, broadly categorized alpha naphthenic acids are more corrosive than beta acids (Kane & Chambers, 2011). Speciation of the measured crude feed TAN to differentiate between dissolved acid gases, α and β naphthenic acids, was not part of this study, nor could the existing data be used to differentiate between the acid types in the crude feed. This could, however, be a plausible explanation for the increase in corrosion, although TAN was still relatively low and had not increased significantly.

5.4.1 Behavior of Different Materials in HTS & NAC Conditions

The dirty washoil corrosion process loop, which is constructed of 316 SS material, had predicted and measured low corrosion rates. The heat exchanger E7714 was replaced in 316 SS material from 5Cr material in 1999, with no corrosion reported since the metallurgy upgrade. The corrosion rates were within expectations for the high alloy 18 wt%Cr material with up to 3 wt%Mo. The 5 wt%Cr material of the furnace coils and transfer lines in the vacuum distillation unit had high modelled and measured corrosion rates, as predicted by El Kamel et al. (2010), who claimed that there was little benefit in using 5Cr material over carbon steel. This can be seen where in the atmospheric distillation unit the temperature of the heavy gasoil corrosion process loop was up to 315°C and the measured corrosion rate was high for the carbon steel material.

5.4.2 Corrosion Morphologies Observed

NAC and HTS differ in morphologies in that while general corrosion without an observable surface pattern is common for HTS, NAC is characterized by heavy localised pitting. NAC pitting was found in both the atmospheric and vacuum distillation furnace tubes. The worst affected areas were the radiant section tube bends, which leaked on numerous occasions, as reported in their histories (Appendix 3). The transfer lines from the furnaces to the distillation columns also showed the same scalloped pitting morphology, which was also detected mainly at bends and reducers. These findings were as expected, due to the two-phase flow conditions in the radiant heaters and transfer lines, and were predicted as such by the models. With vapourisation, the local TAN in the oil increased as naphthenic acids remained in the liquid phase, and highly concentrated acidic droplets corroded the metal surface. With two-phase flow conditions, the impingement of liquid particles on the metal surface also increased shear stresses on the metal, which increased corrosion rates and caused the scalloped appearance on the metal surface.

The heavy and light waxy sections in the vacuum distillation unit had more general wall loss, demonstrating more HTS dominance, as indicated by the V7702 equipment history in Appendix 3. The visual inspections reported that the corrosion was not visually identifiable, except by protrusion of the welds and wall thickness measurements. From 2004 to 2015, the amount of pitting observed increased, which also demonstrated the effect of increasing TAN in the unit feed over this time period, Figures 4.2 and 4.3. The heat exchangers E7108A-H SH also displayed a similar transition from general HTS corrosion to NAC associated pitting in more recent reports. In the distillation columns, general wall loss and pitting corrosion was observed on the column wall, even on the 405 SS cladding, as well as carbon steel base material. Even though 405 SS has approximately 12 wt%Cr, without the additional molybdenum alloying additions, it was still susceptible to corrosion by NAC.

NAC pitting was reported on the carbon steel HGO equipment, V7107 and C7102, as carbon steel did not have chromium nor molybdenum to afford it better resistance to NAC. On the LGO equipment, mainly general corrosion was reported, apart from isolated shallow pitting reported in E7104 SH. This was as expected for the lower process temperatures where less naphthenic acids began to boil off, therefore less NAC was expected.

NAC pitting was also reported in the short residue equipment, on E7715 SH and E7701A/B SH, but to a lesser extent than in the HGO. Although both sections have 5Cr material at temperatures in excess of 300°C, HGO had higher TAN levels than short residue, Figures 4.5 and 4.7.

5.5 Limitations & Potential Error Sources

There are numerous potential error sources in the correlation of the modelled and measured corrosion rate data, the first of which being the data that were used as inputs into the process modeling software tool, Pro/II. Crude assay data are loaded into the simulation software, however, the crude assay data are often outdated. Actual measurements of the crude cut TAN and sulphur were sporadically taken, with some lengthy time periods when no measurements were taken. It should also be noted that the Pro/II modeling is not based on the actual crude diet that was historically processed, but was approximated based on the typical crude basket of the refinery and the required products. The second source of potential errors is inherent in the Pro/II modeling software itself. The selected thermodynamic model for simulation should converge to minimize the error margin, which it did.

The corrosion modeling software also introduces errors into the corrosion rate data. The temperatures used to calculate corrosion rates were averaged over the operational history of the units. Also, only a single corrosion rate was determined, instead of calculating a corrosion rate for each operational mode and the associated temperature. There was also uncertainty over the wall shear stresses which are determined from the flow conditions, which may be locally different in the equipment and piping components.

As mentioned in Chapter 3.4, the corrosion rate measurements are also a potential source of errors. Depending on the inspection technique used, the technician taking the measurements and the location where measurements are taken, the corrosion rates measured can vary considerably.

The impact of the combination of the aforementioned error sources is either self-correcting or has little appreciable impact on the correlation of the modelled corrosion rates with those measured and observed in the field. It is also possible that because the corrosion rates are measured in ranges (L, M, H) and not exact wall loss, that errors are masked within these defined measurement ranges.

It should also be noted that the corrosion rate ranges low, medium and high are set based on design corrosion allowances. There exists the issue that design corrosion allowances are reported on design drawings including safety factors. The measured corrosion rate is designated as “high” when there have been failures within the design life of the equipment, as well as if the measured corrosion rate exceeds the design corrosion rate (Figure 3.1). Due to these design safety factors, it is possible that a component may corrode at a rate above the design rate without ever resulting in a loss of pressure containment within the design life. In practice, when the design corrosion rate of a pressure equipment component has been consumed, a new corrosion allowance called the future corrosion allowance (FCA) may be calculated according to fitness for service principles (API 579, 2016). These specialized calculations come at a cost to the plant as do production losses from in-service leaks, therefore it was deemed fit to define the “high” corrosion rates in this way, despite this apparent flaw.

6. CONCLUSIONS

Corrosion maps were produced based on results of the empirical based industry high temperature corrosion model, Predict Crude^{TM}. According to this assessment, the atmospheric distillation furnace radiant coil and the transfer lines from the furnace to the distillation column had the highest corrosion rates; the crude oil was in two-phase flow in both these corrosion process loops. In the vacuum distillation section, the furnace radiant coil, transfer lines to the distillation column and the heavy waxy distillate corrosion process loop had the highest corrosion rates.

The measured corrosion rates were assessed qualitatively against the corrosion rates predicted by the model, using the desired design life and design corrosion allowances. To determine the measured corrosion rates, both the equipment history and wall thickness measurements were taken into account. The empirical corrosion model was found to be in good agreement with the actual measured corrosion rates on the units. The corrosion model also accurately highlighted the areas with high corrosion rates where failures within design life may be expected, based on modelled process conditions and materials of construction of the various equipment and piping. The materials of construction behaved as predicted by the model, depending on the alloying additions thereof. Materials with higher chromium and molybdenum contents were more resistant to NAC and the associated pitting was not observed. There was also a transition from the more general wall loss of HTS to increased reports of pitting more akin to NAC, over the passage of time, as the plant increased the crude feed TAN levels.

Although there was an overall decrease in the sulphur level associated with the increase in crude feed TAN, no direct correlation between the sulphur and TAN was found. It was determined that the concentration of sulphur in relation to changes in TAN of crude oil blends was mainly dependent on the crude oils mixed into that blend.

In general, the TAN distribution increased for each distillation cut with increased crude feed TAN, except for the vacuum distillation 0.8 TAN case where the dirty washoil and short residue had lower TAN than the 0.35 and 0.5 TAN cases. It was determined that the TAN in each distillation cut in relation to changes in crude feed TAN of crude oil blends was mainly dependent on the crude oils mixed into that blend.

7. RECOMMENDATIONS FOR FUTURE WORK

The corrosion rates were not systematically and periodically measured and rigorous review of inspection reports had to be conducted, however application of a permanently installed online corrosion monitoring system could allow for examination of the effect of discreet changes in process conditions on corrosion rates.

Also of interest was that even without considerable increase in TAN, there were increases in corrosion rates and failures observed, which led to the conclusion that different organic acids measured by the collective term TAN vary in corrosivity, and this could be studied in more depth. Speciation of the measured crude feed TAN to differentiate between dissolved acid gases, α and β naphthenic acids could allow for this kind of analysis.

Actual measurement of TAN and sulphur for each distillation cut for use in the corrosion models is recommended to test the effectiveness of the empirical corrosion model more accurately.

Studying the groups of crude oils (by region) and assessing the TAN and sulphur distribution behaviour of these crudes could help refiners to more accurately predict the process constituents of the crudes that are processed.

It was not possible to discuss the performance of the different materials of construction for the equipment components in this study. To investigate further, the corrosion rates and types of corrosion on the different materials, it would be required to compare sites with similar crude diets but different metallurgies.

REFERENCES

API 581 Risk Based Inspection Methodology, third edition, April 2016.

API RP 939-C Guidelines for Avoiding Sulfidation (Sulfidic) Corrosion Failures in Oil Refineries. API Subcommittee on Corrosion & Materials, Version 5.0, February 2008.

Babaian-Kibala E., Nugent M.J. (1999) Naphthenic Acid Corrosion Literature Survey. *NACE Corrosion 1999,* Paper No. 378.

Bhowmick S. (2011) Ultrasonic Inspection for Wall Thickness Measurement at Thermal Power Stations. *International Journal of Engineering Research and Technology,* Volume 4, Issue 1 (2011), 89-107.

Bota G.M., Qu D., Nesic S., Wolf A. (2010) Naphthenic Acid Corrosion of Mild Steel in the Presence of Sulfide Scales Formed in Crude Oil Fractions at High Temperature. *NACE Corrosion 2010,* Paper No. 10353, NACE International, San Antonio TX.

Chambers B.D., Srinivasan S.; Kane, R. D., Blades M. A. (2012). An Experimental Method for Evaluation of Crude Corrosivity - Naphthenic Acid and Sulfidic Corrosion of Oil Fractions. *NACE Corrosion 2012,* Paper No. 1564, NACE International, Salt Lake City UT.

Cobanoglu M., Altinsoy N. (2014) Wall Thickness Measurement of Pipes by Using Digital Radiography. *4th International Congress APMAS2014*, Fethiye Turkey.

Craig H.L. (1996) Temperature and Velocity Effects in Naphthenic Acid Corrosion. *NACE Corrosion 1996,* Paper No. 603, NACE International, Denver CO.

Derungs W.A. (1956) Naphthenic Acid Corrosion – An Old Enemy of the Petroleum Industry. *Corrosion 12*, Issue 12, 41-46.

Dettman H., Li N., and Luo J. (2009) Refinery Corrosion, Organic Acid Structure, and Athabasca Bitumen. *NACE Corrosion 2009*, Paper 09336, NACE International, Atlanta GA.

Doust A.M., Shahraki F., Sadeghi J. (2012) Simulation, Control and Sensitivity Analysis of Crude Oil Distillation Unit. *Journal of Petroleum and Gas Engineering*, Vol. 36, 99-113.

Dube G., Pistorius P., Simon D., Xaba N., Koenis R., Dowling N. (2012) Unexpected Mechanism of Crude Oil Heater Convection Section Failures. *Ferrous and Base Metals Development Network Conference 2012,* AMI, SAIMM Symposium Series S73, 405-414, Magaliesburg.

El Kamel M., Galtayries A., Foulonneau G., Roumeau X., Morel G., Marcus P. (2010) High temperature Corrosion of Sulphided Steel in Naphthenic Acid Environments. *EuroCORR 2010*, Moscow, Paper 9377.

Farraro T., Stellina R.M. Jr. (1996) Materials of Construction for Refinery Applications. NACE Paper 614, *NACE International*, Houston TX.

Farrell D., Roberts L. (2010) A Study of High Temperature Sulfidation Under Actual Process Conditions. NACE Paper 10358, *NACE International,* San Antonio TX.

Global Petrol Prices, Chart: Historical prices of crude oil (1861 - 2014), viewed 27 April 2018, from *www.globalpetrolprices.com/articles/28*, 2015.

Groysman A., Brodsky N., Penner J. (2005) Study of Corrosiveness of Acidic Crude Oil and its Fractions. *NACE Corrosion 2005*, Paper 05568, NACE International, Houston TX.

Hau J.L. Yepez O.J., Torres L.H., Vera J.R. (2003) Measuring Naphthenic Acid Corrosion Potential with the Fe Powder Test. *Revista de Metalurgia Madrid,* Vol. 1, 116-123.

Haydary J., Pavlik T. (2009) Steady State and Dynamic Simulation of Crude Oil Distillation using ASPEN PLUS and ASPEN DYNAMICS. *Pet Coal 2009,* Vol. 1, 100-109.

Huihua Y., Wei M., Xiaofeng Z., Hu L., Songbai T. (2014) A Method for Crude Oil Selection and Blending Optimisation Based on Improved Cuckoo Search Algorithm. *China Petroleum Processing and Petrochemical Technology*, Vol. 16, Issue 4, 70-78.

Honeywell, viewed 17 May 2018, from https://www.honeywellprocess.com/en-US/explore/products/advanced-applications/software-operations-excellence/corrosion-prediction/Pages/predict-crude.aspx, 2018.

Hucińska J. (2006). Influence of Sulphur on High Temperature Degradation of Steel Structures in the Refinery Industry. *Advances in Materials Science*, Vol. 6, Issue 1, 16-25.

Kane R.D., Cayard M.S. (2002) A Comprehensive Study on Naphthenic Acid Corrosion. *NACE Corrosion 2002,* Paper No. 02555, NACE International, Houston TX.

Kane R.D., Trillo E., Maldonado J.G. (2004) Naphthenic Acid Corrosion: Roles of Velocity. Alloying, TAN and Sulphur Species. *EuroCORR 2004*, European Federation of Corrosion, Budapest.

Kane R.D. (2006) "Corrosion in Petroleum Refining and Petrochemical Operations", Corrosion: Environments and Industries. *Metals Handbook*, Vol. 13C, ASM Handbook, ASM International, 967-1014.

Kane R.D., Chambers B. (2011) High Temperature Crude Oil Corrosivity: Where Sulphur and Naphthenic Acid Chemistry and Metallurgy Meet. *Corrosion Solutions Conference 2011*, Paper 4a, 137-144.

Kanukuntla V., Qu D., Nesic S., Wolf A. (2009). Experimental Study of Concurrent Naphthenic Acid and Sulfidation Corrosion. *NACE Corrosion 2009*, Paper 02764, NACE International, Houston TX.

Kolmetz K., Mardikar A., Gulati H., Ng W.K., Lim T.Y., Cheah P.S. (2007) Design Guidelines for Using Distillation Simulation Software in the Field. *Invensys Process Systems Users Conference,* Bangkok.

Kumar A., Rajkumar K.V., Palanichamy P., Jayakumar T., Chellapandian R., Kasiviswanathan K.V., Raj B., Patankar V.H., Joshi V. M. (2006) Development and Applications of C-Scan Ultrasonic Facility, *NDE2006,* Hyderabad.

Lai G. 2007, High Temperature Corrosion and Materials Applications. *ASM International*, Ohio, 212.

McConomy H. (1963) High Temperature Sulfidic Corrosion in Hydrogen-Free Environments. *API Proceedings 43*, 78-96.

NACE 34103 (2014 revision), Overview of Sulfidation (Sulfidic) Corrosion in Petroleum Refining Hydroprocessing Units.

Nugent M.J., Dobis J.D. (1998) Experience with Naphthenic Acid Corrosion in Low TAN Crudes. *NACE Corrosion 1998*, Paper No.577, NACE International, San Diego CA.

Parker Kittiwake, Heavy Fuel Refinery Process, viewed 15 April 2018, from *http://kittiwake.com/refineryprocess*, 2015.

Piehl R.L. (1988) Naphthenic Acid Corrosion in Crude Distillation Units. *Materials Performance*, Vol. 27, Issue 1, 37-43.

Przybylski K., Mrowec S. (2003) High Temperature Sulphide Corrosion and Transport Properties of Transition Metal Sulphides. *JAERI Conference 2003,* Tokyo, 44-51.

Qing W., Digital Refining, Processing high TAN crude: part I, viewed 27 April 2018, from *http://www.digitalrefining.com/article/1000524*, 2010.

Qu D.R., Zheng Y.G., Jing H.M., Jiang X., Ke, W. (2005) Erosion-Corrosion of Q235 and 5Cr1/2Mo Steels in Oil with Naphthenic Acid and/or Sulphur Compound at High Temperature. *Material Corrosion,* Vol. 56, Issue 8, 533-541.

Rebak R. (2011). Sulfidic corrosion in refineries - A review. *Corrosion Reviews*. 29. 10.1515/CORRREV.2011.021.

Schempp P., Preuss K., Troeger M. (2016) About the Correlation Between Crude Oil Corrosiveness and Results from Corrosion Monitoring in an Oil Refinery. *Corrosion 2016,* Vol. 72, Issue 6, 843-855.

Schneider Electric, Pro/II Process Engineering, viewed on 26 March 2018, from

http://software.schneider-electric.com/products/simsci/design/pro-ii, 2018.

Slavcheva E., Shone B., Turnbull A. (1999) Review of Naphthenic Acid Corrosion in Oil Refining. *British Corrosion Journal*, Vol. 34, Issue 2, 125-131.

Spectro, Ultrasonic Theory, viewed on 30 March 2018, from *www.spectro.co.th*, 2010.

Turnbull A., Slavcheva E., Shone B. (1998) Factors Controlling Naphthenic Acid Corrosion. *Corrosion*, Vol. 54, Issue 11, 922-930.

Turcotte J., Rioux P., Lavoie J. (2016) Comparison Corrosion Mapping Solutions using Phased Array, Conventional UT and 3D scanners. *19th World Conference on Non-Destructive Testing*, Munich.

U.S. Energy Information Administration, Today in Energy, Crude oils have different quality characteristics, viewed on 30 March 2018, from www.eia.gov/todayinenergy, 2012.

Warner R. (2017) Western European refineries and acidity in crude oil, viewed on 6 June 2017, from www.platts.com

Xaba N., Dowling N., Dube G. (2012) Erosion in Oil Refinery High Vacuum Furnace Bends. *Ferrous and Base Metals Development Network Conference 2012,* AMI, SAIMM Symposium Series S73, 415-420, Magaliesburg.

Xaba, N., Cornish, L.A., Mulaudzi, F.M.L. (2015) Challenges in the Development of a High Temperature Corrosion Model for a Crude Oil Refinery Unit. *Nuclear Materials Development Network Conference*, AMI, SAIMM Symposium Series S87, 113-121, NMMU, Port Elizabeth.

Yeung T.W. Digital Refining, Evaluating opportunity crude processing, viewed 27 April 2018 www.digitalrefining.com/article/1000644, 2006.

Zscherpel U., Ewert U., Infanzo S., Rastkhan N., Vaidya P.R., Einav I., Ekinci S. (2006) Radiographic Evaluation of Corrosion and Deposits in Pipelines: Results of an IAEA Co-ordinated Research Programme. *ECNDT 2006 Proceedings,* Vol. 38, Issue 5, 1360.

APPENDICES

1. AMI 2015 Conference Paper
2. Confidentiality agreement sample
3. Equipment History Summaries

Appendix 1

The Southern African Institute of Mining and Metallurgy
Advanced Metals Initiative
Department of Science and Technology
Nuclear Materials Development Network Conference 2015
N. Xaba

CHALLENGES IN THE DEVELOPMENT OF A HIGH TEMPERATURE CORROSION MODEL FOR A CRUDE OIL REFINERY UNIT

N. Xaba[1,2,3], **L.A. Cornish**[2,3], **F.M.L. Mulaudzi**[2,3,4]

1. Shell and BP Refineries South Africa, Durban
2. School of Chemical and Metallurgical Engineering, University of the Witwatersrand, Johannesburg
3. DST-NRF Centre of Excellence in Strong Materials, University of the Witwatersrand, Johannesburg
4. Advanced Materials Division, Mintek, Randburg

Abstract

Following three major loss of primary containment (LOPC) events in a crude oil refinery due to naphthenic acid corrosion, a review of the plant's crude oil diet properties and operational conditions in critical units was conducted. In order to predict possible future failure events due to high temperature corrosion phenomena, a corrosion model was developed. The main high temperature corrosion mechanisms active in the crude oil refinery, crude distillation and high vacuum units were high temperature sulphidic corrosion and naphthenic acid corrosion. These corrosion mechanisms were influenced by the construction materials, process temperatures, active sulphur species concentration, type and concentration of naphthenic acids present in the process, as well as process flow regimes. A basic model has been developed to predict areas of high corrosion in the crude oil distillation and high vacuum units using theoretical knowledge of the behavior of sulphidic and naphthenic acid corrosion. Due to the unpredictability associated with naphthenic acid corrosion rates, the model is able to provide theoretical sulphidic corrosion rates for different product streams, but can only flag areas where naphthenic acid corrosion may take place.

Measurements of corrosion rates of these circuits will be conducted when the units are offline in May-June 2015, and thereafter there will be an analysis of the correlation of the model data against the measured system results.

1. Introduction

There were three unanticipated equipment material failures on a petrochemical oil refinery within one calendar year which resulted in an investigation into the failure mechanisms. All the equipment failures were in the high temperature circuits of the crude distillation and vacuum distillation Fluid Catalytic Cracking feed preparation units. Failure investigations revealed the primary corrosion mechanism responsible for the material failures was naphthenic acid corrosion (NAC) in conjunction with high fluid velocity effects, more commonly referred to as flow assisted corrosion.

The first failure was on a crude distillation furnace radiant section outlet line at a 90° bend as shown in Figure 1 which is a photograph of the internal pipe surface of the failure, the globules observed on the failure surface in Figure 2 are remaining product residue after cleaning. The second failure was found at the bends and some straight sections of the vertical heater coils of vacuum distillation radiant heater downstream in the aforementioned crude distillation furnace. In Figure 2 the morphology of the observed naphthenic acid corrosion is depicted, and Figure 3 shows the material gouging observed on the tube straight sections. Figure 4 shows the third failure which was also located in the bend of the crude furnace radiant heater coil, just upstream of the first failure.

In each failure case, the observed material degradation was at the extrados of a 5Cr1/2Mo material bend with product temperatures at approximately 360°C. The observed failure surfaces were heavily pitted with a pronounced material scalloping effect. Naphthenic acid corrosion is typically characterized by having more localized attack, pitting corrosion and grooving in high velocity areas [1] as shown in Figure 3.

2. Naphthenic Acid Corrosion

The amount of naphthenic acid present in a crude oil is most commonly indicated by a neutralization number or Total Acid Number (TAN). There is a degree of uncertainty in the potentiometric measurement method used to measure TAN, which is based on the amount of potassium hydroxide (KOH) in mg required to neutralize an oil sample of 1 gram. TAN actually measures all organic acids, different naphthenic acids, sulphides and other acid gases that react with KOH [1]. Although there are other means to measure naphthenic acid content of oils and condensates TAN still remains the most popular [2].

The factors which influence naphthenic acid corrosion rates are similar to sulphidic corrosion, namely active sulphur content of the process streams, materials of construction, process temperatures, flow regimes and/or resultant wall shear stresses as well as concentration and type of naphthenic acid [3].

There are two basic types of naphthenic acids with differing corrosive properties, namely α and β. Generally, α naphthenic acids have lower molecular weights than β naphthenic acids, which makes them more easily absorbed into the material's surface and hence they are more corrosive. Steric hindrance reduces the reactivity of the larger more complex β naphthenic acids [4]. It is possible for crude oils of the same amount of naphthenic acids to have differing corrosivities, due to this distinction between the types of naphthenic acids.

In addition to this the different type of acids may be corrosive at varying temperatures. Naphthenic acid corrosion occurs in the liquid phase and has its most severe effects at temperatures close to the naphthenic acid boiling points and upon condensation [5]. The α naphthenic acids also have boiling points of up to 385°C, whereas β naphthenic acids boil at temperature ranges between 357°C and 816°C; however naphthenic acids are thermally decomposed at temperatures above 400°C and much less corrosion is expected above this temperature.

Equations 1-3 represent the classical naphthenic acid corrosion theory [6]. Equation 1 is the formation of iron naphthenate from corrosion of the metal by α naphthenic acid with the general chemical formula RCOOH and in Equation 2 the metal is also corroded by the action of sulphides in the process stream. The iron sulphide layer formed during high temperature sulphidation is soluble and may be dissolved by naphthenic acid. The aggressive nature of naphthenic acid corrosion is illustrated by the third equation where the sulphides in the crude oil stream in solution with the unstable iron naphthenate corrosion product of Equation 1 (which is also highly soluble in oil) react to form more naphthenic acids. The resultant TAN is therefore much higher than the measured TAN of the crude oil.

$$Fe + 2RCOOH \Leftrightarrow Fe(RCOO)_2 + H_2 \qquad \text{(Equation 1)}$$

$$Fe + H_2S \Leftrightarrow FeS + H_2 \qquad \text{(Equation 2)}$$

$$Fe(RCOO)_2 + H_2S \Leftrightarrow FeS + 2RCOOH \qquad \text{(Equation 3)}$$

3. Interaction between NAC and Sulphidic corrosion

In recent years, it was discovered by Nugent and Dobis [7] that although naphthenic acid corrosion was thought to be most severe at high TAN levels (typically classified as crude TAN above 0.5 and crude fractions with TAN greater than 1.5), it may also occur at low TANs with the processing of sweet crudes, crude oil with sulphur content below 0.5wt%. It was also noted that the processing of sweeter low TAN primarily West African Crudes (WAF) on crude distillation and high vacuum units designed for sour Persian Gulf (PG) Crudes lead to corrosion damage of major process equipment at Tosco Trainer oil refinery in the early 1990s. These findings were later supported by the JIP [8] which proposed an apparent window of sulphidic corrosion inhibition. Sulphur acts as an agent of protection against naphthenic acid corrosion, for sulphur levels between 0.1wt% and 2.2wt%, with measured corrosion rates lower than for both low and high sulphur concentrations.

Due to the complex relationship between naphthenic acid and sulphidic corrosion, the Naphthenic acid corrosion index (NACI) has been proposed as a tool to determine which of the two mechanisms is more dominant [9]. It is expressed as the ratio of the corrosion rate to the weight of corrosion product. The underlying principle is that sulphidation produces an insoluble iron sulphide layer and the naphthenic acid corrosion product, iron naphthenate, is said to be oil soluble. NACI values above 10 are for naphthenic acid corrosion, and any values above 100 constitute a system with severe naphthenic acid corrosion. This index has not been used in the model, since the iron sulphide layer may also be mechanically removed in systems with high flow velocities.

4. Process Conditions that Support NAC

The amount of WAF crude in the refinery's crude oil feed has increased from an average of 25 to 80% from 2005 to 2014, and the maximum allowable crude TAN was increased from 0.35mg KOH/g to 0.5mg KOH/g in 2010. A graph in Figure 5 demonstrates the increased WAF crude processing. Although the annual scheduled crude TAN remained below 0.37mg

KOH/g, as depicted in Figure 6, there were fluctuations in the actual TAN seen by the unit. These fluctuations may be caused by the following:

1. Recycling of slops, waxy and long residues of possibly higher TAN and unknown sulphur into the crude feed
2. Crudes do not always mix homogenously, and some crude tanks do not have mixers which may result in layering of crudes with differing densities.
3. Scheduled crude TAN is based on crude ASSAY data, which is not always updated
4. Operational issues and unit upsets, which occasionally result in unscheduled crude diets being processed.

Increased wall shear stresses were also observed to be a contributory factor to all of the material failures experienced on the crude and vacuum distillation units which were all located on the tubes' extrados. High shear wall stresses are caused by the transition from liquid to two phase flow at the furnace coil outlet as the naphthenic acids boil off and the change in flow direction at the bends. Kane et al. [10] demonstrated with hot oil flow loop (HOFL) tests that NAC attack is more prominent at higher TANs and fluid flow rates. Above 100fps, the effects of impingement attack were observed.

In addition to the increased flow rates that increase wall shear stresses in the failure locations it has been observed that corrosion rates may have been aggravated by the gradually reducing crude sulphur content, Figure 7 illustrates the progressive drop in processed crude sulphur levels, which is understood to reduce the formation of the protective iron sulphide layer.

5. Modelling Methodology

Progress has been made in the prediction of naphthenic acid corrosion rates; Craig [11] developed a mathematical model for naphthenic acid corrosion that includes velocity effects and Qu et al. [12] also investigated the flow effect of naphthenic acid corrosion using jet impingement. The latter discovered that depending on TAN concentration and the type of alloy used, the naphthenic acid corrosion rate can either increase linearly with velocity, or exhibit a velocity threshold, above which the corrosion rate sharply increases. Despite these developments, the interaction between the two mechanisms is not well understood and is yet to be quantified.

In order to improve the predictability of high temperature corrosion mechanisms in oil refining and therefore increase reliability of the plant, the plant was modelled to predict areas of high corrosion and the estimated corrosion rates at those locations. The empirical model data developed by McConomy [13] for different materials of construction in contact with products at various temperatures and active sulphur concentrations was used to predict theoretical sulphidic corrosion rates. A corrosion map of the plant was developed indicating process loops, changes in temperature and materials of construction for various equipment.

Naphthenic acids concentrate in crude fractions with higher boiling points during distillation, therefore higher TAN levels than the crude oil feed are expected in these cuts namely residues, gasoils and waxy distillates. It is also possible for certain areas to have localised high TAN concentrations due to boiling / evaporation and condensation effects, which can result in higher naphthenic acid corrosion rates in those areas. The model does not include these effects, which would also require geometric modelling of the plant. Although the crude unit long residue circuit has an estimated TAN below 0.75, it is possible to have localised areas with higher TAN levels.

Corrosion rates of product streams with sulphidic corrosion dominance were estimated using the modified McConomy curve data. The proposed model developed was semi-empirical in nature. The empirical data used were from the Modified McConomy curves.

6. Expected Inspection Results and Future Work

Corrosion rates will be measured at the crude furnace outlet line where renewals were conducted upon failure. The vacuum distillation tubes which were replaced upon failure will also be inspected by wall thickness testing, as well as visual methods for material damage. The TAN and sulphur in the process stream are known, as well as process temperatures and materials of construction. In these circuits, there naphthenic acid corrosion dominance is expected as the naphthenic acids will concentrate in the heavier, higher boiling point crude fractions. The vacuum distillation column which is subject to high temperature sulphidation will also be inspected by wall thickness testing to estimate corrosion rates at selected locations along the column shell wall. Selected piping in the gasoil and waxy sulphidation circuits will also be measured for comparison to the estimated modified McConomy corrosion rates. The naphthenic acid corrosion rates are for information, and will be evaluated as they are anticipated to be higher than the sulphidic corrosion rates particularly with the reduced sulphur levels in the refinery's crude oil diet.

API 581 has tables which may be used to determine combined naphthenic and sulphidic corrosion rates that also attempt to account for flow effects by multiplying by a factor 5 when flow velocities exceed 100fps. The estimated corrosion rates on these tables is a function of material of construction, sulphur, TAN, and temperature. The flaw in the use of these tables is the absence of the sulphur species NAC inhibition phenomenon for medium sulphur levels. The results of inspections will also be compared to the API 581 tables.

Based on the results obtained from inspections, an online corrosion monitoring system is to be designed to measure corrosion rates in these high temperature sulphidic and naphthenic acid corrosion circuits.

The model is limited in its prediction of corrosion rates as it does not differentiate between active and total sulphur in the process stream. Further limitations include wall shear stresses which are not accounted for. The interaction of NAC and high temperature sulphidation is additionally not represented. Added to this is the uncertainty of the actual TAN and sulphur levels in the crude fractions. The following recommendations can be made to better estimate corrosion rates:

1. Measuring TAN in different fractions, and streams
2. Differentiating between Total sulphur, active sulphur and mercaptans
3. Insertion of corrosion coupons which provide more accurate corrosion rate estimation

7. Conclusions

High temperature corrosion modelling in oil refining poses many challenges in adequately predicting corrosion rates as unanticipated processed crude property changes are not accounted for, the parameters that influence corrosion at various areas are not effectively monitored and the interaction between NAC and HTS is not well understood.

8. References

1. Kane R.D., Cayard M.S. (2002) A Comprehensive Study on Napthenic Acid Corrosion. *NACE CORROSION 2002,* Paper No.02555

2. Piehl, R.L. (1988) Naphthenic Acid Corrosion in Crude Distillation Units. *Materials Performance*, Vol. 27, Issue 1, 37-43

3. Bota G.M., Qu D., Nesic S., Wolf A. (2010) Naphthenic Acid Corrosion of Mild Steel in the Presence of Sulfide Scales Formed in Crude Oil Fractions at High Temperature. *NACE Corrosion 2010,* Paper No. 10353

4. Turnbull A., Slavcheva E., Shone B. (1998) Factors Controlling Naphthenic Acid Corrosion. *Corrosion*, Vol. 54, Issue 11, 922-930

5. Derungs W.A. (1956) Naphthenic Acid Corrosion – An Old Enemy of the Petroleum Industry. *Corrosion 12*, Issue 12, 41-46

6. Babaian-Kibala E., Nugent M.J. (1999) Naphthenic Acid Corrosion Literature Survey. *NACE CORROSION 1999,* Paper No. 378

7. Nugent M.J., Dobis J.D. (1998) Experience with Naphthenic Acid Corrosion in Low TAN Crudes. *NACE Corrosion 1998*, Paper No.577

8. Chambers, B. D., Srinivasan, S.; Kane, R. D., Blades, M. A. (2012). An Experimenta lMethod for Evaluation of Crude Corrosivity - Naphthenic Acid and Sulfidic Corrosion of Oil Fractions. *NACE Corrosion 2012,* Paper No. 1564

9. Craig H.L. (1996) Temperature and Velocity Effects in Naphthenic Acid Corrosion. *NACE Corrosion 1996,* Paper No.603

10. Kane R.D., Trillo E., Maldonado J.G. (2002) Naphthenic Acid Corrosion: Roles of Velocity. Alloying, TAN and Sulphur Species. *Eurocorr/2004*, European Federation of Corrosion, Budapest, Hungary, October, 2003

11. Craig H.L. (1995) Naphthenic Acid Corrosion in the Refinery. *NACE Corrosion 1995.* Paper No.333

12. Qu, D. R., Zheng, Y. G., Jing, H. M., Jiang, X., Ke, W. (2005) Erosion-Corrosion of Q235 and 5Cr1/2Mo Steels in Oil with Naphthenic Acid and/or Sulphur Compound at High Temperature. *Material Corrosion,* Vol. 56, Issue 8, 533-541

13. McConomy H. F.(1963) High-Temperature Sulfidic Corrosion in Hydrogen Free Environment, *Proceedings of the American Petroleum Institute, Refining Division* Vol. 43 (III), 78-96

9. Figures

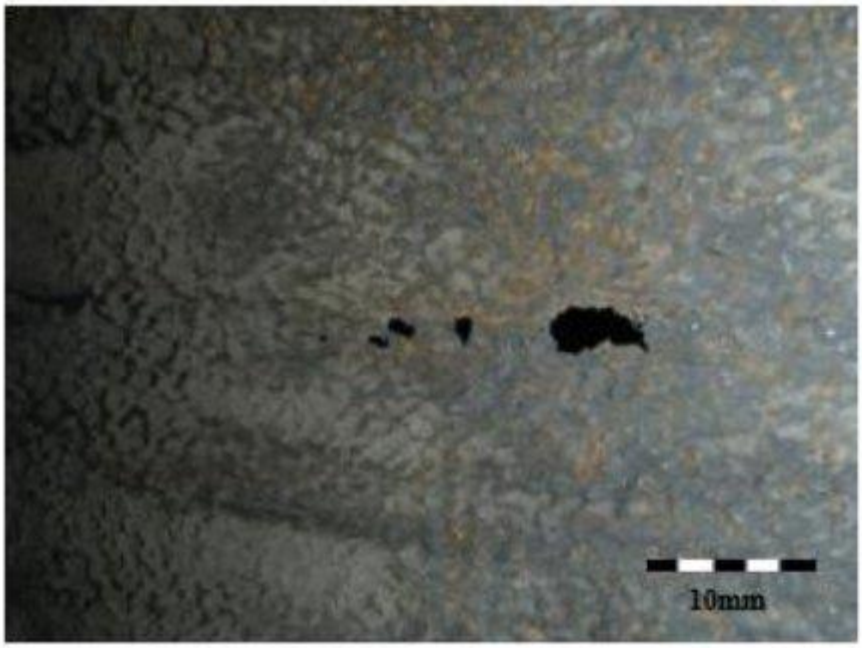

Figure 1: Photograph of the internal failure surface of crude furnace outlet line

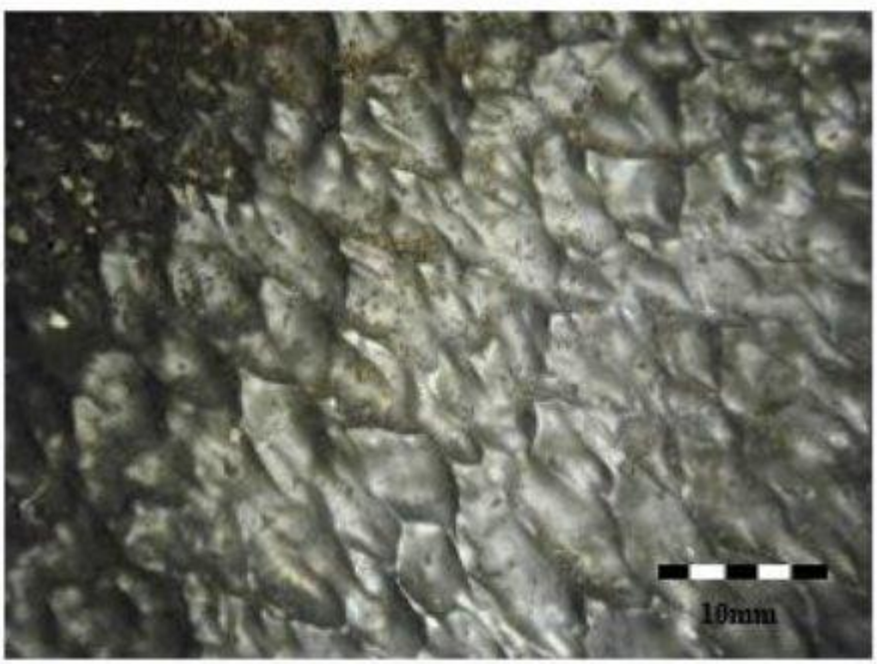

Figure 2: Photograph of internal pitting observed on vacuum distillation furnace tube bends

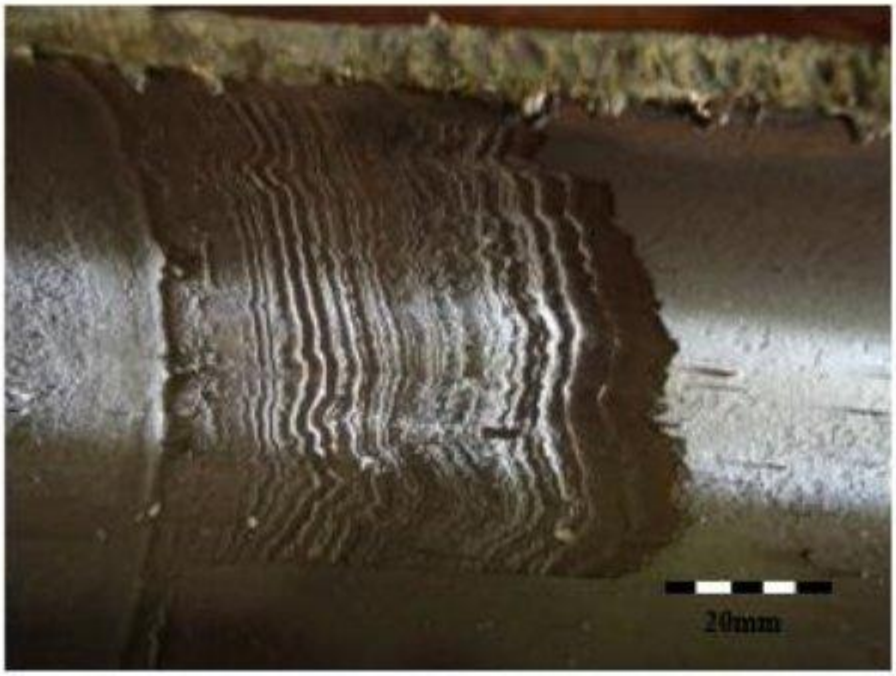

Figure 3: Photograph of material gouging observed on internal surface of vacuum distillation furnace tube straight sections

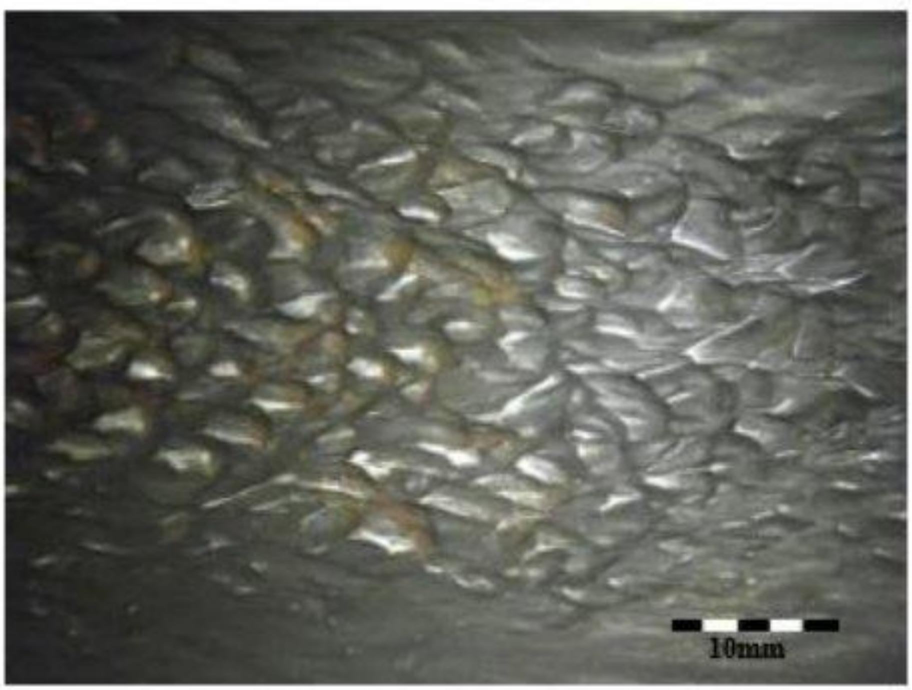

Figure 4: Photograph of internal pitting observed in crude furnace radiant heater tube bend

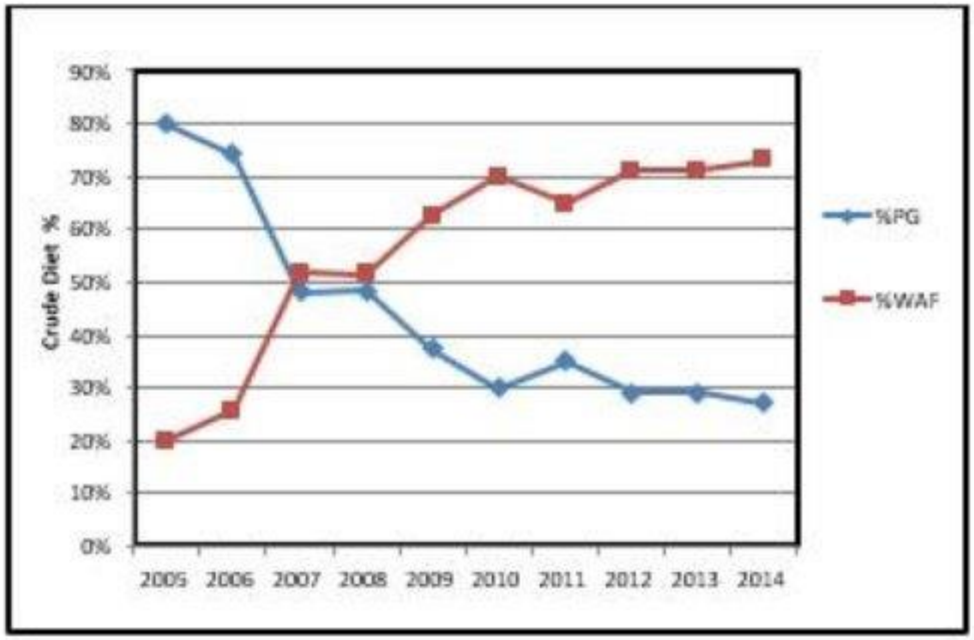

Figure 5: Proportion of West African (WAF) and Persian Gulf (PG) crude processing from 2005 - 2014

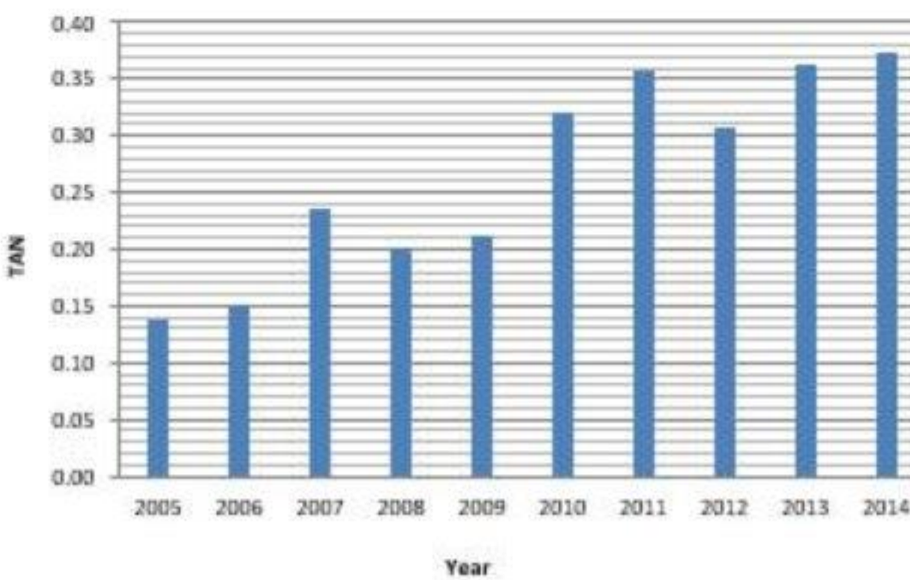

Figure 6: Refinery average crude TAN values from 2005 - 2014

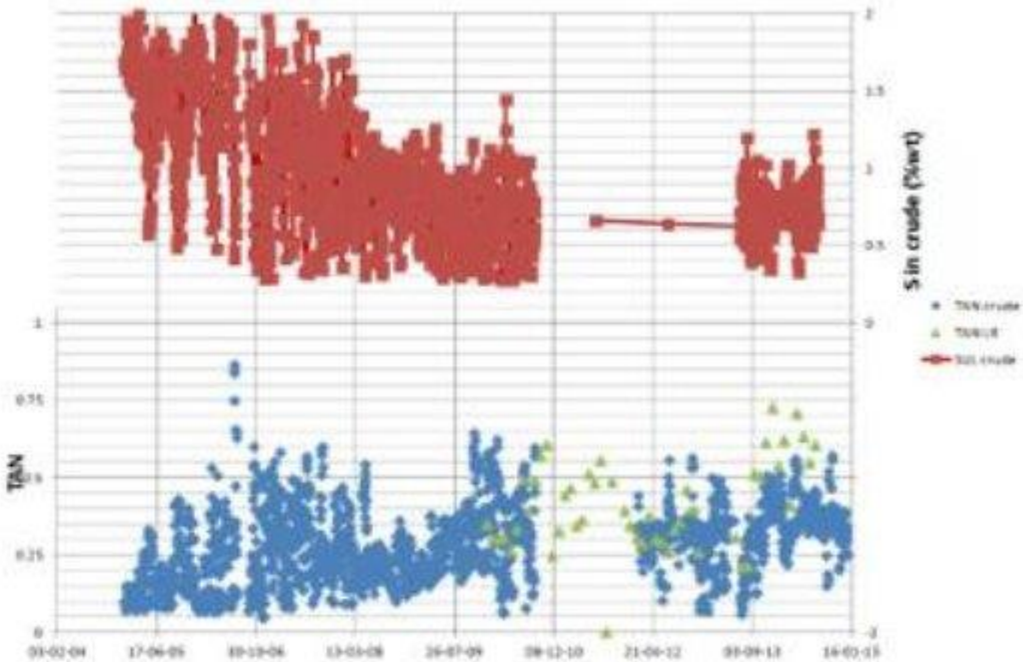

Figure 7: Transformation of crude properties showing progressive drop in crude sulphur level and increase in TAN

Appendix 2

CONFIDENTIALITY AND RESTRICTED USE AGREEMENT

SHELL AND BP SOUTH AFRICA PETROLEUM REFINERIES (PTY) LTD
Registration No. 1960/000007/07
("referred to as SAPREF")
and

University of Witwatersrand
____.
("referred to as RECIPIENT")

RECITALS

1. RECIPIENT wishes to have access to information belonging to SAPREF and which SAPREF considers confidential, proprietary and / or valuable; and

2. SAPREF is willing to disclose such information as SAPREF deems appropriate, and RECIPIENT is willing to receive such information, for the **Purpose** (as defined) on the following terms and conditions.

NOW THEREFORE IT IS AGREED AS FOLLOWS:

1. The following expressions shall have the meanings specified in this Clause.

    1.1 "**Affiliate** of SAPREF" means Shell SA Refining (Pty) Ltd and BP Southern Africa (Pty) Ltd;

    1.2 "the **Effective Date**" means the date of the last party signing this agreement;

    1.3 "the **Purpose**" means the investigation into the potential effectiveness and economic viability of the implementation of an online corrosion monitoring system on Sapref crude distillation and high vacuum units

    1.4 "**SAPREF Information**" relates to data regarding crude distillation and high vacuum units piping and equipment design, history, corrosion rates, and estimated remaining life as well as past processed crudes' corrosivity properties which includes but is not limited to Total Acid Number(TAN) and Sulphur content. Information on the process conditions, namely temperatures, pressures and flow rates of the before mentioned equipment may also be used in the investigation.

2. In consideration of the disclosure of **SAPREF Information** to RECIPIENT, RECIPIENT agrees:

   2.1 save as set forth in Clause 3, not to disclose any **SAPREF Information** to any third party, (including, for the avoidance of doubt, disclosure in any patent application or to any patent office); and

   2.2 not to use **SAPREF Information** except for the **Purpose**;

3. Notwithstanding the provisions of Clause 2, RECIPIENT may disclose such **SAPREF Information** as is reasonably necessary to carry out the **Purpose** to those employees of RECIPIENT who (i) have a reasonable need to know and use such information in furtherance of completing the **Purpose**; (ii) have been informed of the confidential nature of the **SAPREF Information** in question; and (iii) are bound by written obligations no less stringent than those assumed by RECIPIENT hereunder.

   Where it is reasonably necessary for the carrying out the **Purpose** for RECIPIENT to disclose information to any third party, RECIPIENT guarantees that secrecy obligations not less stringent than those contemplated in this Agreement shall be observed by such third party, to which **SAPREF Information** will be disclosed.

4. The provisions of Clause 2 above shall not apply to any **SAPREF Information** which, at the time it is received or obtained by RECIPIENT,

   4.1 is lawfully known to RECIPIENT without binder of secrecy; or

   4.2 is publicly available

   and shall cease to apply to any **SAPREF Information** which, after it is received or obtained by RECIPIENT,

   4.3 is received or obtained by RECIPIENT without restriction on disclosure from a source free to disclose it other than SAPREF or an agent or **Affiliate** of SAPREF; or

   4.4 becomes publicly available through no act or omission on the part of RECIPIENT.

   The foregoing exceptions shall only be effective to the extent that RECIPIENT can prove the facts.

5. Specific disclosures made hereunder shall not be deemed to be subject to any of the above exceptions merely because they are embraced by general disclosures in the public knowledge or literature or in the possession of RECIPIENT, and any combination of features disclosed hereunder shall not be deemed subject to the above exceptions merely because individual features are in the public knowledge or literature or in the possession of RECIPIENT but only if the combination itself is publicly available or lawfully known to RECIPIENT without binder of secrecy.

6. RECIPIENT shall have the right, to the extent necessary to carry out the **Purpose**,

   6.1 to make copies of **SAPREF Information**; and
   6.2 to use, reproduce, transform or store any **SAPREF Information** in a computer or electronic information retrieval system under control by RECIPIENT.

7. If RECIPIENT receives a subpoena, order, notice or other legal process seeking disclosure of **SAPREF Information**, RECIPIENT shall immediately notify SAPREF in order to allow SAPREF

the opportunity to oppose the order, notice or process, or seek a protective order. If requested by SAPREF, RECIPIENT shall co-operate fully with SAPREF in contesting such disclosure. Except as such demand shall have been limited, quashed or extended, RECIPIENT may thereafter comply with such demand, but only to the extent required by law. Where a protective order is obtained by SAPREF, nothing in this Agreement shall be construed to authorise RECIPIENT to use in any manner or disclose **SAPREF Information** to Third Parties other than such governmental or judicial agency or body or beyond the scope of the protective order.

8. At the request and option of SAPREF, RECIPIENT shall

   8.1 either destroy or return promptly to SAPREF, or its nominee, all tangible records containing **SAPREF Information** or excerpts or portions thereof or other information derived from **SAPREF Information**, which are in the possession of RECIPIENT; and

   8.2 remove all **SAPREF Information** or excepts or portions thereof (including any backup copies) from any computer and/or other electronic storage system and in such case RECIPIENT shall, if so requested by SAPREF, provide independent auditor's confirmation of completion of such removal.

9. Nothing in this Agreement shall be construed as granting RECIPIENT a licence under intellectual property rights of SAPREF or an **Affiliate** of SAPREF, or any rights in respect of **SAPREF Information** other than those specifically set out herein. Furthermore, RECIPIENT shall have no right to make any changes, modifications or enhancements to **SAPREF Information**, or to create any derivative work from such **SAPREF Information**.

10. SAPREF shall not be liable in negligence or otherwise for any loss, damage, cost and expenses arising from or in connection with the use made by RECIPIENT of any **SAPREF Information** or any allegation that such use infringes any third party intellectual property right or otherwise. RECIPIENT shall indemnify SAPREF against any third party claim for loss or damage (including personal injury or death) arising from or in connection with RECIPIENT's use of any **SAPREF Information**.

11. RECIPIENT hereby certifies that in exercising its rights and in carrying out its obligations under this Agreement, it shall comply with all applicable governmental laws, regulations, decrees and orders. This clause shall survive the termination or expiry of this Agreement.

12. SAPREF makes no representation and extends no warranty, express or implied, and assumes no responsibilities whatsoever with respect to the completeness, utility or accuracy of any **SAPREF Information**; merchantability or fitness for a particular purpose; or the freedom from infringement of any third party intellectual property rights by RECIPIENT's use of **SAPREF Information**.

13. RECIPIENT shall not assign any of its rights or obligations arising from this Agreement without the prior written consent of SAPREF.

14. This Agreement shall be effective from the **Effective Date**.

15. This Agreement, and the relationship between SAPREF and RECIPIENT under this Agreement, shall in all respects be interpreted in accordance with and governed by the law of South Africa and the Parties agree to submit to the exclusive jurisdiction of the South African High Courts in relation to any dispute arising out of or in connection with this Agreement (whether based in contract, delict (including negligence) or otherwise).

SIGNED at ________________________ this _ day of ____________ 2013

As witnesses

____

For **SAPREF**

1.__________________________

who hereby warrants that (s)he is duly authorised to sign this agreement on its behalf

2.___________________________

Full names ....

Designation ....

SIGNED at ________________________ this _ day of ____________ 2013

As witnesses

____

For RECIPIENT

1.__________________________

who hereby warrants that (s)he is duly authorised to sign this agreement on its behalf

2.___________________________

Full names ....

Designation ....

Appendix 3

C7101 – ATMOSPHERIC COLUMN	
Equipment:	C7101
Service (product):	CRUDE
Process temperature:	115-350 °C
Material of construction:	BS 1501 151 28A + clad A240 TP405. (CS + SS clad TP405). (Up to tray 16. ±8.5m elevation)
Internally coated/clad	*Bottom section clad SS TP405 up to* ±8.5m elevation.

Was the column (partially) renewed? If yes; at what date and why?	No
Was the column or components repaired? If yes; at what date and why?	Yes, 2001 major repairs carried out due to HTS & NAC

Installation date:	1971
Internal inspection dates:	**Inspection history:** *NB. Report only on location of internal corrosion, depth, type, extent and possible cracks or other forms of distortion like blisters. Also report when there is no degradation.*
August 1998	TRAY 1 - 12: NB: 405 original cladding extents to tray 10 support ring. Strip lining carried out in 1992 was from above tray support ring 10 to below tray 13 support ring. TRAYS 13 - 16: The c/s strip between 13 and 14 was corroded to perforation. Trays 14 & 15 were removed and the area between tray 13 up to tray support ring 16 was gritblasted for strip lining. 13 & 14: General crater type pitting corrosion up to 4.0mm measured, especially in the north section extending about 5 metres circumferentially. The 2 tray support beam gussets (c/s) had corroded from 10mm down to 2mm. Tray support had 2mm corrosion. General crater type pitting up to 4.5mm measured, throughout shell. DRAW OF NOZZLES N6/N7 - 14" (Nom w/t 12.7mm): Ultrasonics indicated minimum w/t of 12.0mm. Since the nozzles were located in the strip lined area they were sleeved in S/S 316 and the flange section was machined back 3mm and weld overlayed with E309 and machined. The flat bar cross section which acts as a vortex beaker was made S/S 410 plate. TRAY SUPPORT RING 49: Found to be severely corroded to perforation in places. Complete new tray support ring in S/S 410 was welded in with 309 consumable.
2001	CDU2 was shutdown as planned to carry out tray modification work to the stripper tray section of the column. A new tray no. 2 was installed. New down-comers were installed in existing trays 1, 3, 4, 5, and 6.
	From Tray 16 the shell is stainless steel clad including the bottom head. The cladding was found still to be in a satisfactory condition without any abnormalities being evident. Only in the vicinity of tray 13 minor areas of the carbon steel were exposed. All the nozzles that were accessible were found to be in the same condition as the shell

	within the nozzle area. The man way necks were noted to have wide spread pitting of ±1mm in depth. All the tray rings were still in a satisfactory condition except for number 48 had corroded to perforation and about 2.5 meter had to be replaced on the West side of the column. On tray ring 16 a 2 meter section was replaced.

NDT dates:	**NDT history:** *NB. Report wall thickness results separately for sections in different corrosion loops and report NDT technique.*
Sep 2011	Internal visual noted ±3mm pitting on the top head and ±1.5mm general corrosion on the shell just above the cladding. Man way neck in the vicinity of tray 13 has pitting corrosion of ±1mm

Design corrosion allowance:	3.0 mm
Design Life:	30 years
Measured CR:	Bottom section & LGO – L HGO section - H

C7102 – HGO STRIPPER

Equipment:	C7102
Corrosion Loop(s):	CL7100-08
Service (product):	HGO Steam
Process temperature:	277 °C
Material of construction:	BS 1501 151 28A. (CS)
Column specifics:	*Trays 8 off*
Internally coated/clad	*None*

Was the column (partially) renewed? If yes; at what date and why?	No
Was the column or components repaired? If yes; at what date and why?	No

Installation date:	1971
Internal inspection dates:	**Inspection history:** *NB. Report only on location of internal corrosion, depth, type, extent and possible cracks or other forms of distortion like blisters. Also report when there is no degradation.*
February 2011	The top head was noted to display general surface roughness and wide spread pitting corrosion of±2mm The shell from the head down to the tray was noted to have pitting corrosion of ±1mm deep. The shell section below the bottom tray down to the bottom head where noted to have isolated pitting corrosion of ±0.5mm. All the nozzles were found to have the same condition as the shell. The man way neck internal was noted to have widespread pitting of ±2mm . All the trays were replace during this outage as requested.

Design corrosion allowance:	3.0 mm
Design Life:	30 years
Measured CR:	M

C7103 – LGO STRIPPER

Equipment:	C7103
Corrosion Loop(s):	CL7103-08
Service (product):	LGO, STEAM
Process temperature:	240 °C
Material of construction:	BS 1501 151 28A. (CS)
Column specifics:	*Trays 10 off*
Internally coated/clad	*None*

Was the column (partially) renewed? If yes; at what date and why?	No
Was the column or components repaired? If yes; at what date and why?	No

Installation date:	1971
Internal inspection dates:	**Inspection history:** *NB. Report only on location of internal corrosion, depth, type, extent and possible cracks or other forms of distortion like blisters. Also report when there is no degradation.*
November 1976	Vessel internal is in a very good condition. Minor surface roughening on walls and trays. All tray down comers secure. All nozzle & fitting secure.
September 2011	The internal surface was recorded as having general corrosion of ±1mm throughout. The bottom head displayed general corrosion of 1.5mm concentrated around the vortex breaker.All the trays, tray rings,down comers and dowm comer brackets display general corrosion of 1mm and still securely in postion. All the nozzles were noted to have general corrosion of ±1mm

NDT dates:	**NDT history:** *NB. Report wall thickness results separately for sections in different corrosion loops and report NDT technique.*
September 2011	UT Wall thickness on the shell revealed a minimum of 9.2mm and a maximum of 9.8mm from original of 11.1mm. Loss of 1.9mm
August 2011	Profile RT was carried out on the small bore nozzles K5&6 revealed a minimum of 6.89mm from original of 8.74mm. Loss of 1.85mm

Design corrosion allowance:	3mm
Design Life:	30 years
Measured CR:	L

C7701 HIGH VACUUM COLUMN

Equipment:	C7701
Service (product):	Short residue
Design temperature:	Top: 350°C, Bottom: 405°C
Material of construction:	Top: HII plate Carbon steel, middle: 15Mo3 internally cladded with SS410/405, bottom: 15Mo3 internally cladded with SS410/405
Column specifics:	Column has 3 packed sections and trays
Internally cladded?	The bottom section up to and including the swage section is internally cladded with SS410S or SS405, most probably roll bonded (supported by observed bulging of SS clad in 2004).

Was the column (partially) renewed? If yes; at what date and why?	no
Was the column or components repaired? If yes; at what date and why?	no

Installation date:	1976
Internal inspection dates:	Report only on location of internal corrosion, depth, type, extent and possible cracks or other forms of distortion like blisters. Also report when there is no degradation.
13-Oct-2011	The demister was renewed. The tray supports in bottom section were completely corroded and had to be renewed. The baffles between the draw off trays of tray 3 were all completely corroded and were therefore renewed. The baffle metallurgy was upgraded from 410SS to 304SS. The 410SS shell cladding was pitted in areas, most significantly along a weld on the west side of the column. The worst pitting measured 1.8mm deep.
August 1990	Severe fouling with coke of spargers. Fouling also found in bottom section of column.
July 1982	All vanes removed and renewed in AISI 316. Several of the old vanes were found to have eroded at the point of product contact, several to perforation. Other parts no abnormalities.
May 1981	Schoepentoeter – partially dislodged, two sections collapsed broken away. Vane attachment throughout cracked and torn. AISI 410 material found severely embrittled. Heating to 600ºC then water quenching removed brittleness fully. Severe fouling with coke of pall rings. Other parts no abnormalities.
February 1979 & 1978	The schoepentoeter was very badly damaged and required extensive welding to repair the cracked welds and torn plates. Other parts no abnormalities.

NDT dates:	Report wall thickness results separately for sections in different corrosion loops
Sept. 2013	North side 11.0 mm was measured and 10.8 mm on the South West section on strake just above swage, from original thickness of 17mm. This area is not clad with 410SS

Design corrosion allowance:	3mm
Design Life:	30 years
Measured CR:	Middle: H, bottom: M

F7101A – CRUDE FEED FURNACE

Equipment:	F7101A
Service (product):	Preflashed Crude Oil
Process temperature:	300 - 360°C
Material of construction:	A106 Gr.B (Tubes 1 – 8). (CS) A335 Gr.P5 (Tubes 9 – 30). (5Cr½Mo).
PWHT? (Y/N)	Yes. A335 Gr.P5 (Tubes 9 – 30). (5Cr½Mo).
Furnace specifics:	*Radiant, Vertical, 4 coils with 30 tubes each, 8 off 6" CS. 16 off 6" 5Cr and 6 off 8" 5 Cr*

Were the coils ever renewed? If yes; at what date and why?	Furnace tubes 9 to 30 upgraded to 5Cr½Mo material. September 1992
Were coils or other components repaired? If yes; at what date and why?	Yes, The U bends were replaced on all the 8" tubes. July 2015

Installation date:	1971/2
Internal inspection dates:	**Inspection history:** ***NB. Report only on location of internal corrosion, leaks depth, type, extent and possible cracks, coil distortion & swelling/bulging, external & internal fouling, hanger rods, sliding supports, shadow test. Also report when there is no degradation. Report on any metallurgical investigations done***
1986	31 tubes replaced due to internal corrosion All CS
1987	Cross over's renewed
January 1988	1 tube leaked and repaired
October 1988	1 tube leaked and repaired
September 1989	1 tube leaked and repaired
September 1992	Furnace tubes upgraded to 5Cr
November 2004	All the tubes were removed so that the refractory lining can be replaced. The tubes were noted to be still in a good condition.
October 2014	Furnace shut down due to a tube leak. The return bend on the tubes 29a and 30a was found to be leaking. The reason for the failure is due to internal corrosion/erosion.. The return bend and was replaced. The corrosion was heavy pitting/ scalloped surface concentrated at the bends.
July 2015	The crossover spool between the 6" and the 8" tubes displayed server NAC on the bends and the reducer, heavy localised pitting. The elbows were replaced, and the reducers were weld repaired. On the 8" section of the coil the bottom U bends and 500mm of tubing were replaced due to NAC with the bends being 9 Cr and the tubes being 5 Cr.

NDT dates:	**NDT Results:** ***NB. Report wall thickness results separately for sections in different corrosion loops and report NDT technique.***
	N/A

Design corrosion allowance:	3mm
Design Life:	30 years
Measured CR:	H

F7101B – CRUDE FEED FURNACE

Equipment:	**F7101B**
Service (product):	**Preflashed Crude Oil**
Process temperature:	**300 - 360°C**
Material of construction:	**A106 Gr.B (Tubes 1 – 8). (CS)** **A335 Gr.P5 (Tubes 9 – 30). (5Cr½Mo).**
PWHT? (Y/N)	**Yes. A335 Gr.P5 (Tubes 9 – 30). (5Cr½Mo).**
Furnace specifics:	***Radiant, Vertical, 4 coils with 30 tubes each 8 off 6" CS 16 off 6" 5Cr 6 off 8" 5 Cr***

Were the coils ever renewed? If yes; at what date and why?	Furnace tubes 9 to 30 upgraded to 5Cr½Mo material. September 1992
Were coils or other components repaired? If yes; at what date and why?	**Only as noted in the internal inspection history**

Installation date:	**1971/2**
Internal inspection dates:	**Inspection history:** ***NB. Report only on location of internal corrosion, leaks depth, type, extent and possible cracks, coil distortion & swelling/bulging, external & internal fouling, hanger rods, sliding supports, shadow test. Also report when there is no degradation. Report on any metallurgical investigations done***
1981	Tube 17d renewed due to excessive bulging.
1986	Wall loss on 31 tubes(4.5mm nominal 11) Renewed 31 tubes CS
1988	Tube 17b leaked and renewed
1989	Tube 29d leaking and renewed. Coking found
1990	Tube 15c leaked and renewed. 8 other tubes with flame impingement
1990	8" coils 25-30 renewed. 6" coils turned 180°
1992	New furnace tubes 5 Cr
September 2011	Minimal measured wall loss
May 2015	Tube 29-30 bends (hottest furnace tubes) cut out for inspection and found severely corroded by NAC which was not detected by intelligent pigging inspection.

NDT dates:	**NDT Results:** ***NB. Report wall thickness results separately for sections in different corrosion loops and report NDT technique.***
	No formal NDT UT wall thickness report available only what was noted in the inspection history reports.
July 2015	UT Wall thickness on the 24/25 6" elbow coil C was recorded at 9.1mm from an original nominal of 10.97mm.

Design corrosion allowance:	3.0 mm
Design Life:	30 years
Measured CR:	H

F7101C – CRUDE FEED FURNACE – CONVECTION SECTION

Equipment:	**F7101C**
Service (product):	**Preflashed Crude Oil / Flue gas**
Process temperature:	**235 - 300°C**
Material of construction:	**A106 Gr.B (Tubes 1 – 8). (CS)** **A335 Gr.P5 (Tubes 9 – 30). (5Cr½Mo).**
Furnace specifics:	***Convection, Horizontal, 3 banks with 16 coils with 5 tubes each, 100 NB SCH 40 (6.04mm)***

Were the coils ever renewed? If yes; at what date and why?	Furnace tubes 9 to 30 upgraded to 5Cr½Mo material. September 1992
Were coils or other components repaired? If yes; at what date and why?	Aug 1998. Complete module constituted of 3 banks and a super heater coil was replaced. Top bank of tubes was replaced in 2013. No reason was given.

Installation date:	**1972**
Internal inspection dates:	**Inspection history:** ***NB. Report only on location of internal corrosion, leaks depth, type, extent and possible cracks, coil distortion & swelling/bulging, external & internal fouling, hanger rods, sliding supports, shadow test. Also report when there is no degradation. Report on any metallurgical investigations done***
May 1981	The sixth tube (tube 6) from the west side on the top bank was renewed because of excessive scaling and loss of wall thickness.
March 1985	4th tube from west bowed upwards. This tube plus the two either side have a light oxidize scale from overheating, all spacer lugs also indicate that they have been overheated.
September 1992	Top man way: 3 tubes found to be cracked open due to overheating. Internal coke lay down in tube to 1mm. Leaking tubes were (from west to east) 8, 7, & 3. Tubes also replaced due to thinning were 10, 9 & 5.
July 1996	F7101C was shut down during July 1996 due to crude leak.
January 1998	Crude was found weeping from tube 15 from east, top row shock tubes. Leak approximately 1m away from the header.
March 2010	Top Bank: Leak on one of the shock tubes due to internal coking. The failure mode was longitudinal cracking at the 12 o'clock position of the
May 2011	Top Bank: Leak on one of the shock tubes due to internal coking & overheating (fish-mouth). The failure mode was the same as that observed in 2010 - longitudinal crack at the 12 o'clock position of the Tube 5.
January 2012	Finned Tubes: CD2 was shut down due to a suspected tube leak. During the inspection 3 tubes were confirmed to be leaking due to longitudinal cracks at a 12 o'clock position. The
January 2013	The top bank comprises of 6 rows of tubes with the top 3 rows of tubes shock tubes. These tubes have been up graded to 5 Cr tubes. The next 3 rows were replaced with C/S finned tubes.

NDT dates:	NDT Results: *NB. Report wall thickness results separately for sections in different corrosion loops and report NDT technique.*
March 2010	RT survey of 4” tubes for coking and wall thicknesses. Min WT recorded = 5.42 mm from original of 6.02 mm

Design corrosion allowance:	3mm
Design Life:	30 years
Measured CR:	H

F7701A – VACUUM HEATER – RADIANT SECTION

Equipment:	**F7701A**
Service (product):	**Long residue, Dirty wash oil**
Process temperature:	**370 - 410°C**
Material of construction:	**A312 TP317L. (SS)**
Furnace specifics:	**Radiant section**

Were the coils ever renewed? If yes; at what date and why?	29/11/2002 – tubes renewed due to internal corrosion
Were coils or other components repaired? If yes; at what date and why?	2002, 2007, 2011, 2013, 2014, 2015

Installation date:	**1976**
Internal inspection dates:	Inspection history: *NB. Report only on location of internal corrosion, leaks depth, type, extent and possible cracks, coil distortion & swelling/bulging, external & internal fouling, hanger rods, sliding supports, shadow test. Also report when there is no degradation. Report on any metallurgical investigations done*
29 Nov 2002	Furnace F-7701A visually and ultrasonically inspected. Severe thinning and scaling found mainly on the 12" outlet tubes. The 12" outlet tube in coil 6 was found sucked inward and perforated. The 12" outlet tube was found to have a pin hole leak.
28 July 2003	FP2 HVU Furnace, have been found in a poor condition due to corrosion.
02/04/2007	A 12"tube leak developed in F7701 (N/E Cell). Cause of the failure was attributed to high temperature sulphur corrosion, coking and external oxidation.
06/05/2010	Leaked on a 8" to 10" short radius 180 degree return bend of the outlet radiant section of coil 13.
26/10/2010	Upon entry into the furnace inspection revealed four of the 6" 180 LR return bends to have leaked. Ultrasonic wall thickness measurements on all 16 return bends indicated thinning in exactly the same region on all of the coils. General erosion pattern corrosion.
26/06/2014	Numerous leaks and repairs instituted on radiant coil tubes
02/07/2015	As a result of internal corrosion and as part of the planned work, the 6-inch top bends of all coils, including a section of pipe/reducer on either side of the return bend, were replaced due to previous severe pitting corrosion. Numerous Leaks and repairs instituted on radiant coil tubes

Design corrosion allowance:	3mm
Design Life:	30 years
Measured CR:	H – numerous failures

F7701B – VACUUM HEATER – CONVECTION SECTION

Equipment:	**F7701B**
Service (product):	**Long Residue, Dirty Wash Oil**
Process temperature:	**345 - 375°C**
Material of construction:	**A335 P5 tubes. (5Cr½Mo)**
Furnace specifics:	***Convection***

Were the coils ever renewed? If yes; at what date and why?	DURING 2015 TA (MAY 2015) THE SHOCK TUBES COMPRISING OF TWO ROWS WERE REPLACED (LIKE FOR LIKE) DUE TO COKE BUILD UP and wall loss.
Were coils or other components repaired? If yes; at what date and why?	

Installation date:	**1976**
Internal inspection dates:	Inspection history: *NB. Report only on location of internal corrosion, leaks depth, type, extent and possible cracks, coil distortion & swelling/bulging, external & internal fouling, hanger rods, sliding supports, shadow test. Also report when there is no degradation. Report on any metallurgical investigations done*
02/04/2011	The shock tubes were found to be snaked and oxidized due to overheating. Oxidation scale up to 2.5mm measured on the tubes between 10 & 2'o clock position. Int coke layer raging from 10mm - 25mm was noted between 10 & 2 ' o clock position. Significant wall thickness thinning between 10 & 2 o clock position, worst area being at 12 o Clock position, min measured was 2.5mm from original of 7.62mm

NDT dates:	**NDT Results:** ***NB. Report wall thickness results separately for sections in different corrosion loops and report NDT technique.***

Design corrosion allowance:	3mm
Design Life:	30 years
Measured CR:	H

S7710A – WASH OIL FILTER

Equipment:	S7710A
Service (product):	Heavy waxy
Process temperature:	265°C to 275°C
Material of construction:	SA 516 Gr 60N
Equipment specifics:	Filter basket, filter element
Internally coated? Or cladded?	None

Was the equipment (partially) renewed? If yes; at what date and why?	2011
Was the equipment or components repaired? If yes; at what date and why?	No

Installation date:	1976
internal inspection dates:	**Inspection history:** ***NB. Report only on location of internal corrosion/erosion, depth, type, extent and possible cracks or other forms of distortion like blisters. Also report when there is no degradation.***
August 1998	Clean and free from visible corrosion / defects.
	No inspection done since after installation of the new filter in 2011.

NDT dates:	**NDT Results:** ***NB. Report wall thickness results separately for sections in different corrosion loops and report NDT technique.***
November 2003	UT wall thickness was done at random areas and revealed minimum reading of 10.94mm on shell
	Latest readings after installation of the new filter not available.

Design corrosion allowance:	3mm
Design Life:	30 years
Measured CR:	H

S7710B – Wash Oil Filter

Equipment:	S7710B
Corrosion Loop(s):	CL7700-3B
Service (product):	Heavy waxy
Process temperature:	265°C to 275°C
Material of construction:	SA 516 Gr 60N
Equipment specifics:	Filter basket, filter element
Internally coated? Or cladded?	Unknown

Was the equipment (partially) renewed? If yes; at what date and why?	2011
Was the equipment or components repaired? If yes; at what date and why?	No

Installation date:	1976
internal inspection dates:	**Inspection history:** ***NB. Report only on location of internal corrosion/erosion, depth, type, extent and possible cracks or other forms of distortion like blisters. Also report when there is no degradation.***
September 1992	In a very good condition.
August 1998	Clean and free from visible corrosion / defects.
	No inspection done since after installation of the new filter in 2011.

NDT dates:	**NDT Results:** ***NB. Report wall thickness results separately for sections in different corrosion loops and report NDT technique.***
November 2003	Ut wall thickness was done at random areas and revealed minimum reading of 11.05mm on shell
	Latest readings after installation of the new filter not available.

Design corrosion allowance:	3mm
Design Life:	30 years
Measured CR:	H

S7711 – Waxy Distillate Filter

Service (product):	Heavy waxy
Process temperature:	220°C to 230°C
Process pressure:	800
Material of construction:	SA 106 Gr.B
Equipment specifics:	Filter basket, filter element
Internally coated? Or cladded?	Unknown

Was the equipment (partially) renewed? If yes; at what date and why?	No
Was the equipment or components repaired? If yes; at what date and why?	No

Installation date:	**1986**
internal inspection dates:	**Inspection history:** ***NB. Report only on location of internal corrosion/erosion, depth, type, extent and possible cracks or other forms of distortion like blisters. Also report when there is no degradation.***
September 1986	The vessel was installed as part of the "Deep Flasher" project and hydraulically tested to 2210kPa after installation.
September 1992	In very good condition, no corrosion. UT measurements Shell 9.5-10.5mm, Shell cover 10.0mm - OK.
August 1998	Clean and free from visible corrosion / defects
October 2001	Surfaces generally roughened and product scaled.
June 2008	Internal surfaces good & coated with tightly adhering product scale.

NDT dates:	**NDT Results:** ***NB. Report wall thickness results separately for sections in different corrosion loops and report NDT technique.***
March 2004	UT was done on the filter and revealed a minimum reading of 10.26mm on the bottom head and the NWT is 9.52mm, no wall loss. Minimum reading of 16.27mm on nozzle N3 and NWT is 16.6mm, wall loss of 0.33mm. Minimum reading of 16.56mm on nozzle N4 and the NWT is 16.6mm, wall loss of 0.04mm.
August 2009	NDT was done on the Nozzles and revealed a minimum reading of 12.8mm on nozzle N4 and the original is 16.6mm, wall loss of 3.8mm.

Design corrosion allowance:	3mm
Design Life:	30 years
Measured CR:	H

V7107 – HGO DRAW OFF POT

Equipment:	**V7107**
Corrosion Loop(s):	**CL08**
Service (product):	HGO
Operating temperature:	277 °C
Material of construction:	BS 1501 151 28A. (CS)
Internally coated? Or clad?	***Nil***

Was the vessel (partially) renewed? If yes; at what date and why?	No
Was the vessel or components repaired? If yes; at what date and why?	No

Installation date:	1971
internal inspection dates:	**Inspection history:** ***NB. Report only on location of internal corrosion, leaks, depth, type, extent and possible cracks or other forms of distortion like blisters. Also report when there is no degradation.***
September 2011	Limited inspection through the hand hole and what nozzles were open revealed slight surface pitting corrosion estimated to 2mm deep. The top head and the bottom cone are in the same condition as the shell. All accessible welds were noted to be well defined. All the nozzle bores revealed surface corrosion pitting of about ±2mm deep.

NDT dates:	**NDT results:** ***NB. Report wall thickness results separately for sections in different corrosion loops and report NDT technique.***
September 2011	UT Wall thickness on the shell revealed a minimum of 11.8mm and a maximum of 12mm from a nominal of 12.7mm
September 2011	UT Wall thickness on nozzle N1 revealed a minimum of 10.8mm and a maximum of 11mm from a nominal of 11.12mm
May 2015	Profile RT on nozzle N1 revealed a minimum of 7mm and a maximum of 7.5mm from a nominal of 11.12mm

Design corrosion allowance:	3mm
Design Life:	30 years

V7702 – LOWER CIRCULATION / REFLUX VESSEL

Equipment:	V7702
Service (product):	Heavy waxy
Operating temperature:	265°C to 280°C
Material of construction:	BS.1501-151-GR.28A. (CS)
Vessel specifics:	Horizontal with vortex breaker
Internally coated? Or clad?	***None***

Was the vessel (partially) renewed? If yes; at what date and why?	No
Was the vessel or components repaired? If yes; at what date and why?	Yes; vortex breaker renewed in 2004 due to thinning caused by high temp sulphur corrosion. In 2015, repairs were done on the Nozzle N4 and Manway A1, due to indications detected with MPI.

Installation date:	1976
internal inspection dates:	**Inspection history:** ***NB. Report only on location of internal corrosion, leaks, depth, type, extent and possible cracks or other forms of distortion like blisters. Also report when there is no degradation.***
July 1982	Surfaces showed very light roughening beneath the scale.
Sep 1992	Internal: In good condition/ no corrosion.
Oct 2004	Shell: General roughening up to 0.5mm maximum measured. The North West side of the shell has some significant erosion taking place; area affected is between 9 & 6 o'clock position. Width of the area is 300mm. East head: General roughening with smooth wastage. West head: Significant erosion noted between 9 & 6 o'clock position. The West dished to shell weld has some erosion/ preferential attack in the root up to 1.75mm in depth 1000mm in length. Vortex Breaker: For outlet nozzle (N1) - was severely thinned due to high temp sulphur corrosion. Nominal w/t is 8.0mm remaining w/t was 2.5mm. The vortex breaker was renewed.
Sep 2011	Shell: In the shell the internal surface was smooth as a result of uniform thinning. The worst visible corrosion was noted along the bottom in the 6 o'clock position where minor pitting to 0.9mm was observed.
May 2015	General pitting corrosion about 0.5mm deep was noted. Drain nozzle with preferential corrosion of +/-1mm deep. Other nozzles with slight preferential corrosion. Slight pitting corrosion <0.5mm on the vortex breaker.

NDT dates:	**NDT results:** ***NB. Report wall thickness results separately for sections in different corrosion loops and report NDT technique.***

May 2015	UT wall thickness was done on nozzles, shell and heads. Minimum reading of 9.1mm on head UT7 and the minimum thickness after forming is 13mm, wall loss of 3.9mm. Minimum required thickness as per calculation is 5.4mm.

Design corrosion allowance:	3mm
Design Life:	30 years
Measured CR:	H

V7703 – WAXY DISTILLATE PRODUCT VESSEL

Equipment:	V7703
Service (product):	Waxy distillate
Operating temperature:	250°C
Material of construction:	BS.1501-151-GR.28A. (CS)
Vessel specifics:	Horizontal with vortex breaker
Internally coated? Or clad?	***None***

Was the vessel (partially) renewed? If yes; at what date and why?	
Was the vessel or components repaired? If yes; at what date and why?	Yes, vortex breaker was replaced in 2015, due to erosion corrosion.

Installation date:	1975
internal inspection dates:	**Inspection history:** ***NB. Report only on location of internal corrosion, leaks, depth, type, extent and possible cracks or other forms of distortion like blisters. Also report when there is no degradation.***
July 1982	Walls were corrosion free underneath product scale.
Sep 1992	In good condition/no corrosion.
Oct 2004	Shell: General roughening up to 0.5mm max. MeasuredGeneral roughening on East and West dished heads. No significant defects noted on nozzles. Vortex breaker: For outlet nozzle (N2) was thinned due to high temperature sulphur corrosion. Nominal thickness is 8mm and the remaining wall thickness was 4.5mm.
May 2015	General immeasurable pitting corrosion (<0.5mm) on the shell, heads and nozzles. Vortex breaker: erosion corrosion was noted resulting in remaining wall thickness of 2mm from 10mm NWT, it was replaced.

NDT dates:	**NDT results:** ***NB. Report wall thickness results separately for sections in different corrosion loops and report NDT technique.***
Oct 2004	UT wall thickness on shell show 8.5mm and the nominal wall thickness 10mm, wall loss of 1.5mm.
May 2015	UT wall thickness on shell UT9 show 7.5mm and the nominal wall thickness 10mm, wall loss of 2.5mm. RT profile shot was done on nozzles and the minimum thickness of 8.3mm on nozzle was measured and original is 14.02mm, wall loss of 5.72mm.

Design corrosion allowance:	3mm

Design Life:	30 years
Measured CR:	H

V7712 – DIRTY WASH OIL DRAW-OFF VESSEL

Equipment:	V7712
Service (product):	Overflash
Operating temperature:	300°C
Operating pressure:	Vacuum
Material of construction:	DIN 17155 HII / DIN 17440. (CS + SS 410 clad)
Vessel specifics:	*Vertical*
Internally coated? Or clad?	Clad with 410SS

Was the vessel (partially) renewed? If yes; at what date and why?	No indication from history.
Was the vessel or components repaired? If yes; at what date and why?	No indication from history.

Installation date:	1986
internal inspection dates:	**Inspection history:** ***NB. Report only on location of internal corrosion, leaks, depth, type, extent and possible cracks or other forms of distortion like blisters. Also report when there is no degradation.***
1990 Aug	No visual damage noted.
1992 Sep	No corrosion noted.
2007 Apr	SS Clad still in good condition.
Oct 2011	**Shell:** The shell was internally clad with 410SS. The cladding was in very good condition and no degradation was noted. All of the nozzle to shell welds had good profile and no corrosion was noted. The longitudinal weld was also in very good condition. **Domes:** The top dome was clad with 410SS. In a band around the vessel, approximately 40 to 50mm from the circumferential weld, towards the knuckle, there was random isolated pitting to 1.1mm deep. The rest of the dome was as new, no deterioration was found. **Nozzles:** All the nozzles were clear and the attachment welds had good profile prior to being replaced as part of the DWO project. **Vortex breaker:** The edges of the vortex breaker were not sharp and there was again shallow, mild surface roughening on the top.

NDT dates:	**NDT results:** ***NB. Report wall thickness results separately for sections in different corrosion loops and report NDT technique.***
May 2011	All wall thickness readings by UT and RT of nozzles were above original wall thickness

Design corrosion allowance:	0 mm

Design Life:	30 years
Measured CR:	L

E7102A-D SH - CRUDE/SHORT RESIDUE EXCHANGER

Equipment:	**E7102A-S**
Service (product):	
Process temperature:	
Material of construction shell body:	**BS 1501 151 28A. (CS)**
Material of construction shell cover:	**BS 1501 151 28A. (CS)**
Material of construction channel	**BS 1501 151 28A. (CS)**
PWHT? (Y/N) Specify component.	**Yes. Bonnet and Floating Head only**
Insulated? (Y/N)	**Yes**
Heat exchanger type:	***Floating head***
Heat exchanger specifics:	***Floating head & tubesheet / domed end at each end***
Number of passes:	**1**
Internally coated? Or clad?	***None***

Installation date shell body & cover:	**1971**
Internal inspection dates:	**Inspection history:** ***NB. Report only on location of internal corrosion, leaks, depth, type, extent and possible cracks or other forms of distortion like blisters. Also report when there is no degradation.***
September 1992	Shell internal still in a good condition with scatted isolated pitting of ±2mm throughout. The shell cover is in the same condition as the shell.
November 2004	General slight pitting corrosion less than 1.0mm deep was noted with roughening in the bottom section due to mechanical gouging (Bundle Removal).The sealing faces of both main flanges revealed no relevant discontinuities or mechanical damages All the nozzles which were open and cleaned were inspected. General slight pitting corrosion and roughening was noted less then 1.0mm deep. The sealing faces revealed no relevant discontinuities or mechanical damages.
September 2011	Slight surface corrosion with isolated pitting of ±0.5mm deep was noted in the shell and shell cover. Mechanical marks were noted at the bottom from pulling the tube bundle The tube bundle cage baffle plate location on the shell are clearly visible indicating slight erosion. All the accessible nozzles were noted to have condition similar to both shell and head. The accessible gasket faces did not reveal any sigh of damage.

Design corrosion allowance shell body/cover:	3.0mm
Design Life:	30 years
Measured CR:	L

Shell body NDT	
NDT dates:	**NDT Results:** ***NB. Report wall thickness results, locations and report NDT technique.***
July 2011	UT Wall thickness survey on the nozzles revealed all recordings to be in excess of nominal

<u>Channel history</u>

Channel	
Internal inspection dates:	**Inspection history:** ***NB. Report only on location of internal corrosion, depth, type, extent and possible cracks or other forms of distortion like blisters. Also report when there is no degradation.***
September 1992	Channel head in a good condition. Flange t = 70.3mm Head t = 23.2mm Div plate 13.6mm.
November 2004	General superficial to slight pitting corrosion and roughening up to a maximum off 1.0mm deep was detected on the internal surface. The nozzle bores revealed a black layer under which slight pitting corrosion with roughening up to a maximum of 1.0mm deep. The sealing faces revealed no relevant discontinuities or mechanical damages at the time of inspection. The divider plate revealed slight pitting corrosion up to a maximum of 1.0mm with no relevant impingement noted.
September 2011	both shell and head. The accessible gasket faces did not reveal any sigh of damage

Design corrosion allowance channel:	3.0mm
Design Life:	30 years
Measured CR:	L

Channel NDT	
NDT dates:	**NDT Results:** ***NB. Report wall thickness results, locations and report NDT technique.***
July 2011	UT Wall thickness survey on the nozzles revealed all recordings to be in excess of nominal

E7104 SH – CRUDE/ LGO EXCHANGER

Equipment:	E7104 - SH; E7104 - CH
Service (product):	Light Gas Oil; Crude Oil
Process temperature:	240 to 130; 85 to 100^{0}C
Process pressure Shell side:	100 kPa
Material of construction shell body:	BS 1501-151-28A. (CS)
Material of construction shell cover:	BS 1501-151-28A. (CS)
Material of construction channel	BS 1501-151-28A. (CS)
Heat exchanger type:	*Floating head*
Heat exchanger specifics:	*Top dome present on shell*
Number of passes:	1
Internally coated? Or clad?	*Which parts are clad or coated with which coating/cladding& when applied? N/A*

Installation date shell body & cover:	1971
Internal inspection dates:	**Inspection history:** ***NB. Report only on location of internal corrosion, leaks, depth, type, extent and possible cracks or other forms of distortion like blisters. Also report when there is no degradation.***
September 1992	Shell internal revealed general slight pitting corrosion throughout to approximately 0.5mm deep. Isolated pitting corrosion was noted along the bottom nozzle measured approximately to 1.5mm deep. Shell cover internal displayed general pitting corrosion to a depth of 0.5mm.
September 2011	Shell and shell cover internal revealed slight surface rust with isolated pitting corrosion to approximately 0.5mm deep. Mechanical marks due to bundle removing were noted at the bottom shell areas.

Shell body NDT	
NDT dates:	**NDT Results:** ***NB. Report wall thickness results, locations and report NDT technique.***
September 2011	Ultrasonic wall thickness testing was done in isolated areas as per inspection strategy. No significant metal loss was noted.

Design corrosion allowance shell:	3.0mm
Design Life:	30 years
Measured CR:	L

Channel history

Channel	
Internal inspection dates:	**Inspection history:** ***NB. Report only on location of internal corrosion, depth, type, extent and possible cracks or other forms of distortion like blisters. Also report when there is no degradation.***
September 2011	Channel head and channel cover surface rust and isolated pitting corrosion to approximately 0.5mm deep were noted.

Design corrosion allowance channel:	3.0mm
Design Life:	30 years
Measured CR:	L

E7108A-H SH – PREFLASHED CRUDE/LOWER CIRCULATING REFLUX

Equipment:	E7108A-SH; E7108A-CH
Service (product):	Crude oil
Process temperature:	214-245 ^{0}C
Process pressure Shell side:	Data not available on Inventory list
Material of construction shell body:	BS 1501-151-28A. (CS)
Material of construction shell cover:	BS 1501-151-28A. (CS)
Material of construction channel	BS 1501-151-28A. (CS)
PWHT? (Y/N) Specify component.	Yes (Channel & floating head to be stress relieved after welding)
Insulated? (Y/N)	Yes
Heat exchanger type:	*Floating head.*
Heat exchanger specifics:	*Dome present on shell*
Number of passes:	1
Internally coated? Or clad?	*Which parts are clad or coated with which coating/cladding& when applied? N/A.*

Installation date shell body & cover:	1971
Internal inspection dates:	**Inspection history:** ***NB. Report only on location of internal corrosion, leaks, depth, type, extent and possible cracks or other forms of distortion like blisters. Also report when there is no degradation.***
November 1976	Shell revealed no significant deterioration noted.
August 1986	**Shell:** Proud areas within the shell, coincident with baffle positions of bundle, indicated general corrosion losses along the bottom 1/3 of shell of 1 mm deep. Otherwise the shell was in good condition. Also some isolated pitting corrosion of 1mm deep along bottom
September 2011	**Shell/ shell cover**: Slight surface rust with isolated pitting corrosion of approximately 0.5mm deep was noted in the shell and shell cover. **Nozzles**: Severe measured wall loss – corrosion allowance consumed and nozzles replaced

Shell body NDT	
NDT dates:	**NDT Results:**

	NB. Report wall thickness results, locations and report NDT technique.
September 2011	**Non destructive testing**: UT readings with 3.75mm wall loss on some nozzles

Design corrosion allowance shell body/cover:	3.0mm
Design Life:	30 years
Measured CR:	M

<u>**Channel history**</u>

Channel	
Internal inspection dates:	**Inspection history:** ***NB. Report only on location of internal corrosion, depth, type, extent and possible cracks or other forms of distortion like blisters. Also report when there is no degradation.***
November 1976	Channel in a satisfactory condition. Minor corrosion causing surface roughening was evident.
August 1986	Channel head in good condition with no corrosion noted. Gasket faces in good condition.
September 2011	**Channel/ channel cover** No change has been noted from was previously reported. Surface rust and isolated pitting corrosion of approximately 0.5mm deep was noted.

Channel NDT	
NDT dates:	**NDT Results:** ***NB. Report wall thickness results, locations and report NDT technique.***
September 2011	**Non destructive testing**: Ultrasonic wall thickness testing: No significant metal loss was noted.

Design corrosion allowance channel:	3.0mm
Design Life:	30 years
Measred CR:	L

E7109A-B SH – PREFLASHED CRUDE / LOWER CIRCULATING REFLUX	
Equipment:	E7109A-SH ; E7109A-CH
Service (product):	Gas oil ; Preflashed crude oil
Process temperature:	248 to 230ºC ; 177 to 191ºC
Material of construction shell body:	BS1501-151-28A. (CS)
Material of construction shell cover:	BS1501-151-28A. (CS)
Material of construction channel	BS1501-151-28A. (CS)
Heat exchanger type:	***Floating head***
Heat exchanger specifics:	***Boot or top dome present on shell/Internal or external bellow***
Number of passes:	
Internally coated? Or clad?	***Which parts are clad or coated with which coating/cladding& when applied?***

Installation date shell body & cover:	**1972**
Internal inspection dates:	**Inspection history:** ***NB. Report only on location of internal corrosion, leaks, depth, type, extent and possible cracks or other forms of distortion like blisters. Also report when there is no degradation.***
1976	Shell - In very good condition. Minor surface roughening found on the bottom of the shell at the south end - between nozzle and flange
1982	Shell - In satisfactory condition. Light surface pitting throughout, slightly heavier along the bottom. There is grouped pitting to 1.0 mm at the bottom of both shell flanges and in one area near the center of the shell.
1986	Shell - Light internal pitting in the bottom. Preferential corrosion at baffle locations.
1992	Shell in good condition. Internal - general pitting to 0.5 mm - 1 mm with isolated 1.5mm.
Sep 2011	**SHELL/ SHELL COVER:** Slight surface rust with isolated pits of +/- 0.5mm deep was noted in the shell and shell cover. **NOZZLES:** All the accessible nozzles were noted to have condition similar to both shell and heads. The accessible gasket faces did not reveal any sign of damage.

Design corrosion allowance shell body/cover:	**3 mm**
Design Life:	**30 years**
Measured CR:	**L**

Channel history

Channel	
Internal inspection dates:	**Inspection history:** ***NB. Report only on location of internal corrosion, depth, type, extent and possible cracks or other forms of distortion like blisters. Also report when there is no degradation.***
1976	Channel- good condition.
Sep 2011	**CHANNEL/ CHANNEL COVER/ FLOATING HEAD:** No change has been noted from was previously reported in the 2004 shutdown. Surface rust and isolated pits of about 0.5mm deep were noted. **NOZZLES:** All the accessible nozzles were noted to have condition similar to both shell and heads. The accessible gasket faces did not reveal any sign of damage.

Design corrosion allowance channel:	3 mm
Design Life:	30 years
Measured CR:	L

E7110A-B SH – KERO STRIPPER REBOILER

Equipment:	E7110A-SH ; E7110A-CH
Service (product):	Gasoil ; Kerosene
Process temperature:	310 to 230ºC ; 210 to 220ºC
Material of construction shell body:	BS1501-151-28A. (CS)
Material of construction shell cover:	BS1501-151-28A. (CS)
Material of construction channel	BS1501-151-28A. (CS)
Heat exchanger type:	*Floating head*
Heat exchanger specifics:	*Shell internal bellow present, but there is no boot or top dome present*
Number of passes:	
Internally coated? Or clad?	*None specified*

Installation date shell body & cover:	**1972**
Internal inspection dates:	**Inspection history:** ***NB. Report only on location of internal corrosion, leaks, depth, type, extent and possible cracks or other forms of distortion like blisters. Also report when there is no degradation.***
1974	Shell: Shell in fair condition, thickness just below top flange is 11 - 12 mm. No internal corrosion.
1976	Shell - good condition. Minor isolated roughening.
1982	Shell **-** Areas cleaned, light roughening noted throughout with isolated 0.5 mm pitting.
1986	Shell - in good condition with light general pitting in the lower section and light preferential attack of the welds. Pitting measured at less than 1mm.
1992	Shell - Internally the shell was in a good condition.
1998	INTERNAL: Good condition
2011	Both channel and shell cover flange joints have been furmanited due to leaking in service.

Shell body NDT	
NDT dates:	**NDT Results:** ***NB. Report wall thickness results, locations and report NDT technique.***
Sep 2011	UT's conducted on N4 revealed a wall loss of 4.7mm from a NWT of 12.7mm to a RWT of 8.0mm.

Design corrosion allowance shell body/cover:	3.0mm
Design Life:	30 years
Measured CR:	H

Channel history

Channel	
Internal inspection dates:	**Inspection history:** ***NB. Report only on location of internal corrosion, depth, type, extent and possible cracks or other forms of distortion like blisters. Also report when there is no degradation.***
Sep 2011	Both channel and shell cover flange joints have been furmanited due to leaking in service.

Design corrosion allowance channel:	3.0mm
Design Life:	30 years
Measured CR:	H

E7135 SH – PREFLASHCRUDE/HGO EXCHANGER	
Equipment:	**E7135-S**
Service (product):	**Heavy Gas Oil**
Process temperature:	**210 165 °C**
Process pressure Shell side:	**1250 – 1150 kPa**
Material of construction shell body:	**SA 516 Gr 60N. (CS)**
Material of construction shell cover:	**SA 516 Gr 60N. (CS)**
Material of construction channel	**SA 516 Gr 60N. (CS)**
Heat exchanger type:	***Floating Head***
Heat exchanger specifics:	***Dome present on channel, Impingement plate***
Number of passes:	**1**
Internally coated? Or clad?	***Nil***

Installation date shell body & cover:	**1998**
Internal inspection dates:	**Inspection history:** ***NB. Report only on location of internal corrosion, leaks, depth, type, extent and possible cracks or other forms of distortion like blisters. Also report when there is no degradation.***
September 2011	The shell / shell cover internal surface displayed superficial corrosion with isolated pitting of ±0.5mm.

Shell body NDT	
NDT dates:	**NDT Results:** ***NB. Report wall thickness results, locations and report NDT technique.***

Design corrosion allowance shell body/cover:	3mm
Design Life:	30 years
Measured CR:	L

<u>Channel history</u>

Channel	
Internal inspection dates:	**Inspection history:**

	NB. Report only on location of internal corrosion, depth, type, extent and possible cracks or other forms of distortion like blisters. Also report when there is no degradation.
September 2011	No change has been noted as was previously reported. superficial corrosion with isolated pitting of ±0.5mm in depth. All the accessible nozzles were noted to have conditions similar to both the shell and shell cover The gasket faces did not reveal any sign of damage.

Channel NDT	
NDT dates:	**NDT Results:** ***NB. Report wall thickness results, locations and report NDT technique.***
July 2011	All thickness recorded are in excess of original and these recordings are only on the nozzles.

Design corrosion allowance channel:	3mm
Design Life:	30 years
Measured CR:	L

E7136 CH – PREFLASHCRUDE/HGO EXCHANGER

Equipment:	**E7136-S**
Service (product):	**Gas Oil**
Process temperature:	**280 265 °C**
Process pressure Shell side:	**750 – 650 kPa**
Material of construction shell body:	**SA 516 Gr 60N. (CS)**
Material of construction shell cover:	**SA 516 Gr 60N. (CS)**
Material of construction channel	**SA 516 Gr 60N. (CS)**
Heat exchanger type:	***Floating Head***
Heat exchanger specifics:	***Dome present on channel, Impingement plate***
Number of passes:	**1**
Internally coated? Or clad?	***Nil***

Installation date shell body & cover:	**August 1998 Installed as new.**
Internal inspection dates:	**Inspection history:** ***NB. Report only on location of internal corrosion, leaks, depth, type, extent and possible cracks or other forms of distortion like blisters. Also report when there is no degradation.***
September 2011	The shell / shell cover internal surface displayed superficial corrosion with isolated pitting of ±0.5mm.

Shell body NDT	
NDT dates:	**NDT Results:** ***NB. Report wall thickness results, locations and report NDT technique.***
September 2011	Only the 2” vent and drain nozzles on the shell were thickness checked and recordings were found to be in access of nominal.

Design corrosion allowance shell body/cover:	3mm
Design Life:	30 years
Measured CR:	L

Channel history

Channel	
Internal inspection dates:	**Inspection history:** ***NB. Report only on location of internal corrosion, depth, type, extent and possible cracks or other forms of distortion like blisters. Also report when there is no degradation.***

July 2001	The exchanger and connecting piping were installed new in August 1998 shutdown
September 2011	No change has been noted as was previously reported. superficial corrosion with isolated pitting of ±0.5mm in depth. All the accessible nozzles were noted to have conditions similar to both the shell and shell cover The gasket faces did not reveal any sign of damage.

Channel NDT	
NDT dates:	**NDT Results:** ***NB. Report wall thickness results, locations and report NDT technique.***
September 2011	Only the inlet, outlet and vent nozzles were thickness checked and found to be in excess of nominal.

Design corrosion allowance channel:	3mm
Design Life:	30 years
Measured CR:	L

E7206 CH – DEBUTANISER REBOILER

Equipment:	**E7206**
Service (product):	**Shell side - Light Naphtha/Light gasoline mix** **Tube side – Heavy Waxy**
Process temperature – tube side (°C):	**275-240**
Process temperature – shell side (°C):	**150-120**
Material of construction shell body:	**BS1501-151-28A. (Carbon Steel).**
Material of construction shell cover:	**BS1501-151-28A. (Carbon Steel).**
Material of construction channel	**BS1501-151-28A. (Carbon Steel).**
PWHT? (Y/N) Specify component.	**Yes. Floating Head & Channel Only.**
Insulated? (Y/N)	**U-Bundle**
Heat exchanger type:	Fixed tube sheet /floating head
Heat exchanger specifics:	Boot or top dome present on shell/Internal or external bellow
Number of passes:	1
Internally coated? Or clad?	None.

Renew/ Repair History:

Date	**Component Renewed/ Repaired**
1971	Installation of shell body & cover and commission
1981, 1986	Partial re tube 1981 and 1986, New 1998
1998	New bundle

Inspection History - Shell:

Date	**Inspection Findings** *NB: Report only on location of internal corrosion, leaks, depth, type, extent and possible cracks or other forms of distortion like blisters. Also report when there is no degradation.*
Last internal inspection date:	**Last internal inspection finding:**
Aug 1998	Internally - general surface roughening isolated pit to 0.75mm.
Sept 2011	Shell: The standard of cleanliness was not good but sufficient to make judgment on the shell. The shell exhibited a general rough oxidized surface texture with wastage estimated to be no more than 1 mm. Shell Cover: Exhibits a general washed oxidized appearance, lightly scaled in places and weld profiles in good condition. Wastage estimated at no more than 0.5 mm. Nozzles: Bores lightly scaled. Floating Head: In good serviceable condition. General surface roughness on the inner surface with wastage to no more than 0.5mm. External surface in good condition.
June 2017	The shell found superficially corroded. The middle section noted with a thin product layer.

	The dome was superficially corroded and hard patches of scale were noted at the bottom section. SHELL NOZZLES/FLANGES Nozzles found superficially corroded and a thin product layer was noted at certain areas. Nozzle to shell welds were ground flush with no defects noted visually.

Design corrosion allowance:	3mm
Design Life:	30 years
Measured CR:	L

Inspection History - Channel:

Date	**Inspection Findings** *NB: Report only on location of internal corrosion, leaks, depth, type, extent and possible cracks or other forms of distortion like blisters AND/OR when there is no degradation.*
Last internal inspection date:	**Last internal inspection finding:**
Sept 2011	Channel Cover: Both the shell and division plate has a relatively smooth surface texture exhibiting original weld bead profiles. The channel and the partition plates covered with a thin product layer.

Design corrosion allowance:	3mm
Design Life:	30 years
Measured CR:	H

E7701A SH – PREFLASHED CRUDE/SHORT RESIDUE EXCHANGER

Equipment:	E7701A-SH ; E7701A-CH
Service (product):	Short residue
Process temperature:	295 to 270ºC
Material of construction shell body:	BS-1501-161-28A. (CS)
Material of construction shell cover:	BS-1501-161-28A. (CS)
Material of construction channel	BS-1501-161-28A. (CS)
Heat exchanger type:	Floating head
Heat exchanger specifics:	***Floating head / domes on channel heads***
Number of passes:	**1**
Internally coated? Or clad?	***None***

Installation date shell body & cover:	**1976**
Internal inspection dates:	**Inspection history:** ***NB. Report only on location of internal corrosion, leaks, depth, type, extent and possible cracks or other forms of distortion like blisters. Also report when there is no degradation.***
Oct 2011	Corrosion allowance (3mm) consumed on nozzle.
2015TA	Internally. General slight pitting corrosion+/-0.50mm deep,

Shell body NDT	
NDT dates:	**NDT Results:** ***NB. Report wall thickness results, locations and report NDT technique.***
2011	Corrosion allowance (3mm) consumed on nozzle

Design corrosion allowance shell body/cover:	3.0mm
Design Life:	30 years
Measured CR:	M

Channel history

Channel	
Internal inspection dates:	**Inspection history:** ***NB. Report only on location of internal corrosion, depth, type, extent and possible cracks or other forms of distortion like blisters. Also report when there is no degradation.***

2015	**Findings:** The heat exchanger had clamps installed on the channel and floating head cover flanges. Clamps removed during the 2015TA. **Channel cover:** after gtiblbasting slight pitting corrosion 1.0mm deep noted on the internal section of the cover and sealing face areas. Divider section revealed general pitting corrosion.

Channel NDT	
NDT dates:	**NDT Results:** ***NB. Report wall thickness results, locations and report NDT technique.***
2015	1. Pitting corrosion 1.0mm deep noted on the internal section of the cover and sealing face areas 2. No wall loss deterioration recorded on the nozzles (N1 and N2).

Design corrosion allowance channel:	3.0mm
Design Life:	30 years
Measured CR:	L

E7702A-B SH OVERFLASH PRODUCT COOLER

Equipment:	E7702A-SH ; E7702A-CH
Service (product):	Short Residue ; Tempered Water
Process temperature:	Above 300°C - SH ; 45 to 50ºC - CH
Material of construction shell body:	ASTM A515 Gr 60 Clad 410S. (CS & SS cladding).
Material of construction shell cover:	ASTM A515 Gr 60 Clad 4. (CS & SS cladding).
Material of construction channel	HII. (CS).
Internally coated? Or clad?	*Cladding on shell and shell cover applied i*n 1976.

Installation date shell body & cover:	1976
Internal inspection dates:	**Inspection history:** ***NB. Report only on location of internal corrosion, leaks, depth, type, extent and possible cracks or other forms of distortion like blisters. Also report when there is no degradation.***
1979 Feb	No defect observed
2011 Sep	No defects were noted in the cladding.

Shell body NDT	
NDT dates:	**NDT Results:** ***NB. Report wall thickness results, locations and report NDT technique.***
2011 TA	NDT results available. Based on History, HX not affected by severe corrosion. Perform LTCR calculations.

Design corrosion allowance shell body/cover:	3.0mm
Design Life:	30 years
Measured CR:	L

<u>**Channel history**</u>

Channel	
Internal inspection dates:	**Inspection history:** ***NB. Report only on location of internal corrosion, depth, type, extent and possible cracks or other forms of distortion like blisters. Also report when there is no degradation.***
1986	**Channel** – t-10.1mm. int. light roughening – isolated 0.5mm pits. Gasket faces good. Division plate good. T=10.2mm. Channel cover – good. Int. machine marks still visible t = 40.4mm.

1992	**Channel –** 13.2mm thick – caliper measurement – external scaling 2mm – good internally. UT measurements – channel 10.5mm.
2011	**Channel:** The gasket faces were defect free. No corrosion was observed on the channel internal surfaces. The partition plate was slightly bent, but there was no concern. The minimum UT readings were recorded at 10.1mm (Nom. 10.0mm). The nozzles were clear and no corrosion was noted. The UT readings of the nozzles were N1 = 8.6mm (Nom. 8.56mm) and N2 = 8.4 (Nom. 8.56mm).

Channel NDT	
NDT dates:	**NDT Results:** ***NB. Report wall thickness results, locations and report NDT technique.***
2011 TA	NDT results available. Based on History, HX not affected by severe corrosion. Perform LTCR calculations.

Design corrosion allowance channel:	3.0mm
Design Life:	30 years
Measured CR:	L

E7708A/B SH – WAXY DISTILLATE COOLER

Equipment:	E7708A-S
Corrosion Loop:	CL7700-04 / CL7700-55
Service (product):	Waxy distillate / Tempered water
Process temperature:	160 to 250°C
Material of construction shell body:	BS-1501-151-28A. (CS)
Material of construction shell cover:	BS-1501-151-28A. (CS)
Material of construction channel	BS-1501-151-28A. (CS)
PWHT? (Y/N) Specify component.	Channel & floating head only
Insulated? (Y/N)	No
Heat exchanger type:	Floating head
Heat exchanger specifics:	Nil
Number of passes:	1
Internally coated? Or clad?	No indication from history.

Installation date shell body & cover:	1976
Internal inspection dates:	**Inspection history:** ***NB. Report only on location of internal corrosion, leaks, depth, type, extent and possible cracks or other forms of distortion like blisters. Also report when there is no degradation.***
Sep 1992	Shell: Good condition with minor roughening next to the inlet nozzle up to 0.2mm max.
April 2007	Internal surfaces of shell not properly cleaned. A thin layer of product coated the inner surface. Isolated pitting of 2.0mm noted.
Oct 2011	Isolated pits noted inside the shell 0,6mm deep. 0.8mm pitting corrosion noted inside shell cover.

Shell body NDT	
NDT dates:	**NDT Results:** ***NB. Report wall thickness results, locations and report NDT technique.***
October 2011	wall loss of 2.6mm measured

Design corrosion allowance shell body/cover:	3mm
Design Life:	30 years
Measured CR:	M

<u>Channel history</u>

Channel	
Internal inspection dates:	**Inspection history:** ***NB. Report only on location of internal corrosion, depth, type, extent and possible cracks or other forms of distortion like blisters. Also report when there is no degradation.***
April 2007	There were no signs of any corrosion or pitting.
Oct 2011	The barrel of the channel had uniform wastage and was smooth.

Channel NDT	
NDT dates:	**NDT Results:** ***NB. Report wall thickness results, locations and report NDT technique.***
Sep 1992	UT measurements - Channel 17.0mm.
2011	UT wall thickness was done, no wall loss measured.

Design corrosion allowance channel:	3mm
Design Life:	30 years
Measured CR:	L

E7711A/B SH – SHORT RESIDUE COOLER

Equipment:	E7711-S
Service (product):	Short residue / Tempered Water
Process temperature:	200 to 50°C
Process pressure Shell side:	800 to 750 kPa
Material of construction shell body:	BS 1501-151-28A. (CS)
Material of construction shell cover:	BS 1501-151-28A. (CS)
Material of construction channel	BS 1501-151-28A. (CS)
Heat exchanger type:	Floating Head
Heat exchanger specifics:	Nil
Number of passes:	1
Internally coated? Or clad?	Nil

Installation date shell body & cover:	1976
Internal inspection dates:	**Inspection history:** ***NB. Report only on location of internal corrosion, leaks, depth, type, extent and possible cracks or other forms of distortion like blisters. Also report when there is no degradation.***
1976	Commissioned
July 1982	No corrosion noted at the time of inspection.
Aug 1986	No corrosion noted at the time of inspection.
Sep 1992	Scattered pitting corrosion through out the shell with a max pit of 1mm.
Jan 2004	Isolated pitting corrosion between 1mm-1,5mm internal surface of the shell.
May 2015	General pitting corrosion of about ±0.5mm was noted on the entire shell.

Shell body NDT	
NDT dates:	**NDT Results:** ***NB. Report wall thickness results, locations and report NDT technique.***
Sep 1992	UT measurement - shell 20.0mm. Shell covers 19.5mm
May 2003	UT wall thickness was done and minimum reading of 17.83mm on shell and orginal was 18mm, wall loss of 0.17mm.Minimum reading of 8.28mm on nozzle N5 and original was is 8.74mm, wall loss of 0.46mm.
May 2015	UT wall thickness was carried out on the shell and a minimum of 17.4mm was measured from a nominal of 18mm, wall loss of 0.6mm. Shell cover revealed a minimum of 17.1mm from an

	original of 18mm, wall loss of 0.9mm. Minimum reading of 7.4mm on nozzle N5 and original was 8.74, wall loss of 1.34mm.

Design corrosion allowance shell body/cover:	3mm
Deisgn Life:	30 years
Measured CR:	M

Channel history

Channel	1976
Internal inspection dates:	**Inspection history:** ***NB. Report only on location of internal corrosion, depth, type, extent and possible cracks or other forms of distortion like blisters. Also report when there is no degradation.***
1976	Commissioned
Aug 1986	No corrosion.
Jan 2004	Internally product scaled / roughened.
May 2015	Superficial corrosion was noted on the entire channel.

Channel NDT	
NDT dates:	**NDT Results:** ***NB. Report wall thickness results, locations and report NDT technique.***
May 2015	UT wall thickness carried out on the channel revealed minimum of 12.5mm and original was 12mm. Minimum reading of 11.8mm on nozzle N1 and original was 12.7mm, wall loss of 0.9mm.

Design corrosion allowance channel:	3mm
Design Life:	30 years
Measured CR:	L

E7714 SH & CH – PREFLASHED CRUDE / DIRTY WASH OIL EXCHANGER

Equipment:	E7714-SH ; E7714-CH
Corrosion Loop:	CL7700-03 ; CL7100-05
Service (product):	Overflash, Pre-Flashed Crude
Process temperature:	Ambient - 280ºC – SH ; 241ºC - CH
Process pressure Shell side:	0 to 2000kPa
Material of construction shell body:	SA 240 – 316L. (SS)
Material of construction shell cover:	SA 240 – 316L. (SS)
Material of construction channel	SA 240 – 316L. (SS)
Heat exchanger type:	*Floating head*
Heat exchanger specifics:	***Floating head / domed end at each channel***
Number of passes:	**1**
Internally coated? Or clad?	***None***

Installation date shell body & cover:	**1999**
Internal inspection dates:	**Inspection history:** ***NB. Report only on location of internal corrosion, leaks, depth, type, extent and possible cracks or other forms of distortion like blisters. Also report when there is no degradation.***
1999 Dec	E7714A and B made redundant due to severe high temperature sulphur corrosion found during August 1998 shutdown. One new exchanger installed, full stain less steel.
2011 Oct	No visual damage noted on the stainless steel shell. Shell cover: A new shell cover was installed as part of a project. The old shell cover was in very good condition, as new. The welds were perfect and the nozzles had no evident degradation.

Shell body NDT	
NDT dates:	**NDT Results:** ***NB. Report wall thickness results, locations and report NDT technique.***
2011 Oct	Ultrasonic measurements taken 0.5m into the shell on both sides showed the shell to be at least 11.01mm (Nom. 12mm). Nozzle N3 was also measured by UT and returned a minimum reading of 27.3mm (Nom. 27.6mm). UT reading on cover was 11.35mm (Nom. 12mm).

Design corrosion allowance shell body/cover:	0.0mm
Design Life:	30 years
Measured CR:	L, previously H before metallurgy upgrade to 316L SS

Channel history

Channel	
Internal inspection dates:	**Inspection history:** ***NB. Report only on location of internal corrosion, depth, type, extent and possible cracks or other forms of distortion like blisters. Also report when there is no degradation.***
2011 Oct	No visual damage noted.

Channel NDT	
NDT dates:	**NDT Results:** ***NB. Report wall thickness results, locations and report NDT technique.***
2011 Oct	The thickness of the channel was 11.58mm (Nom. 12mm).

Design corrosion allowance channel:	0.0mm
Design Life:	30 years
Measured CR:	L

E7715 SH & CH – PREFLASHED CRUDE / SHORT RESIDUE EXCHANGER

Equipment:	E7715-SH ; E7715-CH
Corrosion Loop:	CL7700-07 ; CL7700-05
Service (product):	Short residue ; Preflashed crude
Process temperature:	350 to 320 ºC - SH ; 241 to 260ºC - CH
Material of construction shell body:	SA387 Gr5 Cl1. (5Cr½Mo)
Material of construction shell cover:	SA387 Gr5 Cl1. (5Cr½Mo)
Material of construction channel	SA387 Gr5 Cl1. (5Cr½Mo)
Heat exchanger type:	Floating Head
Heat exchanger specifics:	Nil
Number of passes:	1
Internally coated? Or clad?	Nil

Installation date shell body & cover:	**1985**
Internal inspection dates:	**Inspection history:** ***NB. Report only on location of internal corrosion, leaks, depth, type, extent and possible cracks or other forms of distortion like blisters. Also report when there is no degradation.***
1992 Sep	Shell: Shell internally in good condition/no corrosion.
2011 Oct	**Shell:** The nozzles were clear but had isolated pitting as per the rest of the internals. All the welds had decent profile. The thickness of the cover was measured to be 16.1mm from original 20.81mm

Shell body NDT	
NDT dates:	**NDT Results:** ***NB. Report wall thickness results, locations and report NDT technique.***
1992 Sep	UT measurements - shell 21.0mm. Shell cover 21.5mm.
2011 Oct	UT Readings taken on the shell revealed a minimum wall thickness of 18.8mm (Original. 20mm). The thickness of the shell cover was measured to be 16.1mm (Original 20.81mm A/F), which equates to a 4.71mm wall loss.

Design corrosion allowance shell body/cover:	3.0mm
Design Life:	30 years
Measured CR:	H

Channel history

Channel	
Internal inspection dates:	**Inspection history:**

	NB. Report only on location of internal corrosion, depth, type, extent and possible cracks or other forms of distortion like blisters. Also report when there is no degradation.
2011 TA	**Channel:** Shallow pitting to 0.5mm deep The nozzles had no corrosion evident and were clear.

Channel NDT	
NDT dates:	**NDT Results:** ***NB. Report wall thickness results, locations and report NDT technique.***
2011 TA	UT measurements on nozzles gives a maximum 2.60mm wall loss.

Design corrosion allowance channel:	3.0mm
Design Life:	30 years
Measured CR:	M